6TH SYMPOSIUM ON

Meteoroids, Meteors & Meteorites

Messengers from Space



ABSTRACT VOLUME

26-27 October 2026

Kalidas Auditorium, IIT Kharagpur

Organised by the Department of Geology & Geophysics, IIT Kharagpur
in partnership with Physical Research Laboratory, Ahmedabad

metmess.iitkgp.ac.in

Contents

Session I: Early Solar System Processes & Organics

ABS027	From Galactic Matter to Planetesimals: Insights from Meteorites and Sample Returns	**Kuljeet Kaur Marhas** PRL Ahmedabad · Keynote	**6**
ABS008	Beyond the Solar Neighborhood: A New Perspective on Presolar Grain Origins	**Antariksha Mitra** PRL Ahmedabad · Oral	**7**
ABS011	From Stardust to Supernovae: an Integrated 1D-3D Nucleosynthetic Mixing Framework for Tracing the Origin of Presolar Grains	**Divyadharsini R** PRL Ahmedabad · Oral	**8**
ABS032	Elemental and Oxygen Isotope Composition of CM Meteorite Constituents: Constraints on Origin of Solar System	**Gopalan Srinivasan** CSSEH Bhopal · Keynote	**9**
ABS003	Characterization of Nanoglobule-like Organics in Mukundpura (CM2): a Coordinated NanoSIMS-hrtem Study	**Shreeya Natrajan** PRL Ahmedabad · Oral	**11**
ABS012	Nanoscale Carbon and Nitrogen Isotopic Anomalies in Insoluble Organic Matter from the Norton County Aubrite and Parsa Enstatite Chondrite: A NanoSIMS–HRTEM Study	**Neha** PRL Ahmedabad · Oral	**12**
ABS034	The Construct of Solar System: Deconstructed from High Precision 26Al-26Mg Systematics in Meteorites	**Ritesh Kumar Mishra** AMETEK India, Bengaluru · Keynote	**13**
ABS009	Origin and Evolution of Enigmatic Corundum Inclusions in the Bhuka IAB Iron Meteorite: Insights from ^{26}Al–^{26}Mg and Oxygen Isotope Systematics	**Ankit Prakash Singh** PRL Ahmedabad · Oral	**14**
ABS019	Stable isotope variations of major elements in planet forming materials	**Yogita Kadlag** PRL Ahmedabad · Invited	**15**
ABS054	C, H, and N isotopic studies of C2 and C1-type clasts from a polymict ureilite breccia.	**Subhasmita Swain** NISER Bhubaneswar · Oral	**16**
ABS055	Unique olivine-rich volatile-rich C1 clasts in two polymict ureilites	**Subhasmita Swain** NISER Bhubaneswar · Oral	**17**
ABS068	Oxygen Isotope Concentration of Carbonate and Olivine Grains within C1 and CM-like Clasts in Achondritic Breccia Meteorites.	**Neetha Thomas** IISER Berhampur · Oral	**18**
ABS014	High resolution spectroscopy and laboratory astrochemistry @IIT Kharagpur	**Arijit Roy** Dept. of Chemistry, IIT Kharagpur · Poster P01	**19**
ABS016	ℓ-type Doubling in HC2n+1N and HC2n+1P Linear Molecules of Astrochemical Interest	**Ratul Paul** IIT Kharagpur · Poster P02	**20**
ABS050	Raman Spectroscopic Constraints on the Formation Conditions of Presolar Silicon Carbide Grains from the Murchison Meteorite	**Aadhya Tripathi** IISER Mohali · Poster P03	**21**
ABS071	Radiative Transfer Modeling of Molecular Line Profiles in the Hot Corino Proto-binary Ngc 1333 IRAS4A	**Bratati Bhat** PRL Ahmedabad · Poster P04	**22**
ABS076	Mineralogical, Chemical and Shock-Metamorphic Characterization of Chondrule Populations in the Dergaon H5 Chondrite	**Kalpana Singh Verma** IIT Roorkee · Poster P05	**23**

Session II: Asteroids, Comets, Micrometeorites & Returned Samples

ABS006	Meteorite Mineralogy and Indian Meteorite Fall	**Dipak Kumar Panda** PRL Ahmedabad · Keynote	**24**
ABS059	Deciphering Pre- and Post-Accretionary Processing of Organic Matter in Asteroidal Materials	**Rahul Kumar** IIT (ISM) Dhanbad · Oral	**25**
ABS021	Phosphate mineralogy and fluid-assisted alteration in the Khalwat-Nimgaon L5 ordinary chondrite: Implications for S-Type asteroid parent bodies	**Garima Arora** PRL Ahmedabad · Oral	**26**
ABS038	Cosmic Ray Exposure Ages of Meteorites and Surface Exposure Systematics of Planetary Objects	**Ramakant R. Mahajan** PRL Ahmedabad · Keynote	**27**
ABS035	Neutron Signatures in Ordinary Chondrites	**Satvika Jaiswal** PRL Ahmedabad · Oral	**28**
ABS073	Thermal Overprinting by Fusion Crust Controls Back-transformation of High-pressure Phases in the Katol L6 Chondrite	**Kishan Tiwari** IIT Kharagpur · Oral	**29**

ABS041	Shock Features in Ordinary Chondrites: Observations from the Geological Survey of India Archive	**Arindam Dutta** GSI Kolkata · Keynote	**30**
ABS048	Olivine-ringwoodite transformation mechanism in Bori L6 chondrite. Implication for slab rheology	**Rajesh Kumar Behera** IIT Kharagpur · Oral	**31**
ABS029	Interpreting the Entry Conditions for the Development of Different Textures in Micrometeorites	**Vijay Pratap Singh** CSIR-NIO Goa · Oral	**32**
ABS020	Evaluation Of Highly Oblique Impact Crater Near Luobusa Ophiolite Using, Numerical Models, Ultra High-Pressure Minerals and Tektites	**Mahesh Patil** SSRI Ahmedabad · Oral	**33**
ABS082	Extraterrestrial Dust Influx and Biogeochemical Footprints: Constraints from Antarctic Ice and Central Indian Ocean Basin Records	**Vijay Pratap Singh** CSIR-NIO Goa · Oral	**34**
ABS018	Textural and Environmental Discrimination of Extraterrestrial and Terrestrial Spherules: Evidence from Central Indian Ocean Basin Sediments and Antarctic Cryoconite Sediments.	**Krishnaveni D** CSIR-NIO Goa · Poster P06	**35**
ABS044	Noble Gas Isotope Systematics of H Group Ordinary Chondrites	**Avadh Kumar** PRL Ahmedabad · Poster P07	**36**
ABS079	Spectral Signatures of Simulated Asteroid Regoliths: Linking Physical Properties to VNIR–SWIR Characteristics	**Sritama Das** IIT Kharagpur · Poster P08	**37**
ABS080	OH, Organics, and CO_2 in the Outer Solar System: A JWST/NIRSpec Spectral Investigation.	**Arnab Chatterjee** IIT Kharagpur · Poster P09	**38**

Session III: Differentiated Bodies: Asteroids, Moon, Mars

ABS075	End Member Models in Planetesimal Formation: Constraints from Differentiated Meteorites	**Nachiketa Rai** IIT Roorkee · Keynote	**39**
ABS033	Non-traditional Isotope Geochemistry of Planetary Materials	**Ramananda Chakrabarti** IISc Bengaluru · Keynote	**40**
ABS058	Petrography of the Polymict Ureilite Northwest Africa (NWA) 15112: Clast Diversity and Implications for Reduction and Impact Processing	**Aishanya Sharma** IIT Roorkee · Oral	**41**
ABS066	Late homogenization of mantle sources recorded by 182W isotope signatures from the Singhbhum Craton	**Arathy Ravindran** IISER Thiruvananthapuram · Oral	**42**
ABS022	Diversity of Lunar Feldspathic Highland Crust: the View After CHANDRAYAAN-3	**Dwijesh Ray** PRL Ahmedabad · Keynote	**43**
ABS057	How Did Some Basalts on the Moon Become So Rich in Titanium?	**Himela Moitra** IIT Kharagpur · Oral	**44**
ABS049	Identification and Characterization of Previously Unidentified Events from Apollo Passive Seismic Data	**Omkar Kumar Gupta** PRL Ahmedabad · Oral	**45**
ABS002	Late-stage Silicic Differentiation on Mars: Evidence from Si–Na–K-rich Mesostasis and Inclusions in the Shergotty Shergottite	**Manoj Jat** PRL Ahmedabad · Poster P10	**46**
ABS042	Reconstructing the Geological Past of Mars: Insights from Olivine Alteration in the Nakhlite Yamato-593	**Aditya Das** PRL Ahmedabad · Poster P11	**47**
ABS060	Textural Study of the Martian Meteorite - Shergotty	**Mahima Sharma** IIT Roorkee · Poster P12	**48**
ABS061	Petrographic and Mineralogical Insights into Winona and NWA 14344: Implications for Winonaite Petrogenesis	**Nishant Pandey** IIT Roorkee · Poster P13	**49**
ABS045	Probing the origin of Earth's apparent non-chondritic Mg isotope signature	**Soumyadip Haldar** IISER Kolkata · Poster P14	**50**
ABS026	Geochemical Insights into Basalt Weathering on Mars: a Case Study of Lyot Crater	**Sneha Bhowmik** IIT Kharagpur · Poster P15	**51**
ABS064	Spectral Anomalies and Possible Iron-meteorite Origins of FE-RICH Float Rocks at Jezero Crater, Mars: a Mastcam-z and Supercam Investigation.	**Subham Sarkar** IISc Bengaluru · Poster P16	**52**

Session IV: Space Weathering, Meteors, Atmosphere & Ionosphere

ABS037	The PAH problem in the ISM, Bottom-up or Top-down	**Bhalamurugan Sivaraman** PRL Ahmedabad · Keynote	**53**
ABS024	Mid-infrared Spectroscopic investigation of a sample of asteroids	**V. Venkataraman** SPL VSSC Thiruvananthapuram · Oral	**54**

ABS070	Pulsed Laser Irradiation of Three CM Chondrites: Micrometeorite related Space Weathering on Organic-rich Asteroids	**Swarna Prava Das** NISER Bhubaneswar · Oral	**55**
ABS078	Solar- and Cosmic Ray Tracks in Regolith Breccia Meteorites	**Neetha Thomas** IISER Berhampur · Oral	**56**
ABS051	Stony meteorites at hypervelocities in Venusian atmosphere, An experimental approach	**Arijit Roy** PRL Ahmedabad & IIT Kharagpur · Oral	**57**
ABS031	The Largest Peptide-like Molecule in the ISM- Propionamide in Astrochemical Icy Conditions	**Ipshita Sen** Mizoram University · Poster P17	**58**

Session V: Planetary Analogues

ABS043	Role of Fluid into the Origin of Ancient LIP Rhyolite and Large Granitoid: Implications for Martian Silicic Rocks	**Sarajit Sensarma** University of Lucknow · Oral	**59**
ABS077	Combined Radiogenic K–CA and RB–SR Isotopic Age Constraints of the Dhala Impact Structure, India	**Gaurav Singh Papola** IISc Bengaluru · Oral	**60**
ABS072	Significance of Terrestrial Analogues for Lunar Exploration: Insights from the Sittampundi Anorthosite Complex, India	**Rajesh V. J.** IIST Thiruvananthapuram · Keynote	**61**
ABS030	Evaporative Polygons: An Indication of Transient Brine Activity on Mars	**Angana Samanta** IIT Bombay · Oral	**62**
ABS053	3D printing of space bricks and radiation shield using planetary analogues	**Thirukumaran Venugopal** Chikkaiah Govt. College, Erode · Oral	**63**
ABS069	Laboratory Studies for Planetary Science: Developing a New Experimental Facility at SINP, Kolkata, India	**Sankhabrata Chandra** SINP Kolkata · Invited	**64**
ABS001	Extremophile microbiomes hosted in planetary analogue sites across the Indian subcontinent	**Yamini Jangir** IIT Kanpur · Oral	**65**
ABS017	Biosignature Preservation in Travertine Deposits from Tapovan Hotspring, Uttarakhand: Implications for Mars	**Pallabi Das** PRL Ahmedabad · Oral	**66**
ABS047	Geochemical Studies of Impact-melt Rocks from the Lonar Crater	**Anagha S M** PRL Ahmedabad · Poster P18	**67**
ABS015	Impact-melt spherules at Lonar crater, India, and Jezero crater, Mars: A Terrestrial Analogue perspective	**Himangshu Deka** PRL Ahmedabad · Poster P19	**68**
ABS056	Mineralogical signatures of basaltic laterites from India: Implications for Fe-rich alteration history on Mars	**Aindrila Mukherjee** PRL Ahmedabad · Poster P20	**69**
ABS067	Shock Driven Chemical Processing of Lunar Analogues	**Roshan Nath** GITAM Bengaluru · Poster P21	**70**

Session VI: Planetary Remote Sensing & Instrumentation

ABS005	MRO-HiRISE observations of aeolian characteristics at the Arkhangelsky crater on Mars	**Anirban Mandal** NIT Rourkela · Oral	**71**
ABS004	Simulation of neutron and gamma spectra of Mars: Constraints on thickness of CO2 frost layer	**Debabrata Banerjee** PRL Ahmedabad · Oral	**72**
ABS062	Chandrayaan-3 provides intriguing insights into thermophysics and geo-technical environment at lunar high-latitudes	**Karanam Durga Prasad** PRL Ahmedabad · Invited	**73**
ABS065	3D Thermophysical Modelling of Martian Surface and Subsurface Temperatures: Validation Against In-Situ Observations	**Karanam Samadhanam Raju** PRL Ahmedabad · Oral	**74**
ABS039	Design and Development of a Miniaturized Neutral and Ion Mass Spectrometer (NIMS) for Future Planetary Missions	**Sanjeev Kumar Mishra** PRL Ahmedabad · Oral	**75**
ABS081	Chemical Fingerprints of Planetary Evolution	**Liton Majumdar** NISER Bhubaneswar · Invited	**76**
ABS007	Studies on Interannual Variability of Argon in the Martian Atmosphere	**Shipra** PRL Ahmedabad · Poster P22	**77**
ABS010	Deep Learning Classification of Martian Impact Crater Degradation from CTX Imagery	**Saksham Badal** IIT (ISM) Dhanbad · Poster P23	**78**

ABS023	Can the Experimental Maturity Sequence Help to Locate Relatively Recent Brine Activity on Mars?	**Adrita Mukherjee** IIT Kharagpur · Poster P24	**79**
ABS025	Deep-Learning-Based Semantic Segmentation of Lunar Swirls	**Subhangini Soni** PRL Ahmedabad · Poster P25	**80**
ABS052	Integrated Assessment of Safe Landing Zones and Traverse Planning at the Lunar South Pole	**Suyash Sharma** IIST Thiruvananthapuram · Poster P26	**81**

FROM GALACTIC MATTER TO PLANETESIMALS: INSIGHTS FROM METEORITES AND SAMPLE RETURNS

K. K. Marhas, Physical Research Laboratory, Navrangpura, Ahmedabad, kkmarhas@prl.res.in

Meteorites and returned extraterrestrial samples provide an exceptional record of how material evolved from stellar and interstellar environments into the Solar System and its earliest planetesimals. They preserve signatures of stellar nucleosynthesis, galactic chemical evolution (GCE), interstellar chemistry, and the physical and chemical processes that operated in the young protoplanetary disk. The growing availability of pristine returned samples, together with the extensive meteorite record, is opening new opportunities to connect these processes across different spatial and temporal scales.

Presolar grains provide direct evidence for the stellar sources that contributed material to the protosolar cloud. Their elemental and isotopic compositions preserve signatures of nucleosynthesis in evolved stars and supernovae, while isotopic variations in primitive minerals and bulk samples provide a broader record of the chemical heterogeneity of the early Solar System. Short-lived radionuclides and their daughter products add a critical chronological dimension, constraining the timing of stellar contributions, formation of the first solids, and subsequent evolution of planetary materials. Together with GCE models, these isotopic records help place the Solar System within the longer history of material cycling through the Galaxy.

An important feature of this history is the non-carbonaceous (NC)–carbonaceous (CC) dichotomy, which reflects distinct isotopic and chemical reservoirs in the protoplanetary disk. Understanding the origin, timing, and persistence of these reservoirs is central to understanding how material was distributed, mixed, and incorporated into planetesimals. Coupled stable isotope, radiogenic isotope, and short-lived radionuclide systematics in meteorites and returned samples provide constraints on the establishment and evolution of these reservoirs. Their mineral-scale distributions further allow the history of refractory inclusions, chondrules, presolar grains, matrix material, secondary phases, and organic matter to be investigated within their original contexts.

These questions can now be addressed using a broad range of complementary laboratory techniques. SEM, EPMA, and TEM reveal textures, mineralogy, elemental compositions, crystallography, and nanoscale features. Raman, micro-FTIR, XANES, and AFM-IR provide information on mineral structure, bonding, oxidation state, and organic molecular characteristics, while Auger spectroscopy enables localized surface chemistry to be investigated. High-resolution isotopic measurements using SIMS, NanoSIMS, and TOF-SIMS, together with bulk and compound-specific measurements by IRMS, connect these chemical and mineralogical observations to isotopic provenance and chronology. The integration of these approaches is particularly powerful for heterogeneous materials in which the history of an individual grain is encoded in both its composition and its immediate surroundings.

Organic matter provides another important link between interstellar chemistry and the early Solar System. Its molecular, elemental, and isotopic characteristics, considered together with mineralogical context, can help distinguish material inherited from the interstellar medium from compounds formed or modified during disk and parent-body processing. Such studies provide insight into how carbon-bearing material was incorporated into planetesimals and how much of the early chemical inventory survived subsequent processing.

Together, meteorites and sample returns allow us to follow Solar System material from stellar sources, through the protosolar cloud and protoplanetary disk, to planetesimals, while linking its provenance to a progressively better-constrained chronology. The combination of presolar grains, stable and radiogenic isotopes, short-lived radionuclides, organic matter, and high-resolution laboratory analyses is moving cosmochemistry toward an integrated view of how the mineralogical, isotopic, and chemical diversity of the Solar System was assembled, processed, and preserved.

BEYOND THE SOLAR NEIGHBORHOOD: A NEW PERSPECTIVE ON PRESOLAR GRAIN ORIGINS

Antariksha Mitra[1,2] and Kuljeet Kaur Marhas[1],
[1] Physical Research Laboratory, Ahmedabad, Gujarat, 380009, India (antarikshamitra@prl.res.in) ,
[2] Indian Institute of Technology Gandhinagar, Palaj, Gandhinagar, Gujarat, 382055, India.

Presolar grains provide direct records of stellar nucleosynthesis and the chemical conditions of the interstellar medium (ISM) before the formation of the Solar System. Their isotopic compositions are generally interpreted in terms of the stellar sources from which they originated. Mainstream (M) SiC grains are predominantly associated with low- and intermediate-mass asymptotic giant branch (AGB) stars, while the Y and Z populations are generally associated with low-metallicity AGB stars. X grains are linked to core-collapse supernovae (CCSNe), whereas the AB, C, D, N, and U populations are associated with different stellar sources and nucleosynthetic conditions based on their characteristic C, N, Si, Ti, and other isotopic signatures. Presolar oxide and graphite grains also provide isotopic evidence from a range of stellar environments and nucleosynthetic processes. However, the material from which these parent stars formed had already been enriched by earlier generations of stars. Galactic chemical evolution (GCE) can therefore modify the initial isotopic composition of a star before its own nucleosynthetic evolution. Presolar grains may consequently preserve information not only about their parent stars, but also about the Galactic environment in which those stars were formed (Alexander & Nittler 1999).

We investigate this possibility using a spatially and temporally resolved Markov Chain Monte Carlo Galactic Chemical Evolution (MCMC-GCE) model that follows the evolution of elemental and isotopic abundances across the Galactic disk. The model incorporates a time- and Galactocentric-radius-dependent evolving initial mass function (IMF), constrained by the energy and metallicity conditions of the evolving ISM. The chemical evolution is coupled to stellar enrichment from the major nucleosynthetic sources, including AGB stars, CCSNe, and binary and massive-star nucleosynthesis (BMSN), using mass- and metallicity-dependent stellar yields. The model therefore allows us to follow how the isotopic composition of the ISM changes with both Galactocentric radius and Galactic time, and how this changing composition is inherited by subsequent generations of stars.

We use the predicted isotopic evolution to investigate the Galactic origin of different presolar grain populations, with particular emphasis on SiC grains including M, X, Y, Z, AB, C, D, N, and U populations, together with presolar oxides and graphite. Their measured isotopic compositions are compared with the model predictions to examine whether the different populations can be associated with particular ranges of Galactocentric radius, metallicity, and formation epoch. For the mainstream population, we investigate whether the observed isotopic spread can be understood in terms of the different Galactic environments from which their AGB progenitors originated. For the Y and Z populations, we examine their relation to the lower-metallicity regions and earlier stages of Galactic chemical evolution. The X population is considered in the context of the isotopic signatures produced by massive-star nucleosynthesis and CCSNe, while the AB, C, D, N, and U populations are examined to determine whether their distinct isotopic characteristics can also be related to differences in their Galactic birth environments.

This comparison allows us to examine whether the isotopic signatures traditionally used to identify the stellar sources of presolar grains also contain information about where and when their progenitor stars formed in the Galaxy. In this way, presolar grains can be studied not only as records of stellar nucleosynthesis, but also as potential tracers of the spatial and temporal chemical evolution of the Milky Way before the formation of the Solar System.

References:

[1] Antariksha Mitra and Kuljeet Kaur Marhas (2026), *The Astrophysical Journal* 1008 - 140

[2] Kuljeet K. Marhas, Manish N. Sanghani, Scott R. Messenger, Antariksha Mitra, and Ritesh K. Mishra (2026),
The Astrophysical Journal 997 - 275.

[3] Larry R. Nittler, Conel M. O'D. Alexander (1999), *The Astrophysical Journal* 526 - 249.

FROM STARDUST TO SUPERNOVAE: AN INTEGRATED 1D-3D NUCLEOSYNTHETIC MIXING FRAMEWORK FOR TRACING THE ORIGIN OF PRESOLAR GRAINS

Divyadharsini. R[1] and Kuljeet Kaur Marhas[1]
[1]Physical Research Laboratory, Navrangpura, Ahmedabad, Gujarat 380009 (divyadharsini@prl.res.in)

Introduction: Presolar silicon carbide (SiC) grains of Type X are rare stardust remnants from core-collapse supernovae(CCSN) ejecta, accounting for 1-2% of the total presolar SiC recovered from the primitive meteorites. These grains carry anomalous isotopic signatures relative to solar values (large $^{12}C/^{13}C$ and $^{14}N/^{15}N$ variations, enrichment in ^{28}Si, and depletion of ^{29}Si and ^{30}Si) and provide direct laboratory evidence of stellar nucleosynthesis, its evolution and the chemical enrichment of galaxies. Identifying their stellar sources is therefore essential for understanding the origin and evolution of cosmic dust.[1-4]

Methodology: We investigate the supernova origin of presolar SiC X grains by correlating the measured isotopic ratios from NanoSIMS with the post explosion data of core-collapse supernova nucleosynthesis models (1D and 3D) greater than $8M_{\odot}$. The 1D models include a huge range of progenitor masses, metallicity and explosion energy together with large nuclear networks that deliver precise, zone-resolved isotopic yields, yet they require artificial "ad-hoc" mixing of onion-shell layers that are contrary to multi-dimensional simulations and remnant observations. With the piston driven/thermal bomb explosion method, the 1D models systematically have a mismatch with the electron fraction, temperature histories and neutrino processing of the innermost ejecta. Conversely, the 3D models capture the self-consistent hydrodynamic mixing, stochastic Ye (electron fraction) evolution and long-lived post-bounce accretion that produce realistic clump-scale compositions and compatible with the observations, but remain too computationally expensive for the largest reaction networks.[5-11]

Using the 3D trajectories and ejecta abundance to calibrate the post explosion data of 1D models would yield physically plausible mixing recipes, improved inner-ejecta conditions and multi-element isotopic predictions that can be tested simultaneously against individual grains, while still allowing statistical exploration of progenitor masses. The limitations also include the different physics and codes that have been used to simulate the 1D and 3D explosions of the same progenitor mass.

We developed an integrated modeling framework that combines one-dimensional stellar nucleosynthesis mixing calculation with validation from three-dimensional ejecta abundance and tracer particle analysis to unravel the possible stellar origins of X grains, while keeping the existing limitation in mind. The correlation is performed in two modes by adopting a hybrid optimization scheme to solve the multi-zone mixing problem, minimizing χ^2 while satisfying physical constraints ($\sum x = 1$; $C/O \geq 1$) to reproduce the measured C, N, Si, and S isotopic ratios.

Results and Discussion: The results demonstrate that observed isotopic signatures can be reproduced within analytical uncertainties, with stable mixing solutions across Monte Carlo realizations. Thus, our study contributes to a better understanding of the connection between stellar explosions and the formation of stardust. By integrating laboratory isotopic data with theoretical models, this work helps constrain the stellar environments responsible for presolar grain formation and provides insights into the nucleosynthetic processes that govern the origin and evolution of cosmic dust.

References: [1] Hoppe P. and Zinner E. (2012) *LPS XXXXIII*, Abstract #1659. [2] Hoppe et al. (2015) Meteoritics & Planetary Science , 50(6), 1122–1132. [3] Xu et al. (2015) The Astrophysical Journal , 799(2), 156. [4] Liu, Nan, et al. (2024) Space Science Reviews, 220(8), 88. [5] Liu, Nan, et al. (2024) The Astrophysical Journal Letters, 961(1), L22. [6] M., Bradley S., et al. Meteoritics 30.3 (1995): 325-334. [7] Yoshida, Takashi. The Astrophysical Journal 666.2 (2007): 1048 [8] Wang, T., & Burrows, A. (2024) The Astrophysical Journal, 962(1), 71. [9] Pignatari, Marco, et al. The Astrophysical Journal Letters 771.1 (2013): L7. [10] Wang, T., & Burrows, A. (2024) The Astrophysical Journal, 969(2), 74. [11] Imasheva, L., Janka, H. T., & Weiss, A. (2025) Monthly Notices of the Royal Astronomical Society, 541(1), 116-134.

ELEMENTAL AND OXYGEN ISOTOPE COMPOSITION OF CM METEORITE CONSTITUENTS: CONSTRAINTS ON ORIGIN OF SOLAR SYSTEM. **G. SRINIVASAN**[1], N.G. Rudraswami[2]. [1]Centre for Space Sciences and Earth Habitability, Bhopal 462016, India, [2]National Institute of Oceanography, Dona Paula, Goa 403004, India. [1]gopalan.srinivasan@gmail.com, [2]rudra@nio.org

The exploration of the near-Earth asteroids Ryugu and Bennu in recent years have increased our understanding of the links between carbonaceous chondrites and their parent bodies; Ryugu is a C-type asteroid [1] and Bennu is a B-type and with a hydrated surface [2]. In the Main Belt Asteroids population nearly 13% of all the classified asteroids are C complex asteroids [3,4] and majority (~60%) of this C complex are B, C, Cb, Cg, Cgh and Ch type asteroids showing evidence for hydrated silicates in their spectral signatures [5]. The most abundant member of the carbonaceous chondrite (CC) group are the CM (type meteorite Mighei) chondrites [6]. CM meteorite fragmentsare recognized as xenoliths in CCs groups and other meteorite classes, due to their widespread dispersal or high abundance in the main belt (e.g., [7-8]. This increases their importance for understanding the formation and evolution of the early Solar System and as sources of volatiles to Earth [9]. The CM and CI group of meteorites have undergone intense degrees of aqueous alteration such that their mineralogy is dominated by secondary minerals, e.g., phyllosilicates, carbonates, and oxides [10-11], however, processes resulting in their formation are poorly constrained. Some CM meteorites have undergone low to mild thermal metamorphism (e.g., [12-14]). The various degrees of aqueous alteration are characterised by sub-dividing petrologic group from 3.0 to 2.0 for increasing alteration (e.g., [15-17]. Some are almost completely altered assigned a subtype 2.0 which was earlier classified as CM1 [15-16]. Most CM chondrites are of petrologic type 2 (e.g., [18]. The aqueously altered products of CM meteorite primary matrix and fine grained rims constitute ~ 56-91 vol % of bulk rock in CM meteorites [19-20]. The phases most vulnerable to alteration such as mesostatis glass in chondrules, amorphous material in matrix and melilite in refractory inclusions are preserved only in few mildly altered CMs such as Paris, and Jbilet Winselwan. One way to investigate the early stages of aqueous alteration is to study some of the least altered CM chondrites, e.g., Paris meteorite (e.g., [21- 23]. The less altered lithologies have oxygen isotope composition - as low as d17O = –2.1‰ and d18O = 2.4‰, comparable to the lower end of a linear trend defined by Paris subsamples and bulk CM2 chondrites [21].

Studies of Mukundpura meteorite - fall (June 6, 2017) showed that bulk of the meteorite was matrix 70 vol. %, followed by chondrules (15 vol. %) and refractory inclusions (2 vol. %). Based on mineral-chemical composition Mukundpura was classified as CM2.0 (CM1) chondrite [22-23]. Mukundpura samples have been measured for bulk oxygen isotope composition using standard procedures at Institute of Meteoritics, UNM [24]. The oxygen isotope composition of Mukundpura is different from the general trend shown by other CM chondrites but comparable to Cold Bokkeveld and Sutter Mill is to the right of the Mukundpura trend. It has been observed for that oxygen isotope values of CM meteorite Ca-carbonate values plot above and below the TFL while the bulk values generally plot below the TFL and intersect the CCAM line [25]. As noted earlier the bulk CO-CM-Matrix-carbonate lines are parallel to the CM meteorite-water (CMW) line. Using mass balance equations and some constraints the CM water rock ratio for several meteorites is estimated ~ 0.3-0.4; and similar for water rock ratio in Mukundpura. The water rock ratio has bearing on the formation zones of CC meteorites [26]. The less altered lithology of Paris thus offers a unique opportunity to investigate the origin and petrogenesis of the CM meteorite and its important constituent such as the chondrules; on the other hand the more altered sample such as Mukundpura gives an opportunity to study the effect of this alteration on its lithologies and constituents.

References: [1] Kitazato K. et al. (2019) *Science* **364**, 272–275. [2] Hamilton V.E. et al. (2019) *Nat. Astron* **3**, 332–340. [3] Cloutis E. A., et al. (2011) *Icarus* **216**, 309–346. [4] DeMeo F. E., et al. (2009) *Icarus* **202**, 160–180. [5] Burbine T. H. (2017) Asteroids: Astronomical and Geological Bodies. Cambridge University Press, 367 pp. [6] Weisberg M. K., McCoy T. J., and Krot A. N. (2006) In Meteorites and the Early Solar System II pp. 19-52. [7] Zolensky M.E. et al., (1996) Meteoritics and Planetary Science 31, 518–537. [8] Gounelle M., et al. (2003) Geochim. Cosmochim. Acta 67, 507-527. [9] Alexander C. M. O'D., et al. (2012) *Science* **337**, 721–723. [10] Busemann H., et al. (2007) Meteor. Planet. Sci. 42, 1387-1416. [11] Schrader D. L. and Davidson J. (2017) Geochim. Cosmochim. Acta 214, 157-171 [12] Nakamura T. (2005) J. Mineral. Petrol. Sci. 100, 260-274. [13] Kimura M., Grossman J. N., and Weisberg M. K. (2011) Meteorit. Planet. Sci. 46, 431-442. [14] Tonui E. et al., 2014) Geochim. Cosmochim. Acta 126, 284-306. [15] Zolensky M.E. et al., (1997) Geochim. Cosmochim. Acta 61, 5099–5115. [16] Rubin A.E. et al. (2007) Geochim. Cosmochim. Acta 71, 2361–-382. [17] Rubin A.E. (2015) Meteorit. Planet. Sci. 50, 1595-1612. [18] Zolensky M. E., Barrett R., and Browning L. (1993) Geochim. Cosmochim. Acta 57, 3123–3148. [19] Howard K. T., et al. (2011) *Geochim. Cosmochim. Acta* **75**, 2735–2751. [20] King A. J., et al. (2017) *Meteorit. Planet. Sci.* **52**, 1197–1215. [21] Hewins R.H. et al., (2014) Geochim. Cosmochim. Acta 124, 190-222. [22] Ray, D. and Shukla, A. D. (2018). *Planetary and Space Science* **151**: 149. [233] Rudraswami, N. G., et al. (2019) *Geoscience Frontiers* **10**: 495–504. [24] Potin, S., et al. (2020) *Meteoritics*

& Planetary Science **55**: 1681–96. [25] Sharp, Z.D., et al. (2016) *Geochimica et Cosmochimica Acta* **186**, 105-119. [26] Marrocchi Y. et al. (2018) *Earth and Planet. Sci. Lettt.* **482** 23-32

CHARACTERIZATION OF NANOGLOBULE-LIKE ORGANICS IN MUKUNDPURA (CM2): A COORDINATED NANOSIMS-HRTEM STUDY

S. Natrajan[1] and K. K. Marhas[1], [1]Physical Research Laboratory, Ahmedabad, Gujarat -380009
(shreeya@prl.res.in)

Introduction: Chondritic insoluble organic matter (IOM) is structurally heterogeneous at the nanoscale, comprising a dominant, disordered "fluffy" polyaromatic matrix and a minor population of discrete, often hollow, nanoglobules [1]. Nanoglobules are widely interpreted as tracers of either icy-grain UV/cosmic-ray photoprocessing [2] or aqueous formose-type polymerization [3], and their isotopic anomalies (D, ^{15}N enrichments) are commonly attributed to interstellar or pre-accretionary chemistry. Extreme ^{13}C-depleted "coldspots", the isotopically anomalous counterpart to D/^{15}N anomalies provide complementary insights into its origin and evolution. While bulk IOM in CM chondrites typically exhibits δ^{13}C values ranging from -20‰ to +30‰ relative to terrestrial values (Vienna Pee Dee Belemnite, VPDB) [4] , submicron-scale analyses reveal heterogeneities with localized enrichments (δ^{13}C > +100‰, hotspots) and depletions (δ^{13}C < -50‰, coldspots) [5-6]. However, although very rare, extremely depleted grains have been found in unaltered CM chondrites (~ -400‰, [7]) and IDPs (-200 ± 41‰, [8]). These ^{13}C anomalies may reflect kinetic isotope effects in molecular clouds, photochemical fractionation of CO ice in protoplanetary disks, and thermal processing of organic precursors during parent-body alteration [9–11]. The preservation of both ^{13}C-enriched and depleted domains suggests an incomplete homogenization of isotopically distinct organic reservoirs during solar system formation. To delineate the origin of the coldspots and to evaluate their morphological associations, correlated NanoSIMS HRTEM analyses of extracted insoluble organic matter was undertaken

Methods: Insoluble organic matter extracted from three CM chondrites namely, Murchison (CM2.5), Murray (CM2.4) and Mukundpura (CM2.0) were analyzed for C-N isotopic systematics using the NanoSIMS at Physical Research Laboratory, Ahmedabad, India and IPREM, Pau, France. The same regions were further probed using HRTEM at SAIF, IIT Bombay, India.

Results and Discussion: High-resolution NanoSIMS mapping of insoluble organic matter (IOM) extracted reveals extreme ^{13}C-depletions, with δ^{13}C as low as~ -500‰ in Murray, -257‰ in Murchison and -300‰ in Mukundpura. The majority of "^{13}C-coldspots" exhibit spatial decoupling from ^{15}N-anomalies and aromatic-rich domains.

HRTEM analysis was conducted on a few ^{13}C depleted region of Mukundpura (Fig. 1) We observe hollow nanoglobule in these regions. Fringe analysis indicates that these are likely composed of disordered polyaromatic units with amorphous carbon nano particles. This morphology is coupled with turbostatic lattice fringes and/or sheet like expanded PAH clusters (d=0.2-0.28 nm aromatic in-plane, 0.34-0.38 nm interlayer), distinct from diffuse IOM matrix, which likely formed by aromatization of presolar organic ices, with ^{13}C-depletions exceeding bulk IOM by five times and rivaling IDP extremes (-200‰, [8]).

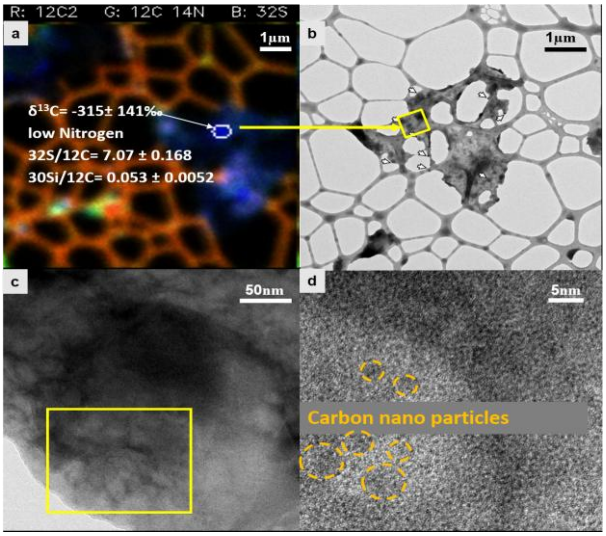


Fig 1: a) NanoSIMS isotope RGB image for Mukundpura region of interest (ROI). b) Bright field image for the ROI. White arrows denote nanoglobule like features.c,d) High resolution TEM image of the selected cold spot.

This suggests that the nanoglobules could likely represent primordial condensates that survived aqueous alteration. These findings demonstrate heterogeneous presolar organic reservoirs also contribute to the Solar System carbon inventory, with selective alteration revealing refractory ^{13}C-depleted carriers as faithful tracers of molecular cloud chemistry.

References: [1] Garvie L.A.J. and Buseck P.R. (2004) *Earth and Planetary Science Letters*, 224, 431–439. [2] Nakamura-Messenger K. et al. (2006) *Science*, 314, 1439–1442. [3] Cody G.D. et al. (2011) *Proceedings of the National Academy of Sciences. U.S.A*, 108, 19171–19176. [4] Alexander C.M.O'D. et al. (2007) *Geochimica et Cosmochimica Acta*, 71, 4380–4403 [5] B.T. De Gregorio, et al., *Meteoritics & Planetary Science*. **48**, 904–928 (2013). [6] L. R. Nittler, et al., *Astrophysical Journal*. 682(2), 1450-1478 (2008). [7] L. R. Nittler, et al., *84th Annual Meeting of The Meteoritical Society* 2021 (LPI Contrib. No. 2609). [8] J.Davidson et al., *Geochimica et Cosmochimica Acta*. **277** ,377-406. (2020) [9]Y. Furukawa et al., *Science Advances*. **7** (2021) [10]W.M. Lawrence et al., *Proceedings of the National Academy of Sciences. U.S.A.* **122** (24) (2025) [11]A.N. Heays et al., *Astronomy & Astrophysics*. **562**, A61 (2014).

NANOSCALE CARBON AND NITROGEN ISOTOPIC ANOMALIES IN INSOLUBLE ORGANIC MATTER FROM THE NORTON COUNTY AUBRITE AND PARSA ENSTATITE CHONDRITE: A NANOSIMS–HRTEM STUDY

Neha [1,2], K.K. Marhas[1], and S. Natrajan[1]
[1]Physical Research Laboratory, Ahmedabad, Gujarat 380009,
[2]Gujarat University, Ahmedabad, Gujarat 380009

Introduction: Insoluble organic matter (IOM) preserves carbon and nitrogen isotopic and structural signatures inherited from interstellar, nebular, and parent-body processes [1, 2]. While such heterogeneities, including ^{15}N- and ^{13}C-anomalous "hotspots" and "coldspots," are well documented in carbonaceous chondrite IOM [3,4], the enstatite meteorite clan remains comparatively unexplored at the sub-micron scale. Enstatite meteorites formed under highly reducing conditions in the inner Solar System and comprise both enstatite chondrites, which preserve primitive textures modified by thermal metamorphism, and aubrites, differentiated achondrites. This contrast makes the enstatite clan a unique testbed for evaluating the survival of organic matter across the primitive-to-differentiated transition. Here we present a coordinated NanoSIMS carbon and nitrogen isotopic survey combined with HRTEM lattice-fringe characterisation of IOM extracted from the Norton County aubrite and its chondritic analogue, Parsa (EH3), to evaluate whether isotopically anomalous organic carriers are indigenous to the aubrite parent body or reflect exogenous, chondritically derived material incorporated after differentiation.

Methods: Extracted IOM residues from the Norton County aubrite and Parsa (EH3) enstatite chondrite were analyzed by NanoSIMS ion imaging for $^{12}C^-$, $^{12}C_2^-$, $^{12}C^{13}C^-$, $^{12}C^{14}N^-$, $^{12}C^{15}N^-$, $^{30}Si^-$, and $^{32}S^-$ to generate $\delta^{13}C$ and $\delta^{15}N$ isotope ratio maps. Isotopic hotspots and coldspots were defined as regions exceeding the mean composition of each sample's IOM population by more than three standard deviations ($\geq$ mean $\pm$ 3σ), following established criteria [3, 4]. HRTEM imaging was performed on the same or adjacent organic domains to measure the (002) interlayer d-spacing and fringe length, thereby classifying the carbon nanostructure as amorphous, poorly graphitised/turbostratic, or highly graphitic/lamellar.

Results and Discussion: NanoSIMS analyses reveal pronounced nanoscale carbon and nitrogen isotopic heterogeneity in the IOM of both Norton County and Parsa, including extreme $\delta^{13}C$ and $\delta^{15}N$ anomalies. A distinct $\delta^{13}C$ coldspot (-300 ± 17‰) is observed in Norton County; neither sample shows the opposite anomaly, a pattern not previously reported within the enstatite meteorite clan. Both samples additionally preserve multiple discrete $\delta^{15}N$ hotspots, reaching roughly 1,800–1,900‰ in Parsa and several thousand per mil in Norton County. Despite the very low IOM abundance in Parsa and Norton County, indicative of extensive thermal processing, its $\delta^{13}C$ values span a range comparable to that reported for Murchison IOM, suggesting that a measurable component of the original IOM isotopic signature has survived the intense thermal processing the meteorite parent body experienced. HRTEM observations further reveal relatively ordered carbon structures, more comparable to or exceeding the structural organisation reported for primitive CI/CM IOM, with no consistent relationship between structural ordering and the magnitude of isotopic anomalies. The combined NanoSIMS and HRTEM observations further demonstrate that isotopic anomalies at the NanoSIMS scale can encompass multiple structurally distinct carbonaceous domains, highlighting the heterogeneous nature of the organic carriers at sub-micrometre scales. HRTEM work is ongoing on the Norton County coldspot regions to test for hollow nanoglobules with turbostratic fringes analogous to presolar aromatic cores in CM chondrite coldspots [5,6&7], which would be the first such identification in the enstatite clan. The persistence of extreme nitrogen anomalies in the aubrite, comparable to its chondritic precursor, is consistent with the incorporation of anomalous organic carriers after differentiation, potentially via late accretion of chondritic material, though an indigenous origin cannot be excluded. Combined isotopic, elemental, and structural results constrain the extent to which primitive organic reservoirs are preserved, modified, or exogenously introduced during differentiation

References: [1] Alexander C. M. O'D., Fogel M., Yabuta H., and Cody G. D. (2007) Geochim. Cosmochim. Acta 71:4380–4403. [2] Alexander C. M. O'D, Cody G. D., De Gregorio B. T., Nittler L. R., and Stroud R. M. (2017) Chemie der Erde Geochemistry 77:227–256. [3] Floss C., Le Guillou C., and Brearley A. (2014) Geochim. Cosmochim. Acta 139:1–25. [4] Matrajt G., Messenger S., Brownlee D., and Joswiak D. (2012) Meteoritics & Planetary Science 47:525–549. [5] Natrajan S. and Marhas K. K. (2026) 88th Annual Meeting of the Meteoritical Society, LPI Contrib. No. 3162, Abstract #5383. [6] Derenne S., Rouzaud J.-N., Clinard C., and Robert F. (2005) Geochim. Cosmochim. Acta 69:3911–3918. [7] Derenne S. and Robert F. (2010) Meteoritics & Planetary Science 45:1461–1475.

THE CONSTRUCT OF SOLAR SYSTEM: DECONSTRUCTED FROM HIGH PRECISION ^{26}Al-^{26}Mg SYSTEMATICS IN METEORITES

R. K. Mishra[1,2] and K. K. Marhas[3], [1]Independent researcher, Village Dhawalpur, Po Kaitha, District Bhagalpur, Bihar, 813211, India, riteshkumarmishra@gmail.com, [2]Ametek Instruments India Pvt. Ltd. Bangalore, Karnataka, [3]Planetary Sciences Division, Physical Research Laboratory, Navrangpura, Ahmedabad, Gujarat, 38009, India.

Introduction: *Major epochs and events determining the grand architecture of any stellar system, including our Solar system, takes place within the first few (0-10 million years) million years of the birth of star* [1-7]. Infra-red, near/sub- infrared and optical astronomy are able to observe disk surfaces, fine dust, and large bodies under fortuitous conditions. However, each of these wavelength regime encounters hard physical limitations imposed by opacity, grain scattering properties, diffraction limits, and thermal emission regimes for the critical growth and evolution phase of solids from 100 microns to a few thousand km sized planetesimals in the protoplanetary disk and *fail to provide any information*.

Meteorites, Methods, and Significance: Fortunately, some of the first forming refractory solar system solids formed during the nascent phase are archived as frozen time capsule in asteroidal belts for 4.56 billion years. These frozen archives recording the diversity of cosmochemical condition, and evolution become available as 'Fall' and 'Find' rocks from space, technically called meteorites. Some of these materials that survived nebular and parent body metamorphism within their parent body can be analyzed using high precision isotopic studies to yield important information about the events and processes 4.5 billion years ago.

In situ studies including the high precision studies using the latest generation analytics has opened the door to obtain very high-resolution (~10 ka) temporal records 4.5 billion years ago [1,4-7]. These isotopic records provide very important results about scale of homogeneity, duration and level of mixing and homogenization of solar system material in addition to evolution of oxygen fugacity, temperature and other cosmochemical conditions in the protoplanetary disk [1-10].

The chronological studies with other isotopic studies present a *new paradigm of a long-lived protoplanetary disk that is rapidly evolving in which the first refractory solids, chondrules, planetesimals and differentiated bodies formed through overlapping and recurrent processes rather than through a single linear sequence*.

References: [1] Villeneuve J. Chaussidon M. and Libourel G. (2009) *Science 325:*985–988. [2] Connelly J. N. et al. (2012) *Science* 338:651-655. [3] Bollard J. et al. (2019) *Geochimica et Cosmochimica Acta 260:*62–83. [4] Mishra R. K. and Chaussidon M. (2014) *Earth and Planetary Science Letters* 390:318-326. [5] Mishra R. K. (2025) *Meteoritics & Planetary Science* 60:2759–2783. [6] Kööp L. et al. (2016) *Geochimica et Cosmochimica Acta* 184:151-172. [7] Kita N. T. et al. (2013) *Meteoritics & Planetary Science 48:*1383–1400. [8] Li H. et al. (2026) *Proceedings of National Academy of Science* 123:(29) e2529765123. [9] van Kooten E. et al. (2026) *Nature Astronomy* 10: https://doi.org/10.1038/s41550-026-02927-1. [10] Siron et al. (2022) *Geochimica et Cosmochimica Acta 324*:312–345.

ORIGIN AND EVOLUTION OF ENIGMATIC CORUNDUM INCLUSIONS IN THE BHUKA IAB IRON METEORITE: INSIGHTS FROM ^{26}AL–^{26}MG AND OXYGEN ISOTOPE SYSTEMATICS

A P. Singh, K. K. Marhas, R. K. Mishra, M Wiedenbeck, M. N. Sanghani ([1]Physical Research Laboratory, Ahmedabad, Gujarat, India, ankitprakash@prl.res.in)

Introduction: Iron meteorites are the cores of differentiated planetesimals and constitute a major category within the broader classification of meteorites [1]. The IABs are also called the silicate-bearing groups, as the primary inclusions within these classes are: sulfide inclusions, nonchondritic silicate inclusions, chondritic silicate inclusions, graphite-rich and phosphate-rich inclusions. The chondritic silicate inclusions further contain olivine, low-Ca pyroxene, high-Ca pyroxene, plagioclase, phosphates, sulfides and metals [2]. The silicate inclusions from IAB can also contain rare phases like sphalerite, K-feldspar, and, here, corundum. Corundum (Al_2O_3) is believed to be the first refractory mineral to condense from a gas having a solar composition (T_{cond} = 1770 K at $P_{tot} = 10^{-3}$ atm) according to thermodynamic equilibrium models [3]. Corundum is one of the least abundant phases amongst all the refractory phases in the Calcium- Aluminium rich inclusions (CAIs), Ameboid-Olivine Aggregates (AOAs) and fragmented remains, even within the chondrites, despite its early formation. A single piece of an iron meteorite (2.42 kg) fell on the 25th June 2005 in Bhuka village, Barmer district, Rajasthan, India [4]. The morphology, micro-texture, modal abundance, metallography, petrology and mineral chemistry of Bhuka have been described previously and is classified as a low-nickel IAB ungrouped iron meteorite [5]. The corundum grains are mostly of either presolar origin or represent some of the earliest-forming solids in the Solar System; their occurrence within a differentiated IAB iron meteorite thus presents an enigma. Here, we present the ^{26}Al-^{26}Mg relative chronology and oxygen isotopic compositions of corundum grains from the Bhuka IAB iron meteorite, gaining insights into the origin and their evolution, whether these corundum grains are presolar, solar or of secondary origin.

Methodology: The major elemental quantification analyses were done at the Physical Research Laboratory, Ahmedabad, using JEOL JXA-8530F Plus Hyperprobe. The corundum grains were analysed for ^{26}Al-^{26}Mg isotope systematics using a nanoSIMS 50 secondary ion mass spectrometer at the Physical Research Laboratory, Ahmedabad, India. Three oxygen isotopic compositions of the corundums in the silicate inclusions were carried out using a large geometry Secondary Ion Mass Spectrometer (LG-SIMS) 1280 HR at GFZ Helmholtz Zentrum for Geoforschung at Potsdam, Germany.

Results and Discussion: The silicate-graphite inclusion in the Bhuka IAB, containing corundum grains, was examined and was named based on its morphological resemblance to familiar shapes: designated as Butterfly, while the others were named for their likeness to a human Foot and Calf. ^{26}Al-^{26}Mg isotopic measurements of corundums within the silicate inclusions show a range in magnesium isotopic ^{26}Mg/^{24}Mg composition from near chondritic (0.13932) to suprachondritic (0.146). The grains yielded ^{26}Al/^{27}Al ratios of (5.2 ± 2.1) × 10^{-5}, (4.6 ± 2.5) × 10^{-7}, and (0.1± 1.7) × 10^{-7}. These grains exhibit distinct but variable oxygen isotopic compositions, with $\delta^{18}O_{SMOW}$ values ranging from -19.4 to -7 ‰, and $\Delta^{17}O$ values ranging from -13‰ to -9 ‰. The observed ratios of ^{26}Al/^{27}Al in the corundum-bearing silicate-graphite inclusions are consistent with the bimodal distribution previously reported from micron sized (<10 μm) corundum grains recovered from the acid residues of chondrites. The two orders of magnitude variation in ratio of ^{26}Al/^{27}Al, but with similar ^{16}O-rich ($\Delta^{17}O \sim -11$‰) composition in the three corundum inclusions can be best explained if these grains having formed in an early homogenous ^{26}Al/^{27}Al, ^{16}O rich reservoir were metamorphosed to varying degrees. Alternatively, the grains could also have incorporated a variable amount of ^{26}Al from the injected refractory dust towards the end of the infall stage only then to be ejected outwards by the dynamics of the evolving protoplanetary disk. These inclusions were incorporated in a very brief period of time of only ~0.3-5 Ma, into the IAB type parent body of Bhuka.

References: [1] Jacquet, E., Dullemond, C., Drążkowska, J., & Desch, S. (2024), *Space Science Reviews*, *220*(7), 78. [2] Benedix, G. K., McCoy, T. J., Keil, K., & Love, S. G. (2000), *Meteoritics and Planetary Science*, *35*(6), 1127–1141. [3] Ebel, D. S., & Grossman, L. (2000), *Geochimica et Cosmochimica Acta*, *64*(2), 339–366. [4] Shrivastava, K. L., Gaur, V., Swadia, J., Bhandari, N., & Shukla, A. D. (2005), *Current Science*, *89*(5), 741–742. [5] Murty, S. V. S., Ranjith, P. M., Ray, D., Ghosh, S., Chattopadhyay, B., & Shrivastava, K. L. (2016), *Planetary and Space Science*, *131*, 119–127.

STABLE ISOTOPE VARIATIONS OF MAJOR ELEMENTS IN PLANET FORMING MATERIALS

Yogita Kadlag[1]
[1]Geosciences Division, Physical Research Laboratory, Navrangpura, Ahmedabad 380009 (yogita@prl.res.in)

Abundances and isotopic compositions of major rock-forming elements, such as Fe, O, Si, and Mg in Earth, meteorites and other planetary materials provide valuable information on the formation and evolution of the protoplanetary disk and the subsequent accretion and differentiation of planetary bodies [1-7]. The accretion and physicochemical processing of dust and gas in the first few million years of the Solar System ultimately shaped the chemical and isotopic composition of planetary bodies. With advanced, high-precision analytical techniques such as MC-ICP-MS, isotopic ratios of Fe, Si, and Mg can be measured with external precision on the order of tens of parts per million (ppm), depending on the isotope system and analytical approach. Primitive meteorites and their components exhibit measurable, often per-mil scale, variations in the stable isotope compositions of major elements. These anomalies are attenuated at the bulk-scale and amplified at smaller spatial scales. Individual components of chondrites, such as refractory inclusions, chondrules, and matrix exhibit substantially larger Si-isotopic anomalies than bulk chondrites [8-13]. Mineral- and component-scale Si-isotope heterogeneity among chondritic components reveals substantial isotopic variability, with δ^{30}Si values ranging from ~ -8 ‰ and ~ 34 ‰ [9, 13]. These results place an upper limit of ~ 8 wt % on the Si content of the Earth's core and suggests that the compositions of terrestrial planets can be derived from variable proportions of chondritic components. Overall, Si-isotope variations in planetary materials suggests that solid-melt-gas fractionation during condensation, high-temperature processing of nebular dust, as well as accretion and planetary differentiation shaped the isotopic composition of planets.

Acknowledgments: I would like to acknowledge Prof. Harry Becker, Prof. Friedhelm von Blanckenburg, Dr. Daniel A. Frick, and Dr. Michael Tatzel for their support and assistance in acquiring the Si stable isotope data used in [8, 9, 11].

References [1] Clayton R. N. and Mayeda T. K. (1996) *Geochimica et Cosmochimica Acta* 60:1999–2017. [2] Poitrasson F., Halliday A. N., Lee D. C., Levasseur S., and Teutsch N. (2004) *Earth and Planetary Science Letters* 223:253–266. [3] Weyer S., Anbar A. D., Brey G. P., Münker C., Mezger K. and Woodland A. B. (2005) *Earth and Planetary Science Letters* 240:251–264. [4] Wiechert U. and Halliday A. N. (2007) *Earth and Planetary Science Letters* 256:360–371. [5] Armytage R. M. G., Georg R. B., Savage P. S., Williams H. M. and Halliday A. N. (2011) *Geochimica et Cosmochimica Acta* 75:3662–3676. [6] Pringle E. A., Savage P. S., Badro J., Barrat J.-A. and Moynier F. (2014) *Proceedings of the National Academy of Sciences of the United States of America* 111:17029–17032. [7] Dauphas N., Poitrasson F., Burkhardt C., Kobayashi H. and Kurosawa K. (2015) *Earth and Planetary Science Letters* 427:236–248. [8] Kadlag Y., Tatzel M., Frick D. A., Becker H. and Kühne P. (2019) Chondrule-Matrix Complementarity in the Allende CV3 Chondrite – A Si Isotope Perspective. *Lunar and Planetary Science Conference*, Abstract #1092. [9] Kadlag Y., Tatzel M., Frick D. A., and Becker H. (2019) *Geochimica et Cosmochimica Acta* 267:300–321. [10] Villeneuve J., Marrocchi Y., and Jacquet E. (2020) *Earth and Planetary Science Letters* 542:116318. [11] Kadlag Y., Tatzel M., Frick D. A., Becker H. and Kühne P. (2021) *Geochimica et Cosmochimica Acta* 304:234–257. [12] Martins R., Chaussidon M., Deng Z., Pignatale F., and Moynier F. (2021) *Earth and Planetary Science Letters* 554:116678. [13] Marin-Carbonne J., McKeegan K. D., Davis A. M., and MacPherson G. J. (2023) *Meteoritics & Planetary Science* 58:546–571

C, H, AND N ISOTOPIC STUDIES OF C2 AND C1-TYPE CLASTS FROM A POLYMICT UREILITE BRECCIA.

S. Swain[1,2], J. Aleon[3], M. Verdier-Paoletti[3], M. Patzek[4], R. R. Mahajan[5], S.S. Rout[1,2]

[1]National Institute of Science Education and Research, Bhubaneswar, Jatni, Khurdha, Odisha, India, 752050. [2]Homi Bhabha National Institute, Training School Complex, Anushaktinagar, Mumbai, India. [3]Institut de Minéralogie, de Physique des Matériaux et de Cosmochimie, Sorbonne Université, Museum National d'Histoire Naturelle (MNHN), CNRS UMR 7590, IRD, 75005 Paris, France, [4]Institut für Planetologie, University of Münster, Wilhelm-Klemm-Straße 10, 48149 Münster, Germany. [5]Planetary Sciences Division, Physical Research Laboratory, Ahmedabad, Gujarat, India, 380009.

*subhasmita.swain@niser.ac.in

Introduction: Volatile-rich carbonaceous clasts in meteoritic breccias are invaluable samples for understanding the distribution and mixing of volatile-rich reservoirs in the early solar system [1-6]. These clasts are known to preserve primitive solar system materials in their fine-grained matrices. In several of these clasts, localized hotspots with extreme D and ^{15}N enrichment are observed, which are thought to have formed in cold molecular clouds or in the outer solar system [7]. Additionally, studies indicate that some anomalous clasts are fragments of parent bodies that are not represented in the current meteoritic inventory [2,4]. Here, we present C, H, and N isotope measurements of the mineralogically distinct anhydrous silicate containing "C2" clasts [8], along with a C1 clast in the polymict ureilite sample DaG 1000, to establish relationships with any known meteoritic groups or clasts and to search for isotopic hotspots.

Methods: Polished thin section (PTS) of Dar al Gani (DaG) 1000, a polymict ureilite (pUrei), was used for this study. The isotopic analysis within the clasts was carried out using a Cameca NanoSIMS N50 ion microprobe (Cs+ beam; 16kV) at the Institute of Mineralogy, Physics of Materials and Cosmochemistry (IMPMC), Paris. Analyses were performed in imaging mode on carefully selected 20×20 μm² areas within the matrix, avoiding fractures, silicate inclusions, other mineral phases, and terrestrial alterations. Electron microprobe analysis (EPMA; 15kV, 15nA) of the matrix and mineral phases in clasts was carried out at the Department of Geology, Mineralogy and Geophysics, Ruhr-University Bochum, Germany.

Results & Discussion: The PTS contains two large C2-type clasts, measuring ~1.9 mm (DaG 1000-01) and ~2.3 mm (DaG 1000-02), and one smaller C1 clast of size ~0.8 mm.

The δD values of the C2 clasts range from ~ -240‰ to 175‰ with a clast mean value of ~84±60‰ for DaG 1000-01, and a value of ~2±107‰ for DaG 1000-02. The reported errors are in 1σ. For both clasts, there is no linear correlation between $^{12}C/H$ and bulk δD values, which may reflect intermixture of isotopically heterogeneous organic matter and phyllosilicates. The measured δD values are in the range of the CM-like clasts in HEDs, C1 clasts in ordinary chondrites, and CI, CM chondrites [2,9,10]. The mean bulk $\delta^{13}C$ value of the C2 clast DaG 1000-01 is -29±5‰ with values ranging from -36 to -19‰. The $\delta^{13}C$ value overlaps with those of the C2-clasts in CH/CB, CR chondrites. The mean bulk $\delta^{15}N$ is 3±16‰, with values ranging from -33 to 25‰, which is similar to that of the bulk values of CI, CM, and CR chondrites, and falls within the range of CM-like clasts in HEDs, C-clasts in CH/CB.

We found a ~1 μm SiC grain corresponding to a ^{13}C hotspot, with a $\delta^{13}C$ value of 611±54‰ ($\delta^{15}N$ ~ -294‰, δD ~ -150‰). There are a few micron- to submicron-scale δD hotspots (699 to 2263‰) in the matrix of the C2 clast DaG 1000-01, which have a similar $^{12}C/H$ ratio to that of the bulk meteorite.

The average δD value of the C1 clast is ~ -13 ± 86‰ (N = 4), which is similar to the range for the studied C2 clasts, and much smaller than the range for previously studied pUrei-hosted C1 clasts (i.e., 950 to 3100‰; [2]). Unlike the C2 clasts, there is a linear correlation between the $^{12}C/H$ and bulk δD (R^2=0.85).

Conclusion: The studied C1 clast is isotopically distinct from the pUrei-hosted C1 clasts, suggesting a diversity in the sources of carbonaceous material accreted by pUrei. All three studied clasts show broad isotopic similarity to those of the CI and CM solar system material. The presence of isotopically heterogeneous organic compounds and D-rich hotspot inherited from the molecular clouds implies that at least some of the material's primitive isotopic heterogeneity was preserved even after parent-body processing.

References: [1] Bonal L. et al. (2010) Geochim. Cosmochim. Acta, 74(8): 2500-2522. [2] Patzek M. et al. (2020) Geochim. Cosmochim. Acta 272: 177-197. [3] Zolensky M. and Ivanov A. (2003) Geochemistry 63(3): 185-246. [4] Patzek M. et al. (2025) Meteoritics & Planetary Science 60(5): 1073-1094. [5] Bischoff A. et al. (2006) Meteorites and the early solar system II: 679-712. [6] Rubin A. E. and William F. B. (2009) Meteoritics & Planetary Science 44(5): 701-724. [7] Kebukawa Y. et al. (2019) Sci. Rep. 9(1): 3169. [8] Swain S. et al. (2026, In Press) 10.1111/maps.70245 [9] Kerridge J. F. (1985) Geochim. Cosmochim. Acta 49(8): 1707-1714. [10] Kolodny Y. et al. (1980) Earth Planet. Sci. Lett. 46(2): 149-158.

UNIQUE OLIVINE-RICH VOLATILE-RICH C1 CLASTS IN TWO POLYMICT UREILITES

S. Swain[1,2,*], E. Mugnaioli[3], A. Musolino[3], M. Patzek[4], B. Hofmann[5,6], S. S. Rout[1,2]

[1]National Institute of Science Education and Research, Bhubaneswar, Jatni, Khurdha, Odisha, India, 752050. [2]Homi Bhabha National Institute, Training School Complex, Anushaktinagar, Mumbai, India. [3]Dipartimento di Scienze della Terra, Università di Pisa, Via Santa Maria 53, 56126, Pisa, Italy, [4]University of Münster, Institut für Planetologie, Wilhelm-Klemm-Str.10, 48149, Münster, Germany, [5]University of Bern, Institute of Geology, Baltzerstrasse 1+3, 3012 Bern, Switzerland, [6]Natural History Museum Bern, Bernastrasse 15, 3005 Bern, Switzerland. *subhasmita.swain@niser.ac.in

Introduction: Xenolithic clasts in meteorites are widely found in various chondritic and achondritic host breccias and are important for understanding the distribution and mixing processes of primitive solar system materials [1-4]. Isotopic studies have shown that C1 clasts in polymict ureilites (pUrei) are distinct from any known chondritic groups and represent previously unsampled material [5,6,7]. Here, we show that some pUrei-hosted C1 clasts exhibit a unique aqueous alteration condition indicative of mild thermal metamorphism associated with shock processing. These observations suggest a potentially diverse distribution of the primitive, volatile-rich carbonaceous materials, with variable alteration histories.

Methods: Polished thin sections (PTS) of Northwest Africa (NWA) 14228 and Dar al Gani (DaG) 164 polymict ureilite samples (Institut für Planetologie, University of Münster) were used for this study. Backscattered electron (BSE) imaging and electron probe microanalysis (EPMA; 15kV, 15nA) were carried out at the Department of Geology, Mineralogy and Geophysics, Central Microanalytical Lab, Ruhr-University Bochum, Germany. Raman analysis of the matrix organics was performed using the LabRAM HR Evolution Raman spectrometer (Horiba Scientific) at the Center of Interdisciplinary Sciences, National Institute of Science Education and Research, Bhubaneswar (532 nm, 600 grooves/mm, <0.3 mW). Focused ion beam (FIB) analysis was carried out using a ZEISS Crossbeam 550 dual beam FIB-SEM at the Center for Instrument Sharing of the Università di Pisa (CISUP), in Italy. Scanning-transmission electron microscopy (STEM) imaging, energy-dispersive X-ray (EDX) spectroscopy, selected area electron diffraction (SAED), and three-dimensional electron diffraction were performed at CISUP with a JEOL JEM-F200 multipurpose transmission electron microscope.

Results & Discussion: Five C1 clasts (NWA 14228-02, -04, -07, -10, DaG 164-03) were identified, which contain abundant magnetites with surrounding Fe-rich alteration phases (Fe-alt); the only other occurrences of such phases are found in the C1 lithologies of Almahatta Sitta pUrei [8]. The abundance and morphology of the Fe-alt phases vary among the clasts. The TEM imaging, electron diffraction, and EDS analysis of the phase revealed them to be well-crystalline magnetite grains intermixed with Fe-rich olivine, with minor phyllosilicates in small pockets. In almost all Fe-alt phases, magnetite is selectively present at the center, which suggests olivine to be a secondary phase formed through the alteration of magnetite [9]. Raman studies of matrix organic matter in these olivine-containing clasts confirm an alteration temperature < 300 °C, similar to that of other CI- and CM-like clasts [10]. Neither the Raman spectra nor the mineralogical study indicates widespread heating (~400-600 °C), required for the onset of dehydration-induced olivine formation.

Based on thermodynamic studies [11], a possible formation scenario for the Fe-rich olivine involves precipitation as a secondary phase from an Fe- and Si-rich alkaline aqueous solution at T > 150 °C and W/R~0.1-0.2. In this case, the source for Fe is likely from the dissolution of magnetite, whereas Si was likely released from dissolution of phyllosilicates. Another possibility for the formation of Fe-rich olivine could be the reduction of magnetite grains in the presence of H_2 gas and SiO_2(aq.).

Conclusion: The parent body/bodies of the Fe-rich olivine-containing C1 clasts have undergone mild to moderate thermal processing due to heterogeneous effects of shock processing. During the shock process the temperature increased to 150-250°C, leading to melting of any residual ice and/or release of residual fluid present in pore spaces, dissolution of carbonate, phyllosilicate and magnetite grains, and precipitation of Fe-rich olivine grains around magnetite grains or formation of olivine around magnetite grains through reduction by a H_2 gas.

References: [1] Brearley, A. J. (1992) Geochim. Cosmochim. Acta 56: 1373-1386. [2] Zolensky, M.E. et al. (1996) Meteoritics & Planetary Science 31: 484-493. [3] Patzek, M. et al. (2018) Meteoritics & Planetary Science 53.12: 2519-2540. [4] Ikeda, Y., and Prinz, M. (2001) Meteoritics & Planetary Science 36: 481-499. [5] Patzek, M. et al. (2020). Geochim. Cosmochim. Acta 272: 177-197. [6] Visser, R. et al. (2019) Geochim. Cosmochim. Acta 261: 210-223. [7] Patzek, M. et al. (2025) Meteoritics & Planetary Science 60: 1073-1094. [8] Goodrich, C.A. et al. (2019) Meteoritics & Planetary Science 54: 2769-2813. [9] Swain S. et al. (2026, In Press) 10.1111/maps.70245. [10] Visser, R. et al. (2018) Geochim. Cosmochim. Acta 241: 38-55. [11] Zolotov, M. Y. et al. (2006) Meteoritics & Planetary Science 41.11: 1775-1796.

OXYGEN ISOTOPE CONCENTRATION OF CARBONATE AND OLIVINE GRAINS WITHIN C1 AND CM-LIKE CLASTS IN ACHONDRITIC BRECCIA METEORITES.

N. Thomas[1], S. Bhowmick[2], S.S. Rout[3], [1]Indian Institute of Science Education and Research, Berhampur (neetha21@iiserbpr.ac.in), [2,3]National Institute of Science Education and Research, Bhubaneswar.

Introduction: Volatile-rich dark clasts in chondritic (e.g., CM, CR, CB, ordinary and R chondrites) and achondritic (e.g., HEDs, Ureilites) breccias represent primitive solar system materials and serve as a proxy for understanding early Solar System processes [1,2]. Some of these volatile-rich clasts have a mineralogy similar to that of CI, CM, and ungrouped C2 chondrites and sample materials that formed in the cold outer protoplanetary disc and rare cometary material unrepresented in the present meteorite collection [1,2,3]. The secondary phases within the clasts which precipitated directly from the aqueous fluid provide information about the nature and evolution of fluid within the parent asteroids [4]. Here we report the in-situ oxygen isotope study of carbonate, apatite, magnesite and olivine grains in some C1- and CM-like clasts to understand the nature of aqueous alteration that happened within the parent body of these clasts, compare them with the known processes in CI and CM chondrites and understand the type of volatile-rich materials that were falling/accreting on the parent body of ureilites and HEDs.

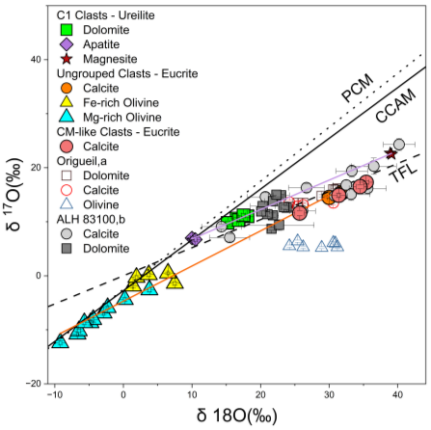


FIGURE 1: Oxygen isotopic composition of C1, ungrouped, and CM-like clasts from Ureilite and Eucrite (bright solid shapes) compared with literature data [5,6]

Samples and Methods: Various dark clasts within the polished thin sections (PTSs) of Northwest Africa (NWA) 7542 (polymict eucrite), NWA 14228 (polymict ureilites), and Sariçiçek (Howardite) were located using optical and JEOL JSM-7001F field emission scanning electron microscope (FE-SEM). Elemental mapping and mineral characterisation were done at 15 kV via energy-dispersive X-ray spectroscopy (EDS). In situ oxygen isotope compositions of the selected phases were subsequently measured via high-resolution secondary ion mass spectrometry with a multi-collector (HRSIMS Cameca IMS-1280).

Results: The oxygen isotopic composition of the calcite and olivine grains from CM-like clasts in polymict eucrite ranges from $\Delta^{17}O$ = -1.7‰ to -1.0‰, and $\Delta^{17}O$= -7.6‰ to $\Delta^{17}O$= -1.3‰. In C1 clasts from polymictic ureilites, dolomite, magnesite, and apatite yield $\Delta^{17}O$ ranges of 1.6‰ to 2.1‰,2.2‰ to 2.5‰, and 1.2‰ to 1.8‰, respectively. The studied secondary minerals within C1 and CM-like clasts plot along or close to the terrestrial fractionation line (TFL), and some others fall on a line with a slope of~0.65. The Mg-rich olivine grains within the unique clast NWA 7452 (X9) are ^{16}O-rich, whereas the Fe-rich olivine replacing them is enriched in ^{18}O and ^{17}O. The calcite within this clast is much more enriched in ^{17}O and ^{18}O.

Discussions & Conclusions: The oxygen isotope data of the secondary minerals from C1 and CM-like clasts analysed in this study overlap with the literature data of secondary phases from the known CI and CM chondrites, capturing the isotopic composition of the fluid which evolved from initially ^{16}O-depleted to progressively more ^{16}O-enriched composition over time. The steeper slopes along which some of the carbonate phases fall relative to the TFL point to precipitation from a fluid that reacted with ^{16}O-rich anhydrous phases. Additionally, the high $^{17,18}O$-enriched signature of the magnesite indicates early precipitation from an isotopically heavier fluid. Some other carbonate grains show constant $\Delta^{17}O$ values and varying $^{17,18}O$ concentrations due to changes in temperature during their formation. The study of carbonate grains shows that the fluid composition (and temperature) within the parent asteroid of the clasts changed with time and its evolution is similar to that seen in CM and CI chondrites.

Acknowledgements: We thank the Centre for Interdisciplinary Sciences (CIS) at the National Institute of Science Education and Research (NISER), Bhubaneswar and Prof. Takuya Kunihiro and group from the Pheasant Memorial Laboratory (PML), Okayama University, especially for their invaluable technical support and guidance.

References: [1] van Kooten, E. et al. (2024) *Science Advances* 10: eadp1613. [2] Patzek, M. et al. (2025) *Meteoritics & Planetary Science* 60: 1073-1094. [3] Bischoff, A. et al. (2006) *Meteorites and the early solar system II*: 679-712. [4] Suttle, M. D., et al. (2021) *Geochimica et Cosmochimica Acta* 299: 219-256. [5] Piralla, M. et al. (2020) *Geochimica et Cosmochimica Acta* 269: 451-464. [6] Telus, M., et al. (2019) *Geochimica et Cosmochimica Acta* 260: 275-291.

HIGH RESOLUTION SPECTROSCOPY AND LABORATORY ASTROCHEMISTRY @IIT KHARAGPUR.

Arijit Roy[1], Ratul Paul[1], Arpita Pati[1], Shuvalaxmi Garnaik[1], and Piyush Mishra[1,*]
[1]Department of Chemistry, Indian Institute of Technology, Kharagpur, West Bengal, India.
*Contact: pmishra@chem.iitkgp.ac.in

With the advent of new-generation space and ground-based telescopes, our idea about the interstellar medium (ISM) and its chemical complexity has largely been enhanced. As of June 2026, about 347 molecules, starting from the simplest molecule H_2 to the complex one C_{60} are known to be present in different parts of the ISM, and the numbers keep growing [1]. A majority of these molecules have been detected using ground-based radio telescopes and space-based infrared telescopes by studying their microwave and infrared spectral features [2]. Our understanding of the formation pathways of these molecules in the ISM is limited. In these circumstances, laboratory astrochemistry supported by high resolution spectroscopy specifically in microwave and IR wavelengths, supported by quantum chemical calculations could provide us with a viable pathway to interpret the telescope data and helps us to understand the formation, evolution and physico-chemical transformation of different molecules in the ISM in great detail [2].

Owing to the importance of high-resolution spectroscopy to astrochemistry, the Gas Phase Chemical Physics Laboratory at the Department of Chemistry, IIT Kharagpur, started working on the four different aspects of high-resolution molecular spectroscopy. The primary focus concentrated on the development of a Modular Chirped-Pulse Molecular Rotational Resonance (CP-MRR) spectrometer. This will enable us to interpret observational data from the radio-frequency to the sub-millimeter wave region, potentially leading to the discovery of new complex molecules in different parts of the ISM.

Parallel ongoing research is high-resolution IR spectroscopy to study molecular processes in the gas-phase like combustion process happening in star-forming regions, planetary prebiotic chemistry, and upper atmospheric (near-space) chemistry. The results from this work can complement interpretations of space-borne IR telescope data, such as ongoing James Webb Space Telescope data and Spitzer mission data. Efforts are also being made to develop a cryogenic buffer gas cell and combine it with IR spectroscopy. The cell will mimic near-space (mesosphere-thermosphere (M-T) region) environments enabling our understanding of complex chemistry in those environments, including studying atmospheric discharges, electromagnetic processes, and dust particle interactions in shaping the dynamics of this region. Additionally, we also want to understand the crucial condensed-phase chemical processes in meteoritic chemistry, specifically by studying the effect of intense laser induced shocks on the meteorite analogs such as the carbonaceous dust soot.

Apart from detection and molecular structure determination and study of non-covalent interactions, we also want to learn about the chemical dynamics by performing quantum state control experiments and precession measurements. In this symposium we will demonstrate a summary of the ongoing research activity of the Gas Phase Chemical Physics Laboratory at the Department of Chemistry, IIT Kharagpur.

References: [1] C. P. Endres, S. Schlemmer, P. Schilke, J. Stutzki, and H. S. P. Müller, The Cologne Database for Molecular Spectroscopy, CDMS, in the Virtual Atomic and Molecular Data Centre, VAMDC J. Mol. Spectrosc. 327, 95–104 (2016). [2] Puzzarini C, Alessandrini S, Bizzocchi L, Melosso M and Rivilla VM (2023), From the laboratory to the interstellar medium: a strategy to search for exotic molecules in space. Front. Astron. Space Sci. 10:1211784.

ℓ-TYPE DOUBLING IN $HC_{2n+1}N$ AND $HC_{2n+1}P$ LINEAR MOLECULES OF ASTROCHEMICAL INTEREST

Ratul Paul[1], Subhankar Bera[1], and Piyush Mishra[1], *
[1]Department of Chemistry, Indian Institute of Technology Kharagpur, Kharagpur, West Bengal, India.
*Contact: pmishra@chem.iitkgp.ac.in

Conjugated linear-chain molecules represent an important class of carbon-rich species with potential significance in atmospheric processes, astrochemistry, and the chemistry of the interstellar medium. Many of these molecules are highly reactive or thermodynamically unstable under terrestrial conditions, making their isolation, characterization, and direct laboratory investigation challenging. A classic illustration of this is the molecules classified as cyanopolyynes ($HC_{2n+1}N$), which have been recognized in cosmic environments[1] . Its phosphorus-containing counterpart, $HC_{2n+1}P$, is hypothesized to exist in cosmic environments, despite HCP being the sole chemical recognized in such media. Notwithstanding the significance of these molecular categories in astrochemistry, astrobiology, and prebiotic chemistry, the laboratory evidence available is constrained by experimental difficulties[2], [3], [4] . Nevertheless, their transient existence and distinctive molecular structures make them promising candidates for detection in gas-phase environments. In this work, we use computational methods to come up with a ℓ-type doubling constant for each degenerate vibrational mode of ($HC_{2n+1}N$, n = 0 – 5), and ($HC_{2n+1}P$, n = 0 – 5). We also investigate the trends of the *ℓ-type doubling* constant in relation to chain length, terminal atom, and vibrational frequency. Since *ℓ-type doubling* is observed in the rotational spectra recorded by radio-telescopes and vibrational spectra recorded by space telescopes, the molecular constants and vibrational frequencies will be beneficial in astrochemical searches and detection.

References:

[1] McGuire B. A. (2022) *Astrophys. J. Suppl. Ser.* 259:30. [2] Bizzocchi L. et al. (2001) *J. Mol. Spectrosc.* 205:110–116. [3] Summers D. P. (2012) *Genesis—In The Beginning: Precursors of Life, Chemical Models and Early Biological Evolution*, 201–216. [4] Walton C. R. et al. (2023) *Nat. Geosci.* 16:399–409.

RAMAN SPECTROSCOPIC CONSTRAINTS ON THE FORMATION CONDITIONS OF PRESOLAR SILICON CARBIDE GRAINS FROM THE MURCHISON METEORITE

A. Tripathi[1] and K. K. Marhas[1]
[1]Planetary Sciences Division, Physical Research Laboratory, Navrangpura, Ahmedabad 380009, Gujarat, India
(e-mail: [kkmarhas@prl.res.in; ms22202@iisermohali.ac.in])

Introduction: Presolar SiC grains condensed in the outflows of evolved stars and supernovae and survived incorporation into the Solar System. Their isotopes record nucleosynthesis in the parent star, whereas their crystal structure (polytype) records how the solid condensed and grew. SiC exists in over 200 polytypes - including both synthetic and terrestrial forms. Presolar grains are dominated by cubic 3C, with rarer 2H, 4H, 6H and 15R [1,2]. This mix differs from terrestrial SiC, where 6H and 4H are common and 2H is scarce. These grains preserve crystallization pathways specific to stellar environments.The astrophysical conditions that govern formation of a particular polytype include - temperature, pressure, gas composition (C/O, metallicity), supersaturation, cooling and expansion of the outflow, and the condensation kinetics [3,4]. Most of these factors remain poorly constrained. Raman spectroscopy of the transverse-optical (TO) phonon mode provides a non-destructive structural probe of presolar SiC [1]. The TO mode is sensitive to the Si–C bonding environment and crystal structure, causing its peak position and linewidth to vary with polytype and structural disorder. Here, we use these Raman signatures to constrain the conditions leading to particular polytypes.

Methods: We studied 124 SiC grains (0.8–1.5 μm, KJF series) from the Murchison meteorite, classified as mainstream (85), AB (19), X (8), Y (6) and Z (6) based on NanoSIMS C, N and Si isotopic analysis. Raman spectra (Mercury Argon Light Source) were acquired and analysed following the approach of Liu et al. [1]: spectra were baseline-corrected and the TO peak was fitted with a Voigt profile to obtain position and FWHM. Based on this analysis, we assigned polytypes for 40 grains.

Results: The TO peak position spans 783.9–802.9 cm^{-1}, while FWHM ranges from 11.1–34.0 cm^{-1} The TO position separates the four identified polytypes, with mean values of 798.6, 792.8, 785.8 and 784.3 cm^{-1} for 3C, 6H, 15R and 4H, respectively. The systematic shift toward lower wavenumbers for non-3C polytypes reflects differences in their Si–C crystal structure and phonon environment [1]. FWHM measures the width of the TO mode and is sensitive to structural disorder, defects and compositional or isotopic heterogeneity. In our data, broader TO features are concentrated among the lower-wavenumber, non-3C grains. This is consistent with the broadened and shifted TO features associated with non-3C structures and disorder reported by Liu et al. [2]. Non-3C polytypes occur in MS, AB, X and Y grains. Thus, polytype diversity is not confined to a single stellar source population.

Discussion: TO position acts as a tracker for polytype. The occurrence of different polytypes across isotopic groups shows that stellar source alone does not determine SiC structure; instead, polytype reflects differences in the local conditions of crystal growth. This is consistent with Liu et al. [2], who found that downward shifts and broader TO peaks are associated with departures from ideal 3C structure, including rare polytypes and structural disorder. In our grains, the systematic separation of TO positions between 3C, 6H, 15R and 4H therefore provides a Raman signature of this polytype diversity. The rare polytypes observed in X grains may further reflect the wider range of physical conditions in supernova ejecta [3]. TO shifts can also be influenced by ^{13}C enrichment, while peak broadening may arise from isotopic heterogeneity, defects or overlapping modes [2]. Together, our results show that Raman spectroscopy can connect the observed crystal structure of presolar SiC with variations in its formation environment.

Acknowledgments: NanoSIMS and Raman measurements were made at the Carnegie Institution for Science.

References:

1. Liu N. et al. (2017) *Meteoritics & Planetary Science* 52:2550–2569.
2. Daulton T. L. et al. (2003) *Geochimica et Cosmochimica Acta* 67:4743–4764.
3. Kodola´nyi J. et al. (2018) *The Astrophysical Journal* 868:34.
4. Gabrielle M. Adams and Katharina Lodders (2025) *The Astrophysical Journal* 985:35.

RADIATIVE TRANSFER MODELING OF MOLECULAR LINE PROFILES IN THE HOT CORINO PROTO-BINARY NGC 1333 IRAS4A

Bratati Bhat[1], [1]Physical Research Laboratory (Physical Research Laboratory, Navrangpura, Ahmedabad, 380009, Gujrat, India, bratati.hooghly@gmail.com)

Abstract: NGC 1333 IRAS4A is a well-studied low-mass, Sun-like proto-binary system with two components, A1 and A2, that exhibit distinct physical and chemical properties. We modeled this hot corino using the RATRAN radiative transfer code to explain the different spectral signatures of CH3OH and H2CO observed toward A1 and A2. Our aim is to understand the kinematical and chemical differences between the two components and to characterize their dust opacity effects. We adopted a one dimensional spherical infalling envelope model including a collimated outflow. High-resolution ALMA observations reveal that the contrasting spectral profiles arise mainly from dust opacity: A1 is optically thick, producing absorption features, while A2 is optically thin and shows emission, including an inverse P-Cygni profile indicative of infall. By extending our model from millimeter to centimeter wavelengths using ALMA and VLA data, we demonstrate reduced opacity effects at longer wavelengths.

Acknowledgments: This work uses ALMA data (ADS/JAO.ALMA 2015.1.00147.S). We thank ESO, NSF, NINS, NRC, MOST, ASIAA, KASI, and the Republic of Chile for supporting ALMA. B.B. acknowledges PRL, Ahmedabad, and IIA, Bengaluru, for research facilities and support.

References:

[1] Bratati Bhat, Ankan Das, Prasanta Gorai, Dipen Sahu. (2026) *Life Sciences in Space Research,* 49, 48-60.

MINERALOGICAL, CHEMICAL AND SHOCK-METAMORPHIC CHARACTERIZATION OF CHONDRULE POPULATIONS IN THE DERGAON H5 CHONDRITE.

K. S. Verma[1], N. Rai[1] and K.K. Marhas[2],
[1]Earth Sciences department, Indian Institute of Technology, Roorkee, 247667, India (ksinghverma@es.iitr.ac.in),
[2]Physical Research Laboratory, Planetary Science, Ahmedabad, India.

Dergaon undifferentiated (H5) ordinary chondrite, with relatively low K-contents, has texturally varied chondrules and shock-induced features which are required to be studied in order to present the complete characterization, quantification and petrogenesis of our sample in an attempt to understand the impact and evolutionary history of this meteorite. In the analysed sample, the chondrule to matrix ratio is high as chondrules are present in large number (~68).

Dergaon H5 ordinary chondrite polished section is studied under optical microscope and thereafter, electron probe micro-analysis (EPMA) was carried out for the identification of minerals, modal mineralogy and matrix and chondrule compositions. The Cameca SX100 EPMA is used in IIT Roorkee, India, where, the conditions for the analysis were 15kV accelerating voltage, 20nA current, 1µm beam size along with 15s of counting time. Raman spectroscopy (Horiba JY LabRAM HR micro-Raman spectrometer, WIHG, Dehradun, India) is carried out to understand the range and polymorphs of the mineral phases.

Two major chondrule classifications has been identified in our studied sample. The first is based on their mineralogical relationship namely, porphyritic olivine pyroxene (POP), barred olivine (BO), porphyritic olivine (PO), porphyritic pyroxene (PP), radial pyroxene (RP), porphyritic olivine pyroxene (ROP) and cryptocrystalline chondrules (C). While, the other classification is based on their shape and presence of fractures, is identified as pristine (25 vol%), mechanically deformed (35 vol%) and partially melted chondrules. Nearly 40 vol% are partially melted with serrated and degraded boundaries indicating thermal metamorphism. The results of the geochemical analysis were presented in the form of ternary and bivariate plots, which suggests average compositional range of pyroxene, olivine and feldspar are Wo 0.40-7.04 En 74.98-84.37 Fs 14.32-17.92, Fo 79.41-81.05 Fa 18.63-19.94 Te 0.02-0.71 and An 6.93-39.01 Ab 36.22-91.51 Or 1.56-8.01 respectively.

Presence of radial cracks, irregular fractures, planar deformational features (PDFs), cataclastic texture suggests the S1-S2 shock stage while the identification of other shock-indicators like chromite veinlets, chromite-plagioclase assemblages (where, Al is higher than unmelted chromite), silicate melt veins and metal- troilite assemblages by raman spectroscopy, propose that the possible source of heat generated for this metamorphism could be via collision impacts (S4-S5). Additionally, based on various shock and impact features, moderately shocked (S4-S5) shock stage is assigned, where corresponding pressure ranging from 30-55 GPa, contrary to S2-S3 (very weakly to weakly shocked) shock stage suggested by previous studies with corresponding pressure 5-20 GPa [1]. Silicate melt veins at some places with olivine composition (Fa 42-43) is different from the olivine of nearby matrix and chondrules (Fa 18-19). Also, in shocked chondrites, olivine melt veins occur at 75-90 Gpa pressure while pyroxene with PDFs observed at 25-90 GPa pressure [2], suggests the pressure at the time of shock metamorphism may be ≥75 GPa.

This study presents the shock features, their formation history and corresponding physical conditions to shock stages (S4-S5), help in understanding the deep earth's mantle system and constrain pressure, temperature conditions which otherwise is very difficult considering the lack of physical access to earth's deep interior.

References: [1] Shukla P. N. et al. (2005) Meteoritics and Planetary Science 40:627-637. [2] Stoffler D. et al. (1991) Geochimica et Cosmochimica Acta 55;3845-3867.

METEORITE MINERALOGY AND INDIAN METEORITE FALL

Dipak Kumar Panda, Planetary Science Division, Physical Research Laboratory
pdipak@prl.res.in; dipakpanda75@gmail.com

Abstract:

The solar system formed 4.56 Ga ago, but a complete understanding of its origin and evolution is still lacking. For this, we need samples from different planets and asteroids, along with Earth samples, to understand the different processes that have occurred in the solar system. The samples from Earth are no longer in pristine condition; we now rely on meteorite samples from asteroids and other planets, such as the Moon and Mars, or on returned samples from planetary missions.

An extraterrestrial solid object that penetrates Earth's atmosphere and falls onto Earth's surface is known as a Meteorite. The Meteorite can be found (collected immediately after it falls on Earth) or found (no record of when it falls on Earth or collected after a long time). The fall-type meteorites are preferred as they are not contaminated or weathered. Meteorites are broadly classified as stony, stony-iron, and Iron. Based on the bulk compositions and texture, the meteorites are classified as chondrites and non-chondrites. Further, non-chondrite is subdivided into achondrite, stony-iron, and Iron. Based on chemistry, oxygen isotopes, mineralogy, and petrography, the meteorites are further classified using a classification scheme that provides insight into the formation history.

For the classification of meteorites, various techniques and instruments are used in petrographic and geochemical studies. Like petrographic information, a petrographic microscope is used. For geochemical information, the instruments include the Electron Micro Probe Analyzer (EPMA), X-Ray Fluorescence (XRF), and Inductively Coupled Plasma Mass Spectrometer (ICP-MS). Phase chemistry can be determined using EPMA, whereas bulk chemistry requires XRF and ICP-MS.

In India, the Geological Survey of India (GSI) is the custodian of Meteorites, and the Physical Research Laboratory was recently recognized as a repository of Meteorites. As per the Meteorite Bulletin, there are 158 meteorite falls/finds in India. As per the type of Meteorite, the collection of meteorites from India comprises carbonaceous (C1, CM), Ordinary (H, L, LL), HED, Aubrite, Ureilite, Iron, and Martian, etc. The classification of these meteorites is based on their chemical composition and oxygen isotope [1,2]. Of the total collection, more than 70% are ordinary chondrites. A few of these ordinary chondrites are primitive and can be used to infer very early events in the solar system.

During the presentation, a brief overview of the classification of meteorites and how some collections of Indian meteorites provided very important scientific results.

Reference:

1. Krot A.N et al. Treatise on Geochemistry, Vol I, “Meteorite and Cosmochemical Process”, 2014
2. Clayton et al, EPSL, 30, 10-18, 1976.

DECIPHERING PRE- AND POST-ACCRETIONARY PROCESSING OF ORGANIC MATTER IN ASTEROIDAL MATERIALS.

Rahul Kumar,[1,2] Tak Kunihiro[2], and Christian Potiszil[2], [1]Department of Applied Geology, Indian Institute of Technology Indian School. Of Mines) Dhanbad, 826004, rahulkumar@iitism.ac.in, [2]Pheasant Memorial Laboratory, Institute for Planetary Materials, Okayama University, Yamada 827, Misasa, Tottori, 682-0193, Japan.

Introduction: Reconstructing the origin and evolution of organic matter (OM) in asteroidal materials remains a fundamental challenge in planetary science [1], [2], [3] . A major difficulty lies in distinguishing between OM properties inherited from pre-accretionary environments such as the interstellar medium (ISM) or protosolar nebula (PSN) and those modified by post-accretionary processes, such as fluid-mediated alteration, oxidation, and mineral associations on parent bodies [4]. This study investigates the size distribution of insoluble organic matter (IOM) in asteroidal materials to infer dominant pre-accretionary processes (fragmentation and coagulation) and assesses OM-mineral associations to evaluate the role of aqueous alteration in shaping OM distribution. Seven Ryugu fragments (2 Ryugu-A, 5 Ryugu-C), three Orgueil (CI1), three Murchison (CM2), and two Murray (CM2) fragments were embedded in indium, dry-polished, and analysed using Scanning Electron Microscope-Energy Dispersive Spectroscopy elemental mapping. Element maps obtained was further processed with image processing and machine learning to identify spatial distribution of phases. OM properties such as diameter, circularity, and mineral associations were quantified. Power-law statistics ($n(d) = kd^{-\alpha}$) were applied to OM size distributions to constrain fragmentation versus coagulation processes. OM size distributions yield power-law indices (α) ranging from –1.2 to –3.0. Ryugu-A exhibits steeper slopes (α = –2.6 to –2.8) indicating dominance of smaller OM grains. Ryugu-C shows shallower slopes (α = –1.5 to –2.1). CI chondrites display α values (–1.9 to –2.1) within the Ryugu-C range, while CM2 meteorites exhibit broader α ranges (–1.2 to –3.0). Lab-synthesized OM via Formose reaction at 80°C and 200°C yields α = –2.9 and –3.1, respectively, overlapping with Ryugu-A. A clear correlation exists between dolomite abundance and α (R^2 = 0.70). Ryugu-A, with lower dolomite content (<1%), preserves steeper α values, suggesting reduced oxidation and better preservation of small OM. Ryugu-C, with higher dolomite (up to 3%), shows shallower α, indicating complete degradation of small OM through extensive oxidation. OM-dolomite abundance exhibits an anticorrelation (R^2 = 0.99), following exponential decay. OM-mineral associations are systematically lower in Ryugu-A compared to Ryugu-C for magnetite, Fe-sulfide, dolomite, and apatite, despite similar phyllosilicate associations. Notably, OM-mineral association is independent of secondary phase abundance. Large OM (1.6-5 μm) shows stronger dolomite and apatite associations than small OM (1-1.6 μm), consistent with partial oxidation where OM portions convert to carbonate or apatite. Irregular OM (circularity 0.4-0.8) exhibits greater mineral association than rounded OM (circularity 0.8-1.0), supporting fluid-driven redistribution.

Acknowledgments: We would like to thank Pheasant Memorial Laboratory members for laboratory maintenance. This work was supported in part by Ministry of Education, Culture, Sports, Science and Technology (MEXT) of Japan. This work was carried out at the JAXA's Hayabusa2 Phase-2 curation facility at Institute for Planetary Materials, Okayama University. This study was performed using joint-use facilities of the Institute for Planetary Materials, Okayama University.

References: [1] C. Potiszil et al., “Organic Matter in the Asteroid Ryugu: What We Know So Far,” Life 2023, Vol. 13, Page 1448, vol. 13, no. 7, p. 1448, Jun. 2023, doi: 10.3390/LIFE13071448. [2] T. Nakamura et al., “Formation and evolution of carbonaceous asteroid Ryugu: Direct evidence from returned samples,” Science (1979)., vol. 379, no. 6634, Feb. 2023, doi: 10.1126/science.abn8671. [3] E. Nakamura et al., “On the origin and evolution of the asteroid Ryugu: A comprehensive geochemical perspective,” Proceedings of the Japan Academy, Series B, vol. 98, no. 6, pp. 227–282, Jun. 2022, doi: 10.2183/PJAB.98.015. [4] L. R. Nittler et al., “Micro-Scale Characteristics of Insoluble Organic Matter in Chondrites: A Coordinated TEM, STXM and SIMS Study”.

PHOSPHATE MINERALOGY AND FLUID-ASSISTED ALTERATION IN THE KHALWAT-NIMGAON L5 ORDINARY CHONDRITE

G. ARORA*[1] AND D. RAY[1]
[1]PHYSICAL RESEARCH LABORATORY, AHMEDABAD, INDIA
*Corresponding author E-mail: garima@prl.res.in

Phosphate minerals in ordinary chondrites (OCs) are important recorders of parent-body thermal metamorphism, impact processing, volatile redistribution, and fluid-rock interaction (Jones et al., 2014; Jones et al., 2016; Lewis and Jones, 2016). Here, we investigate the petrographic, microtextural, and compositional characteristics of apatite and merrillite in the Khalwat-Nimgaon meteorite, a recently recovered L5 ordinary chondrite breccia from India. Petrographic observations combined with electron probe microanalysis (EPMA), X-ray elemental mapping, and Raman spectroscopy reveal compositionally heterogeneous apatite associated and locally intergrown with merrillite along grain boundaries, fractures, and vein-like domains. These textures suggest that the phosphate assemblage records multiple stages of parent-body processing rather than simple equilibrium crystallization.

Apatite exhibits pronounced F-Cl variability, whereas merrillite shows variations in Na, Mg, and Fe. The nominal OH component was calculated from apatite stoichiometry, and the resulting F-Cl-OH compositions were compared with published phosphate data for H, L, and LL ordinary chondrites. The Khalwat-Nimgaon apatites occupy a relatively broad compositional field, indicating significant heterogeneity in volatile-site occupancy and redistribution of F, Cl, and nominal OH during parent-body evolution. Notably, some apatite grains attain high Cl# values (~90), approaching the Cl-rich phosphate compositions reported from the H5 chondrite Sidi El Habib 001 (Che et al., 2023). Together with the Fe-Mg systematics of the associated phosphates, this compositional resemblance suggests that phosphate chemistry may reflect localized physicochemical conditions and secondary volatile redistribution rather than being controlled solely by the bulk H-L-LL chemical group of the meteorite. Similar variations in ordinary-chondrite apatite compositions have been attributed to metamorphic reactions, interaction with Cl-bearing fluids or melts, and redistribution of volatiles during parent-body processing (Jones et al., 2016; Lewis and Jones, 2016; Megevand et al., 2025).

The occurrence of phosphates along fractures and grain boundaries, apatite-merrillite intergrowths, high Cl#, variable F-Cl-OH systematics, and localized elemental heterogeneity collectively support secondary modification of the phosphate assemblage. These features are consistent with localized fluid-assisted or metasomatic alteration superimposed on thermal metamorphism, with subsequent impact-induced fracturing and heating potentially enhancing volatile mobility and phosphate recrystallization. The results therefore suggest that equilibrated ordinary-chondrite parent bodies may have experienced more extensive and spatially heterogeneous volatile processing than generally recognized. Given the established spectral relationship between ordinary chondrites and S-type asteroids, the Khalwat-Nimgaon phosphate assemblage provides additional evidence for localized mobilization of water and halogens within probable S-type asteroid parent bodies and contributes to understanding the distribution, redistribution, and preservation of volatile components in inner Solar System planetesimals.

References:

[1] Jones R. H. et al., 2014. Phosphate minerals in LL chondrites. Geochimica et Cosmochimica Acta 132:120–140.

[2] Lewis J. A., and Jones R. H. 2016. Phosphate and feldspar mineralogy of equilibrated L chondrites. Meteoritics and Planetary Science. 51:1886–1913.

[3] Jones R. H. et al., 2016. Phosphate minerals in the H group of ordinary chondrites, and fluid activity recorded by apatite heterogeneity in the Zag H3–6 regolith breccia. American Mineralogist. 101:2452–2467.

[4] Megevand V. et al., 2025. Petrographic insights into phosphate formation in L and LL ordinary chondrites. Geochimica et Cosmochimica Acta. 408:153–173.

[5] Che S., et al., 2023. In-situ formation of halite in the Sidi El Habib 001 (H5) ordinary chondrite. Geochimica et Cosmochimica Acta. 348:85-106.

COSMIC RAY EXPOSURE AGES OF METEORITES AND SURFACE EXPOSURE SYSTEMATICS OF PLANETARY OBJECTS

R. R. Mahajan[1], [1]Physical Research Laboratory, Ahmedabad, Gujarat, India, 380009.
email: ramakant@prl.res.in

Introduction: Solar system is full of various objects and effects. All objects are exposed to the energetic radiation, called solar cosmic rays (SCR) and galactic cosmic rays (GCR). SCR originates from Sun, while GCR from galactic region. SCRs are MeV particles interacting with the solid objects up to 10 cm, while GCR effects (including primary and secondary) are observable up to 1.8 m. Nuclear transformations are caused by primary cosmic ray protons (GCR and SCR) as well as secondary neutrons and protons (GCR). The cosmogenic noble gas nuclide (stable) is accumulated in the rock as long as the rock is exposed to the GCR and/or SCR [1]. This duration is called as comic ray exposure age (CRE age).

The transit time of the meteoroid from its ejection from parent object till fall on Earth is estimated using the noble gas nuclides produced via cosmic ray interaction in the interplanetary region. The CRE ages derived from noble gas measurements can be used to club together the meteorites from same class to constrain the common ejection events [2]. The CRE ages are conventionally plotted as histograms to decipher the past impact events on the asteroids, that ejected the meteoroids [3]. Ordinary chondrites, the largest meteorite group on Earth, exhibit the exposure age between 1 to 80 Ma, having several clusters, provides the information about collisional events occurred in past in the asteroid belt.

Cosmic ray exposure on airless body: Burial history of the sample from regolith of air body can be estimated using cosmogenic noble gases. Cosmic ray exposure age of samples from regolith of airless bodies is an effective technique for investigating the regolith history. It is to be noted that cosmogenic noble gases of a regolith grain integrated a range of exposures during its residence at different burial depths [4].

Complex exposure history of the meteorites is applicable for few cases [5]. Pre-exposure close to the surface on the parent body, exposure of new surface generated after breaking the meteoroid in space. Loss of cosmogenic gases due to subsequent parent body alteration is also possible.

Uses of cosmic ray exposure effects: Cosmic ray exposure ages of individual presolar grains provide a new observational constraint on the chronology of stellar events preceding solar system formation. Prolonged cosmic ray exposure ages are common in iron and some of the stony-iron meteorites. On the other-hand, short CRE ages are observable in carbonaceous chondrites. The short CRE ages of carbonaceous chondrites may be due to their origin from near earth objects or the long exposure meteorites are lost due to their fragile nature.

Cosmic ray exposure history of fossil meteorites is useful to decipher past impact events on Earth. Chromite grains from these burial sites reveal short transfer time, of 1 Ma from the asteroid belt to Earth [6]. Surface exposure history is also useful to determine the extent of space weathering, which lead to change in the spectral observations of the planetary objects.

Pre-compaction exposure ages in chondrules: Chondrules while freely floating individual objects in the nebula are exposed to the cosmic ray. Determining the CRE age of the individual chondrule is essential in this case. The pre-compaction exposure of the chondrule can be estimated by subtraction bulk meteorite CRE age from that of chondrule CRE age.

Pairing of meteorites: Two types of pairing of the meteorites are applied using CRE ages determined form noble gases. The first is, source crater pairing applied to lunar and Martian meteorites [7]. The second is applied to meteorites recovered from hot and cold deserts, to pair them using CRE age.

Acknowledgments: Department of Space is thankful for funding.

References: [1] Leya I and Masarik (2009) *Meteoritics & Planetary Science* 44:1061-1086. [2] Eugster O. and Michel T. (1995) *Geochimica et Cosmochimica Acta* 59:177-199. [3] Mahajan R. R. (2022) Advances in Space Research 70:2112-2132. [4] Mahajan R. R. (2015) *Planetary and Space Science* 117:24-37. [5] Mahajan R. R., Sarbadhikari A. B. and Sisodia M. S. (2019) *Planetary and Space Science* 165:23-30. [6] Meier et al. (2026) *88th Ann. Met. Soc. Meeting.* Abstract #5156. [7] Mahajan R. R. (2015) *46th LPS*, Abstract # 1166.

NEUTRON SIGNATURES IN ORDINARY CHONDRITES

Satvika Jaiswal[1], Ramakant R. Mahajan[1], Avadh Kumar[1] and Kuljeet K. Marhas[1]
[1]*Physical Research Laboratory, Ahmedabad, 380009, India.*

Introduction: Ordinary chondrites (OCs) are the most abundant meteorites, with H and L groups making up about 70% of recorded falls, and they preserve a comparatively unmodified record of early solar system processes. Their noble gases carry cosmogenic, radiogenic, trapped, and nucleogenic components that together record cosmic-ray exposure (CRE), thermal history, and parent-body gas retention. Among these, neutron-capture products are especially important because they can bias cosmogenic and radiogenic ages if not resolved. Excess ^{80}Kr and ^{82}Kr, produced by ^{79}Br (n, γ)^{80}Kr and ^{81}Br (n, γ)^{82}Kr, record the thermal-neutron effect within the meteoroid and give indirect information on the distribution of halogen-bearing phases, which are otherwise hard to characterize. Quantifying these effects both improves the deconvolution of noble gas components and constrains neutron irradiation conditions and shielding geometry. Here we present a noble gas isotopic study of nine OC falls and finds: five H chondrites (Dhajala, Mahadeva, Balcarce, Dergaon, Devgaon) and four L chondrites (Uhrovec, Gambat, Realicó, Berduc). H and L chondrites have contrasting parent-body histories: the H parent body is a megabreccia that shed fragments with little shock, whereas the L parent body was a monolith that broke up catastrophically at ~470 Ma [1]. We integrate CRE ages with gas retention ages, focus on neutron-capture excesses in the noble gases to assess thermal-neutron effects.

Results and Discussion: The majority of samples show ^{80}Kr and ^{82}Kr excesses that deviate from the cosmogenic spallation trend, and ^{128}Xe excesses that correlate with iodine-derived ^{129}Xe. Together these identify (n, γ) capture on Br and I as the principal source of the anomalies. After subtraction of trapped (phase Q) [2] and spallation components, the neutron-produced ^{80}Kr and ^{82}Kr span nearly three orders of magnitude, from ~7×10^{-13} cm^{3}STP/g in Gambat to ~6×10^{-10} cm^{3}STP/g in Dergaon. This range reflects heterogeneous integrated neutron fluence, shielding conditions, and halogen content. Both Dergaon aliquots carry excesses more than an order of magnitude above the other samples, indicating a substantially higher neutron dose or Br abundance. The $(^{80}Kr/^{82}Kr)_n$ ratios of Dhajala, Uhrovec, Realicó, and Berduc cluster tightly between 1.7 and 2.2, approaching the value of ~2.5 expected for epithermal neutrons (30-300 eV) rather than the thermal value of ~3.3 [3]. This indicates that neutron capture in these meteorites was dominated by intermediate-energy neutrons. Ratios below the Br-capture limit in Mahadeva, Balcarce, and Devgaon, and the high value in Dergaon (7.68), most likely reflect incompletely resolved trapped or spallation contributions, so the reported ratios represent lower limits. Because nucleogenic Kr and Xe are stable and integrate the total neutron fluence, they provide a direct record of neutron irradiation and halogen distribution. Correcting for them is essential for accurate cosmic-ray exposure and gas retention ages in OCs.

Conclusions: Noble gas (He-Xe) isotope data for nine ordinary chondrites show that neutron capture is a significant but heterogeneous contributor to their Kr and Xe inventories. Excesses of ^{80}Kr, ^{82}Kr, and ^{128}Xe (correlated with iodine-derived ^{129}Xe) identify (n, γ) capture on Br and I, with neutron-produced Kr varying by nearly three orders of magnitude (Gambat lowest, Dergaon highest). The $(^{80}Kr/^{82}Kr)_n$ ratios in Dhajala, Uhrovec, Realicó, and Berduc point to capture dominated by epithermal neutrons. Cosmogenic ^{21}Ne exposure ages are more reliable than ^{3}He ages, which are systematically low, and K-Ar ages exceed U, Th-He ages in every sample, reflecting preferential ^{4}He loss. Nucleogenic components must therefore be corrected before Kr and Xe are used for exposure ages, and they provide a probe of neutron fluence and halogen distribution.

Acknowledgments: The authors thank the Department of Space, Government of India, for funding this study.

References:

[1] Korochantseva E. V. et al. (2007) *Meteoritics & Planetary Science*, 42, 113–130.
[2] Busemann H. et al. (2000) *Meteoritics & Planetary Science*, 35, 949–973.
[3] Marti K. et al. (1966) *Zeitschrift für Naturforschung A*, 21, 398–413.

THERMAL OVERPRINTING BY FUSION CRUST CONTROLS BACK-TRANSFORMATION OF HIGH-PRESSURE PHASES IN THE KATOL L6 CHONDRITE.

K. Tiwari[1,2], S. Bhowmik[2], S. Ghosh[2], and D. Ray[1]. [1]Physical Research Laboratory, Ahmedabad – 380059, India (kishantiwari@iitkgp.ac.in), [2]Department of Geology and Geophysics, Indian Institute of Technology, Kharagpur – 721302, India.

Introduction: Meteorites record two major thermal events, shock metamorphism on the parent body and atmospheric heating during entry, each leaving distinct mineralogical signatures [1,2]. Shock-melt veins (SMVs) host high-pressure (HP) polymorphs such as wadsleyite, ringwoodite, majorite, and bridgmanite, whose preservation at ambient pressure depends on the post-shock cooling rate, decompression timescale, and kinetic barriers to reverse transformation [3,4]. Fusion-crust heating during atmospheric entry can additionally drive retrograde (back-)transformation of these HP phases, yet this effect is seldom quantified. Here we examine the Katol L6 ordinary chondrite to quantify how fusion-crust heating controls the back-transformation of HP minerals within an SMV, and we use it to reconstruct the original crust thickness and the mass lost to ablation.

Samples and Methods: A polished section of Katol preserving an SMV network adjacent to intact fusion crust was examined by backscattered-electron (BSE) imaging and 532 nm micro-Raman spectroscopy at PRL, Ahmedabad [5]. The thermal history was modelled with a two-dimensional heat-diffusion scheme (MATLAB) using sample-derived geometry and boundary conditions. Back-transformation timescales were computed from the interface-controlled reverse ringwoodite-olivine kinetics of Kubo et al. [4], with the pre-exponential factor scaled to the dry water content of L6 chondrites.

Results and Discussion: BSE and Raman mapping reveal a sharp zonation across the SMV–crust interface: ringwoodite persists ~555 μm into the SMV and ~425 μm into the adjacent host rock, whereas nearer the crust it is back-transformed to olivine. Kinetic calculations show that forming ~1 μm olivine grains requires only a few seconds at 1273–1310 K, consistent with the luminous phase of atmospheric entry. Heat-diffusion modelling indicates that sustaining temperatures above the ringwoodite–olivine threshold (~1273 K) for a few seconds at the observed depths requires an original crustal layer of ~7.6–8.7 mm at the baseline surface temperature of 2323 K (~3–8 mm across 2000–3000 K). These values are more than an order of magnitude greater than the ~30–125 μm of crust preserved in the sample, implying substantial ablation during flight.

Conclusions: Fusion-crust heating quantitatively explains the retrograde zonation of HP phases in Katol. Beyond delineating the post-shock thermal regime that governs HP-mineral survival, the approach provides a quantitative means to reconstruct the original fusion-crust thickness and thereby estimate the mass lost to ablation—offering new insight into meteoroid entry dynamics, the preservation bias of HP phases, and the flux of extraterrestrial material to Earth.

Acknowledgments: We thank PRL, Ahmedabad, and IIT Kharagpur for analytical facilities and support.

References: [1] Sharp T. G. and DeCarli P. S. (2006) *Meteorites and the Early Solar System II*, 653–678. [2] Tomioka N. and Miyahara M. (2017) *Meteoritics & Planetary Science* 52:2017–2039. [3] Hu J. and Sharp T. G. (2022) *Progress in Earth and Planetary Science* 9:6. [4] Kubo T. et al. (2022) *Progress in Earth and Planetary Science* 9:21. [5] Tiwari K. N. et al. (2025) *Progress in Earth and Planetary Science* 12:6. [6] Ghosh S. et al. (2021) *Proceedings of the National Academy of Sciences* 118:e2108736118. [7] Miyahara M. et al. (2021) *Progress in Earth and Planetary Science* 8:59. [8] Stöffler D. et al. (2018) *Meteoritics & Planetary Science* 53:5–49.

SHOCK FEATURES IN ORDINARY CHONDRITES: OBSERVATIONS FROM THE GEOLOGICAL SURVEY OF INDIA ARCHIVE

Arindam Dutta [1*]

[1]Meteorite and Planetary Science Division (MPSD), Geological Survey of India (GSI), 15, A and B Kyd Street, Central Head Quarters (CHQ), Kolkata-700016, India.

*Corresponding author E-mail: arindam.dutta@gsi.gov.in

Abstract

Shock features in meteorites are developed due to high impact collision of asteroids during the formation and evolution of the solar system. These features are important for constraining the shock P – T – t conditions. The high-pressure shock phases are developed due to hypervelocity impacts, formed by the process of solid state transformations, crystallization of shock melts and instantaneous shock deformation of the host rock and minerals. The study of shock features in meteorites is the prime source of information about the collisional and geological history of their asteroidal parent bodies. Shock metamorphism is a nonequilibrium process that involves in physical, mineralogical and chemical changes of meteorites. The studied ordinary chondrites (equilibrated - uneuilibrated) having almost similar mineralogy with different chemical and petrologic types (L3 to L6-7, LL5 and H3 to H6) resulting from their pristine primordial matter with varied chemistry, temperatures of equilibration and shock metamorphic grade. The internal structure and texture of chondrules indicate rapid quenching, followed by quick solidification, suggesting that the molten and semi-molten droplets were formed separately in the solar nebula by disequilibrium condensation mechanism. The geochemical reservoirs for individual chondrites are significantly different from each other. Assam (L5), Bori (L6), Mirzapur (L5) and Rangala (L6) with different shock grades (S3 – S5) display the presence of different diamond polytypes (B-C), and other carbon phases with Raman peak values ranging from 1308 cm^{-1} to 1370 cm^{-1}. The presence of extraterrestrial diamond polytypes (like 6H, 8H, B-C phase and lonsdaleite - 2H; micro to nano – diamonds; size ~ 1-3 µm) and graphite phases in chondrites were determined from characteristic Raman peaks at 1308 cm^{-1}, 1314 cm^{-1}, 1315 cm^{-1}, 1332 cm^{-1}, 1349 cm^{-1}, 1359 cm^{-1}, 1360 cm^{-1}, 1469 cm^{-1}, 1504 cm^{-1} and 1585 cm^{-1} respectively. The Raman shift towards smaller wavenumber at 1315 cm^{-1} indicates the presence of lonsdaleite with more ordered carbon structure having hexagonal symmetry. Characteristic Raman peaks exclusively represent the presence of wadsleyite and ringwoodite fragments confined within shock melt veins (SMVs) as observed in chondrites. Presence of plagioclase melt glass (maskelynite) along the interstitial/intergranular spaces of olivine and pyroxene chondrules, and within matrices suggests escalation of shock pressures at above ~ 45 GPa, involved in volume expansion and generating radial cracks in Katol (L6-7) chondrite. Shock features in chondrites have been identified by the presence of high pressure polymorphs of olivine like wadsleyite (~ 917 cm^{-1} and 918 cm^{-1}) and ringwoodite (~ 796 cm^{-1}, 797 cm^{-1}, 844 cm^{-1} and 846 cm^{-1}), transformation of plagioclase into maskelynite and/or diaplectic glass and development of pyroxene glass due to high intensity impact induced shock deformation. Presence of ringwoodite and wadsleyite in ordinary chondrites (literally absent in terrestrial rocks) indicates escalation of shock pressures at ~ 13 - 22 GPa and temperatures range from 900 - 1200°C. Considerable mineral chemical disequilibria with wide range of equilibration temperatures (845 - 1100°C) across varied chemical – petrologic types show distinct fractionation and enrichment trends of REEs and TEs. Relatively higher equilibration temperatures are estimated for the L-group chondrites (850 - 1070°C) over the H-group (860-960°C) can be correlated with their varying shock stages (S1 - S6) and increasing petrologic types, though at many instances the shock effects have been annealed to some extent. Identification of several shock metamorphic features, high pressure – high temperature (HPHT) mineral polymorphs, nano to micro-sized (~1-3µm) diamond inclusions within olivine, pyroxene, and also within intergranular spaces, matrices, and presence of isotropic shock veins are investigated by combined petrographic, SEM – BSE studies, Raman Spectroscopy and Cathodoluminescence (CL) imaging to testify impact pressures – temperatures (maximum) at ~ 50 GPa and 800 - 1200ºC. Though these impacts/collisions last for a few seconds to milliseconds (ms), but the resultant shock features provide valuable information regarding meteorite evolution in the cosmochemical environment.

Keywords: *Ordinary chondrite, shock metamorphism, equilibration temperature, cosmochemical process.*

OLIVINE-RINGWOODITE TRANSFORMATION MECHANISM IN BORI L6 CHONDRITE. IMPLICATION FOR SLAB RHEOLOGY

Rajesh Kumar Behera[1], Sujoy Ghosh[1], Kishan Tiwari[1], Masaaki Miyahara[2], Naotaka Tomioka[3], Dwijesh Ray[4], Kuljeet K Marhas[4]

[1] Department of Geology and Geophysics, Indian Institute of Technology, Kharagpur-721302, India; rajeshkumarbehera439@gmail.com

[2] Graduate School of Advanced Science and Engineering, Hiroshima University, Hiroshima-739-8526, Japan

[3] Japan Agency for Marine-Earth Science and Technology, Kochi Institute for Core Sample Research, Nankoku-783-8502, Japan

[4] Planetary Science Division, Physical Research Laboratory, Ahmedabad-380059, India

Abstract: Bori meteorite is a heavily shocked L6 chondrite consist of shock melt vein (SMV) and several melt pockets. In this study, we have observed different modes of transformation of olivine to ringwoodite and the occurrence of metastable individual segmented olivine grains: 1) An olivine grain inside the SMV undergoes the segmentation process with Fe-Mg interdiffusion between them to produce the Fe-rich and Fe-poor segmented individual olivine grains. The Fe-rich olivine grains may be the back-transformation of ringwoodite grains, 2) Another olivine grain inside the SMV undergoes the segmentation process to form the individual segmented olivine grains with interdiffusion of Fe-Mg within the grains producing Fe-rich core and Mg-rich rim, 3) Inside the SMV, an olivine grain undergoes the segmentation process with subsequent transformation into ringwoodite grains. The presence of olivine (Fa_{25}) along the boundary of individual segmented ringwoodite grains (Fa_{31}), suggest the back-transformation of ringwoodite into olivine with interdiffusion of Fe-Mg between them, 4) Along the margin of the SMV, olivine grain transforms into polycrystalline to lamellar ringwoodite grain through the incoherent solid-state transformation mechanism. The coexistence of the metastable olivine and the ringwoodite grains suggest a temperature range of 700 to 1200 °C [1]. Furthermore, Bori meteorite experiences a maximum shock pulse duration of 0.3 s with an impact velocity of 2.54 km/s and the parent body diameter to >1 km. The olivine to ringwoodite transformation causes huge grain size reduction, which can significantly reduce the effective viscosity and affect the rheology of the subducting slab. Furthermore, the release of latent heat during the olivine to ringwoodite transformation increases the local temperature, promoting the stable deformation of slab [2].

Acknowledgments: SG acknowledges the financial support by Kalpana Chawla Space Technology Cell, IIT Kharagpur (Grant no. IIT/KCSTC/Chair/New/P/24-25/01). RKB acknowledges CSIR, New Delhi for providing the fellowship. SG thanks the Head of the Department of Geology and Geophysics, and the DSC members. SG acknowledges the Central Research Facility, IIT Kharagpur, for making the analytical facilities available for this study.

References: [1] Wang Y. et al. (1997) The breakdown of olivine to perovskite and magnesiowüstite. Science 275:510–513. [2] Honda R. et al. (2026) The olivine-ringwoodite transformation triggers deep slab seismicity and rheological weakening. Nature Communications 17:5264.

INTERPRETING THE ENTRY CONDITIONS FOR THE DEVELOPMENT OF DIFFERENT TEXTURES IN MICROMETEORITES

V. P. Singh[1,2,*], N. G. Rudraswami[2]
[1]CSIR- National Institute of Oceanography, Goa, India,
[2]WPI-SKCM[2], Hiroshima University, Higashi Hiroshima, Japan,
*vijaypratap865@gmail.com; vpsingh@hiroshima-u.ac.jp

Abstract:

Cosmic dust undergoes significant textural transformations during its atmospheric entry, evolving into various types of micrometeorites depending on the heating conditions [1, 2]. This study investigates the textural evolution of S-type cosmic spherules by analyzing their dependence on entry parameters, such as velocity, zenith angle, and particle size, alongside precursor composition. We present a refined subclassification of S-type micrometeorites, categorizing barred textures into tabular, platy, and radial forms, and porphyritic textures into equant, skeletal, and chain morphologies. The development of these specific textures is primarily governed by the balance between the degree of overheating above the precursor's liquidus temperature and the subsequent undercooling required for crystallization [3]. Our findings indicate that particles heated below their liquidus temperature typically form scoriaceous or equant porphyritic textures, whereas heating near the liquidus promotes the formation of skeletal or chain porphyritic morphologies. When temperatures exceed the liquidus by approximately 100°C, the distortion of embryos leads to the development of barred textures, with the specific barred type depending on the extent of undercooling. Extreme heating results in cryptocrystalline, glassy, or calcium-aluminium-titanium (CAT) spherules, while temperatures above 2400°C cause over 90% ablation, hindering spherule formation entirely. By comparing the liquidus temperatures of chondritic olivine and residual melts with the peak heating temperatures derived from the CABMOD model, we map the specific atmospheric entry conditions that favor particular micrometeorite textures. For instance, smaller particles (<400 μm) entering at escape velocity with high zenith angles (e.g., 65°–90° for CI precursors) have the highest likelihood of surviving as unmelted, scoriaceous, or porphyritic spherules. Conversely, moderate zenith angles (50°–70°) for similar particles favor barred textures, while steeper angles, higher velocities, and larger particle sizes drive extensive melting and glass formation. Ultimately, this work refines our understanding of the entry conditions that shape micrometeorite textures, providing a framework to better interpret the origins and survival of extraterrestrial dust.

References:

[1] Love SG, Brownlee DE (1991) Heating and thermal transformation of micrometeoroids entering the Earth's atmosphere. Icarus 89(1):26–43.

[2] Genge MJ, Engrand C, Gounelle M, Taylor S (2008) The classification of micrometeorites. Meteorit Planet Sci 43(3):497–515.

[3] Singh, V.P., Rudraswami, N.G. (2025) Textural evolution of S-type micrometeorites. *Prog Earth Planet Sci* **12**, 36.

EVALUATION OF HIGHLY OBLIQUE IMPACT CRATER NEAR LUOBUSA OPHIOLITE USING, NUMERICAL MODELS, ULTRA HIGH-PRESSURE MINERALS AND TEKTITES

Author: Mahesh Patil
Contact:mup124@rediffmail.com
Affiliation: Science and Spirituality Research Institute, 804, Yash Aqua, Navrangpura, Ahmedabad- 380009 (India)

Abstract:

An elliptical formation, measuring roughly 100km by 48 Km is situated near Luobusa Ophiolite in Tibet(28°51'37"N 90°52'11"E To 28°35'46"N 91°47'04"E). This structure exhibits characteristics consistent with hydro code numerical models that simulate highly oblique impacts at less than 10^0 angle to horizontal surface. Oriented in northwest-South east direction, it features a circular formation on northwest side and scars extending towards Southeast. The closeness of this structure to the Luobusa ophiolite, which is notable for ultra-high-pressure findings like coesite with former stishovite along with other UHP finds-typically linked with impact craters further emphasize its significance. The NW-SE alignment of structure also correlates with Australasian strewn field which is a result of highly oblique impact in Indochina region.

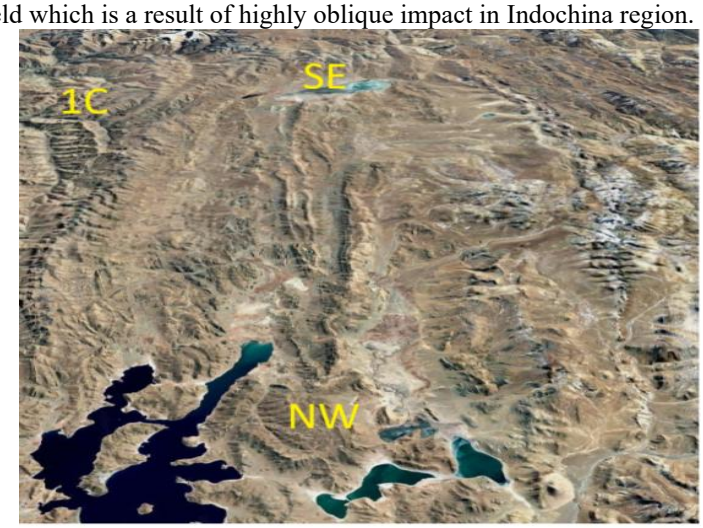


Figure1: Satellite image of elongated structure.

EXTRATERRESTRIAL DUST INFLUX AND BIOGEOCHEMICAL FOOTPRINTS: CONSTRAINTS FROM ANTARCTIC ICE AND CENTRAL INDIAN OCEAN BASIN RECORDS

Vijay Pratap Singh[1,2*], N.G. Rudraswami[2]
[1]WPI-SKCM[2], Hiroshima University, Higashi Hiroshima, Japan [2]CSIR- National Institute of Oceanography, Goa, India,
*vpsingh@hiroshima-u.ac.jp; vijaypratap865@gmail.com

Micrometeorites (MMs), sub-millimeter extraterrestrial dust particles continuously accreting onto Earth, provide an unbiased, representative sampling of Solar System parent bodies, ranging from primitive carbonaceous and ordinary chondritic asteroids to volatile-rich comets. As the sole research group in India dedicated to micrometeoritics, we have established one of the world's most comprehensive and environmentally diverse collections of cosmic dust. This repository spans contrasting modern and ancient depositional regimes, including deep-sea pelagic clays from the Central Indian Ocean Basin (CIOB), polar glacial ice from Antarctica (Maitri Station) and the Arctic, fossilized micrometeorites preserved across deep-time geological horizons (including the Cretaceous–Paleogene / K–Pg boundary intertrappean beds), and urban rooftop deposits [1,2,3]. Through high-resolution petrographic, micro-analytical, and numerical modeling (CABMOD) frameworks, our research elucidates the complex physical and chemical transformations cosmic dust undergoes during hypervelocity atmospheric entry. We trace the spectrum of entry heating, from pristine, unmelted, and scoriaceous fine-grained matrix particles to completely melted porphyritic, barred, cryptocrystalline, and silicate/iron cosmic spherules. Chemical elemental partitioning, isotopic mass fractionations (e.g., oxygen ablation), and relict mineral phase compositions (such as Fe-rich olivines and chondrule fragments) enable us to deconvolve atmospheric modification from primary parent-body characteristics, linking specific particle populations to carbonaceous (CI, CM, CV) and ordinary (H, L, LL) chondrites [4,5].

Furthermore, comparative flux evaluations across marine, polar, and lithified sedimentary archives allow us to constrain spatial and temporal variations in global extraterrestrial accretion rates over millions of years. Beyond planetary science, our work highlights the profound terrestrial footprint of this flux. In deep-sea marine ecosystems, the diagenetic weathering and dissolution of cosmic spherules release essential bio-essential trace metals, most notably bioavailable iron (Fe), nickel (Ni), and manganese (Mn), into pelagic ocean environments, directly connecting extraterrestrial accretion to global ocean biogeochemical cycles [3,6]. This synthesis demonstrates how multi-reservoir cosmic dust studies bridge astrophysics, planetary geology, atmospheric science, and ocean biogeochemistry, opening new frontiers in understanding Earth's co-evolution with interplanetary matter.

References:

[1] Rudraswami, N. G., Fernandes, D., & Pandey, M. (2020). Probing the nature of extraterrestrial dust reaching the Earth's surface collected from the Maitri station, Antarctica. *Meteoritics & Planetary Science*, *55*(10), 2256-2266.

[2] Singh, V. P., Rudraswami, N. G., Chalapathi Rao, N. V., Genge, M. J., Pandey, M., Sreekuttan, S., & Chattopadhaya, S. (2024). Discovery of fossil micrometeorites from the Deccan trap intertrappeans. *Meteoritics & Planetary Science*, *59*(11), 2922-2937.

[3] Rudraswami, N., Singh, V., & Basil Saleem, K. (2025). Central Indian Ocean Basin micrometeorite collections: Type, flux, etching and its implication to ocean biogeochemistry. *Geoscience Frontiers*, *16*(4), 102078.

[4] Singh, V.P., Rudraswami, N.G. Textural evolution of S-type micrometeorites. *Prog Earth Planet Sci* **12**, 36 (2025). Love SG, Brownlee DE (1991) Heating and thermal transformation of micrometeoroids entering the Earth's atmosphere. Icarus 89(1):26–43.

[5] Rudraswami NG, Pandey M, Fernandes D, Carrillo-Sánchez JD, Feng W, Plane JMC, Singh VP (2022) Oxygen ablation during atmospheric entry: its influence on the isotopic composition of micrometeorites. Astrophys J 940(1):25.

[6] Rudraswami, N. G., Pandey, M., Genge, M. J., & Fernandes, D. (2021). Extraterrestrial dust as a source of bioavailable iron contributing to the ocean for driving primary productivity. *Meteoritics & Planetary Science*, *56*(12), 2175-2190. https://doi.org/10.1111/maps.13764

TEXTURAL AND ENVIRONMENTAL DISCRIMINATION OF EXTRATERRESTRIAL AND TERRESTRIAL SPHERULES: EVIDENCE FROM CENTRAL INDIAN OCEAN BASIN SEDIMENTS AND ANTARCTIC CRYOCONITE SEDIMENTS.

D. Krishnaveni[1,2] and N. G. Rudraswami[1,2], [1]CSIR National Institute of Oceanography,Dona paula,Goa,India,403004, [2]Academy of Scientific and Innovative Research, Ghaziabad, Uttar Pradesh, India,201002 (krishnaveniktr@gmail.com)

Introduction: Micrometeorites (MMs) are extraterrestrial dust particles that survive atmospheric entry and reach Earth's surface [1], but identifying them is challenging because terrestrial spherules can resemble them [2,3]. We distinguished cosmic spherules from terrestrial spherules in the Central Indian Ocean Basin (CIOB) on the basis of morphology and compared the CIOB population with cosmic spherules from Antarctic cryoconite [4,5].

Methods: Spherules were handpicked using a stereo zoom microscope and later mounted in epoxy resin, polished, and carbon-coated before imaging in a scanning electron microscope. Micrometeorites are classified as S-, I-, and G-types and are subdivided by texture [1,6]. The CIOB collection comprises roughly around 1000 particles, of which 300 are terrestrial, and the remaining are MMs, whereas the Antarctic collection comprises 306 MMs.

Results: Size does not discriminate between the two groups: median diameters are 244 µm for MMs and 254 µm for terrestrial spherules. Terrestrial spherules make up ~30% of the CIOB particles and rarely contain the Ni-bearing metal beads characteristic of MMs [4].They can be originated from Volcanic, hydrothermal activities. Identification therefore rests on texture: metal beads and relict grains occur almost exclusively in MMs, whereas terrestrial spherules are angular, vesicular and microlite-bearing. Among the MM population,Barred Olivine texture dominates the deep-sea population, while porphyritic texture is predominant in Antarctic cryoconites. Alteration in deep-sea micrometeorites is mineral-selective, with seawater dissolving minerals and redistributing their Mg, Si and Ni into secondary phases, thereby eroding the very textures and chemical signatures used for cosmic identification. Etching affects the majority of MMs from the deep sea[7]. The Antarctic collection comprises more porphyritic (48% of S-types), exceeding barred spherules and little etching.

Conclusion: Compared with Antarctic MMs, CIOB MMs are more etched and altered, richer in barred spherules, indicating that depositional setting and seawater alteration reshape the recovered population. Terrestrial spherules cannot be separated from MMs by Size and are distinguished by texture, morphology and chemical composition. Textural criteria, supplemented by geochemical confirmation, improve the reliability of micrometeorite identification and flux estimates in deep-sea archives.

Acknowledgments: Funding from DST INSPIRE is gratefully acknowledged. We thank CSIR-National Institute of Oceanography for access to the SEM facility. The CIOB samples were collected during cruise SSD-048, and the Antarctic samples during the 35th Scientific Expedition to Antarctica.

References: [1] Genge M.J. et al. (2008) *Meteoritics and Planetary Science.* 43:497–515.[2] Hodge P.W. & Wright F.W. (1964) *Journal of Geophysical Research.* 69:2449–2454. [3] Niyogi A. et al. (2011) *Journal of Earth System Science* 120:1043–1054.[4] Agarwal D.K. & Palayil J.K. (2022) *Scientific Reports.* 12, 6811.[5] Rudraswami N.G. et al. (2020) *Meteoritics and Planetary Science* 55:2256–2266.[6] Genge M.J. et al. (2020) *Planetary and Space Science* 187:104900.[7] Rudraswami N.G. et al. (2025) *Geoscience Frontiers* 16:102078.

NOBLE GAS ISOTOPE SYSTEMATICS OF H GROUP ORDINARY CHONDRITES

Avadh Kumar[1*], R. R. Mahajan[1]
[1]*Physical Research Laboratory, Ahmedabad, India-380009*
[*]*E-mail: avadh@prl.res.in*

ABSTRACT: Meteorites are fragments of small solar system bodies and preserve a record of early solar system processes. Most originate in the main asteroid belt, where collisional disruption of parent bodies and subsequent gravitational perturbation deliver fragments to Earth-crossing orbits. Ordinary chondrites (OCs) are the most abundant meteorite class, making up ~85% of recovered meteorites. Based on bulk chemistry, they are divided into three groups: H (high total iron, 28%), L (low total iron, 22%), and LL (low total iron and low metallic iron) [1,2].

Here we report noble gas data for five H chondrites: Dhajala, Mahadeva, Balcarce, Devgaon, and Dergaon. The cosmic ray exposure (CRE) age is the time a meteoroid spent as a small body (~meter-sized) exposed to galactic cosmic rays, from its liberation from the parent body to its arrival on Earth. It is therefore also referred to as the ejection or transfer age. CRE ages constrain the timing and frequency of impact events on parent bodies and the dynamical transport of meteoroids to Earth [3].

METHODOLOGY: Noble gases were extracted from individual grains of each meteorite using a continuous-wave (CW) Nd:YAG laser (λ = 1.06 μm). All stable Ne isotopes (^{20}Ne, ^{21}Ne, ^{22}Ne) were measured. The cosmogenic component was identified using the Ne three-isotope diagram (^{20}Ne/^{22}Ne vs. ^{21}Ne/^{22}Ne).

Significance of CRE ages: Galactic cosmic rays (GCRs), predominantly high-energy protons (~85%) and α-particles with energies from hundreds of MeV to several GeV, continuously irradiate the surfaces of asteroids and meter-sized meteoroids. Interactions with target elements (principally O, Mg, Al, Si, Fe, and Ni) induce spallation reactions and secondary-particle cascades that produce stable (e.g., ^{3}He, ^{21}Ne, ^{38}Ar). Measuring these nuclides yields CRE ages, which are a primary tool for reconstructing the collisional and dynamical evolution of the solar system. For meteorites, this age corresponds to the time spent as a meteoroid of ~meter size following ejection from the parent body, which is why it is also termed the ejection (transfer) age. CRE ages are therefore a principal tool for reconstructing the collisional and dynamical evolution of small solar system bodies [4].

Discussion: Chronology of Events- The CRE ages obtained here are compared with the established CRE age distribution of H chondrites, which is not continuous but shows discrete clusters of ages. These clusters are widely interpreted as the signature of distinct, large-scale impact events on the H-chondrite parent body that produced populations of meteoroids at specific times. CRE ages allow a chronology of events on the parent asteroid to be established, including the timing and duration of fragmentation, collisional evolution, and the transport to Earth [5].

Acknowledgements: We are very thankful to Department of Space. Government of India for financial support.

Keywords: Meteorites, Cosmic Ray Exposure age, Noble Gas, Ordinary Chondrites.

References: [1] Grady M. et al. (2014) Atlas of Meteorites [2] Pepin R. O. et al. (2012) Acta89, 62-80 [3] Busemann H. et al. (2000) Meteoriti. Planet. Sci. 35, 949-973 [4] Eugster O. et al. (1988) GCA 52, 1649-1662 [5] Dalcher N. et al. (2013) Meteorit. Panet. Sci. 48, 1841-1862.

SPECTRAL SIGNATURES OF SIMULATED ASTEROID REGOLITHS: LINKING PHYSICAL PROPERTIES TO VNIR–SWIR CHARACTERISTICS

S. Das[1], R. Sarkar[2] and E. Cloutis[3], [1]Indian Institute of Technology Kharagpur, Kharagpur 721302, India (sritamadas250226@kgpian.iitkgp.ac.in), [2]Indian Institute of Technology Kharagpur, Kharagpur 721302, India (ranjan@gg.iitkgp.ac.in), [3]University of Winnipeg, Winnipeg, Manitoba R3B 2E9, Canada (e.cloutis@uwinnipeg.ca).

Introduction: Interpreting asteroid reflectance spectra requires isolating spectral features arising from mineral composition from those arising from the physical state of the surface. The low gravity on small asteroids may favour loosely packed, highly porous regoliths [1] whose spectra are expected to differ from those of laboratory powders in which the grains settle under Earth's gravity. In the laboratory, spectrally transparent salts such as KBr have been mixed with meteorite and mineral powders to mimic this porosity [2–4], and salt coatings are known to weaken the features of the material beneath them [5]. In this study, we analyse existing laboratory datasets of asteroid regolith analogues to quantify how grain size, packing density, porosity and surface texture can be constrained from their albedo, spectral slope, band depth, and band centre across the visible to shortwave infrared (~0.4–2.5 μm). This will help us separate compositional and physical effects when interpreting asteroid spectra.

References: [1] Vernazza P. et al. (2012) *Icarus* 221:1162–1172. [2] Izawa M. R. M. et al. (2010) *Journal of Geophysical Research: Planets* 115(E7). [3] King P. L. et al. (2011) *LPS XLII*, Abstract #1985. [4] Yang B. et al. (2013) *Icarus* 223:359–366. [5] Berger J. A. et al. (2015) *Journal of Geophysical Research: Solid Earth* 120:2162–2178.

OH, ORGANICS, AND CO_2 IN THE OUTER SOLAR SYSTEM: A JWST/NIRSPEC SPECTRAL INVESTIGATION.

A., Chatterjee[1] and R., Sarkar[1], [1]Department of Geology and Geophysics, IIT Kharagpur (chatterjeearnab734@gmail.com)

Introduction: Jupiter Trojans are primitive bodies that share Jupiter's orbit. JWST/NIRSpec observations (1.7-5.3 μm) of five Lucy targets (Patroclus, Eurybates, Orus, Leucus, and Polymele) show a broad 3 μm OH band that is deepest on the less-red Eurybates (8.83%) and only marginal on the red Orus and Leucus, which instead carry stronger 3.3-3.6 μm aliphatic organic absorption (2.78% and 1.87%), an apparent inverse trend between OH and organics [1]. The sharp 2.7 μm phyllosilicate band of Ceres, Pallas, and Themis is absent, and so is a carbonate band at 3.7-4.0 μm [1]. We extend the comparison to the JWST Large Program DiSCo-TNOs (Discovering the Surface Composition of trans-Neptunian Objects). It uses NIRSpec to evaluate the spectral properties and ice compositions, such as CO_2 and CO, of minor bodies in the outer solar system. We look at absorption in these spectra and examine how the OH, organic and CO_2 signatures relate across the samples.

References: [1] Wong, I., et al. (2024) *The Planetary Science Journal* 5(4), p.87.

END MEMBER MODELS IN PLANETESIMAL FORMATION: CONSTRAINTS FROM DIFFERENTIATED METEORITES

Nachiketa Rai
Department of Earth Sciences, IIT Roorkee, Centre for Space Science and Technology, IIT Roorkee
(n.rai@es.iitr.ac.in).

The formation and early evolution of terrestrial planets involved the accretion of primitive Solar System materials, followed by varying degrees of internal heating, melting, and chemical differentiation. These processes produced planetary bodies with diverse mineralogical, geochemical, and internal characteristics, reflecting variations in their precursor compositions, thermal histories, and differentiation pathways. Achondritic meteorites preserve important records of these early processes and provide valuable constraints on the formation and evolution of planetesimals.

Asteroid 4 Vesta, the widely accepted parent body of the howardite-eucrite-diogenite (HED) meteorites, has traditionally served as a reference model for understanding early planetary differentiation [1]. However, growing evidence from other achondrite groups, together with recent petrological and geochemical investigations, suggests that early planetesimals underwent a considerably broader range of evolutionary processes than those represented by conventional models of extensive melting and global differentiation [2].

Understanding this diversity requires an integrated investigation of the mineralogical, geochemical, and isotopic characteristics of different achondrite meteorite groups, together with quantitative constraints from petrological and geochemical modelling. Of particular importance are the relationships between chondritic precursor compositions, partial melting, melt extraction, crystallisation, and metal-silicate differentiation. We have examined contrasting evolutionary pathways recorded by differentiated meteorites, ranging from limited partial melting and incomplete differentiation to complex, multistage magmatic evolution in extensively differentiated Planetesimals.

Collectively, these meteorites reveal that planetesimal differentiation was not governed by a single evolutionary pathway, but rather encompassed a spectrum of processes controlled by precursor composition, thermal evolution, melting, and chemical segregation. Their integrated investigation provides important insights into the formation, internal differentiation, and chemical evolution of early planetary bodies, and ultimately into the processes that contributed to the assembly of terrestrial planets.

References: [1] McSween H et al. (2014) *Elements* 10: 39-44. [2] McSween Jr, H. Y., Mittlefehldt, D. W., Beck, A. W., Mayne, R. G., & McCoy, T. J. (2011). HED meteorites and their relationship to the geology of Vesta and the Dawn mission. Space Science Reviews, 163(1), 141-174. [3] Rai, N., et. al. (2020). Geochemical Perspectives Letters.14, 20-25. [4] Goodrich, C. A., Jones, J. H., & Berkley, J. L. (1987). Origin and evolution of the ureilite parent magmas: Multi-stage igneous activity on a large parent body. Geochimica et Cosmochimica Acta, 51(9), 2255-2273. [5] Layak, P., Rai, N., Marhas, K.K. and Downes, H., (2026). Thermochemical evolution of the mesosiderite parent body: Modelling and mineralogical constraints on silicates. Geochemistry, p.126426.

NON-TRADITIONAL ISOTOPE GEOCHEMISTRY OF PLANETARY MATERIALS

Ramananda Chakrabarti[1]
[1] Centre for Earth Sciences, Indian Institute of Science, C. V. Raman Road, Bangalore 560012

Advancements in mass spectrometry have allowed measurements of isotopes of a large suite of elements in the periodic table. These elements include refractories and volatiles, lithophiles as well as siderophiles and variations in their isotopic compositions have provided insights into a wide range of planetary processes from accretion and collisions to differentiation and water-rock interaction. In this talk I'll present some important findings related to the above-mentioned processes based on measurements of metal (not-so-non-traditional-anymore) isotopes.

PETROGRAPHY OF THE POLYMICT UREILITE NORTHWEST AFRICA (NWA) 15112: CLAST DIVERSITY AND IMPLICATIONS FOR REDUCTION AND IMPACT PROCESSING

Aishanya Sharma[1] and Nachiketa Rai[1,2],
[1]Centre for Space Science and Technology, Indian Institute of Technology, Roorkee (aishanya_s@sst.iitr.ac.in),
[2]Department of Earth Sciences, Indian Institute of Technology, Roorkee

Introduction: Ureilites are carbon-rich ultramafic meteorites usually classified as primitive achondrites, composed primarily of coarse-grained olivine and pyroxene (mainly pigeonite) [1]. They are regarded as mantle residues, or restites, of chondritic planetesimals that experienced partial melting. They exhibit evidence of the separation of feldspar-rich silicate melts and sulphur-rich metallic melts. Polymict ureilites are regolith breccias that sample this lithological diversity, preserving clasts of mantle residues, ultramafic cumulates, and feldspathic lithologies, which are largely absent in monomict ureilites [1,2,3]. Detailed investigations of ureilites may therefore provide insights into the evolution of chondritic precursors into differentiated planetesimals in the early Solar System.

This study presents new petrographic and mineralogical observations of NWA 15112. Reflected-light optical microscopy was employed to document clast textures, surface morphology, the distribution of opaque phases (Fe-Ni metal, sulphides, carbon), and shock features. Furthermore, scanning electron microscopy using backscattered-electron imaging and energy-dispersive X-ray spectroscopy (SEM-EDS) was employed to characterize clast boundaries, reduction textures at olivine/pyroxene-carbon interfaces, and the distribution of Fe-Ni metal and sulphides, together with major-element compositional analyses of olivine, pyroxene, and accessory phases. Detailed SEM observations reveal lithological and textural diversity within NWA 15112, providing insights into the evolution of the ureilite parent body (UPB). The sample exhibits carbon-bearing phases associated with well-rounded clasts of olivine and pyroxene. The association of these silicate minerals with carbon-rich phases may reflect the highly reducing, carbon-rich conditions experienced by ureilitic materials. However, the identification and origin of individual carbon polytypes require independent confirmation, particularly because shock metamorphism can modify carbon phases. These observations provide preliminary constraints on the shock and thermal history of the studied material. Integration of petrographic, mineralogical, and compositional observations may further constrain the lithological diversity and reduction processes recorded within the UPB during its early evolution.

Acknowledgements: Aishanya Sharma gratefully acknowledges the receipt of the CSIR-UGC JRF.

References: [1] Barrat, J.-A., Jambon, A., Yamaguchi, A., Bischoff, A., Rouget, M.-L., Liorzou, C., 2016a. *Geochimica et Cosmochimica Acta* 194, 163-178. [2] Bischoff, A., Horstmann, M., Barrat, J.-A., Chaussidon, M., Pack, A., Herwartz, D., Ward, D., Vollmer, C., Decker, S., 2014. *Proc. Natl. Acad. Sci. U. S. A.* 111, 12689-12692. [3] Sanders, I.S., Scott, E.R.D., Delaney, J.S. (2017*). Meteoritics and Planetary Science* 52, 690–708.

LATE HOMOGENISATION OF MANTLE SOURCES RECORDED BY ^{182}W ISOTOPE SIGNATURES FROM THE SINGHBHUM CRATON

Arathy Ravindran [1,2] , Carsten Münker[2], Josua J. Pakulla[2], Jonas Tusch[2], Mario Fischer-Gödde[2], Jaganmoy Jodder[3,4], Axel Hofmann[5], Rajat Mazumder[6]

[1]IISER Thiruvananthapuram (School of Earth, Environmental and Sustainability Sciences, Mathuramala PO, Vithura, Kerala-695551; artyravindran@iisertvm.ac.in), [2]Institute of Geology and Mineralogy, University of Cologne, Germany, [3]Center for Planetary Habitability, University of Oslo, Norway, [4]Evolutionary Studies Institute, University of Witwatersrand, South Africa, [5]Department of Geology, University of Johannesburg, South Africa, [6]German University of Technology in Oman, Oman.

Introduction: Anomalies in the short-lived ^{182}Hf-^{182}W systematics (expressed as μ^{182}W) relative to modern mantle values (μ^{182}W=0) have been preserved in Archean and Proterozoic rocks around the world. These anomalies allow valuable insights into Hadean mantle differentiation processes on Earth, chemical heterogeneities of the mantle, and the evolution of different mantle reservoirs with time. Possible processes explaining μ^{182}W anomalies are early silicate differentiation, missing late veneer or core contributions [1].

So far, only a few ^{182}W data were reported for ancient rocks from India [2,3]. Archean rocks from Dharwar Craton exhibit modern mantle-like μ^{182}W values, indicating that the Dharwar Craton mantle sources were homogenized by ~3.4-3.0 Ga [2]. New μ^{182}W data for Archean rocks including granitoids, komatiites and basalts from the Singhbhum Craton (n=7) as part of our study also show non-resolvable anomalies from the standard. Younger, Proterozoic rocks from the craton (e.g., Dalma basalt, rhyolite from the Lower Chandil Formation) also show no μ^{182}W anomalies (n=6, including replicate measurements of the rhyolite from separate chemical digestions) when compared to the modern mantle. However, dolerite dikes that span in age from ~2.8 Ga to 1.7 Ga [4] show resolvable, negative μ^{182}W anomalies (-2.6±2.2 to -4.4±3.2; n=6 including a replicate measurement of one sample from separate chemical digestions). This signature could reflect interaction with Earth's core when assuming a plume-triggered primary source close to the core-mantle boundary [4,5], resulting in small, negative μ^{182}W values. Another possibility could be a gradual addition of a late veneer component to the Earth's mantle after ~3.0 Ga, as older rocks show a missing component of the late veneer [1, 6, 7]. However, it is also suggested that addition of meteoritic material should have decreased significantly by that time [8]. Ultimately, these findings indicate that the Singhbhum mantle has preserved primordial ^{182}W heterogeneities from the Hadean eon that remained preserved until 2.0 Ga.

Acknowledgments: The corresponding author is grateful to the Alexander von Humboldt Foundation and Swiss National Science Foundation for funding the project. AR is also thankful to University of Cologne for providing the laboratory infrastructure and the use of the Multi-Collector ICPMS for ^{182}W measurements, and to IISER Thiruvananthapuram for hosting when the data interpretation was done.

References: [1] Willbold et al. (2011) *Nature* 477:195-198. [2] Ravindran et al. (2026) *Geochemical Perspectives Letters* 40:12-17. [3] Messling et al. (2023) *Geochemistry Geophysics Geosystems* 24: e2023GC011161. [4] Srivastava et al. (2019) *Precambrian Research* 329:5-17. [5] Pandey et al. (2021) *Lithos* 382-383:105959 [6] Leitzke et al. (2024) *Earth and Planetary Science Letters* 647:119022 [7] Tusch et al. (2021) *Proceedings of the National Academy of Ssciences* 118: e2012626118 [8] Marchi and Korenaga (2025) *Nature* 641: 1111-1120

DIVERSITY OF LUNAR FELDSPATHIC HIGHLAND CRUST: THE VIEW AFTER CHANDRAYAAN-3

Dwijesh Ray, Rishitosh K. Sinha, Santosh Vadawale, M. Shanmugam and Anil Bhardwaj
Physical Research Laboratory
Ahmedabad 380009, India
(dwijesh@prl.res.in)

The lunar Feldspathic Highland Crust is one of the ancient and primary planetary crusts of the solar system. The major information of geological evolution of lunar crust came from remote sensing observations, sample returns (Apollo, Luna and Chang'e 5&6) and assorted collection of lunar meteorites (>700 nos) [1]. Earlier *in situ* exploration missions provided limited geological information particularly from the equatorial regions. The lunar meteorites also present limitations due to lack of their proper geological context and source regions. Earlier studies leveraged lunar highland crusts are subdivided into ferroan anorthosite crust particularly predominant in nearside, while magnesian crust, which is comparatively common in lunar meteorites are prevalent in the farside. This geochemical distinction aligns with crustal dichotomy and its associated asymmetry [2]. The lack of information particularly from the high latitude, southern feldspathic highland terrain (FHT) remains under constrained particularly about the geological evolution of crust and its geological implications.

On August 23, 2023, India's Chandrayaan-3 successfully landed near the southern high-latitude feldspathic highlands of the Moon. The Alpha Particle X-ray Spectrometer (APXS) onboard Pragyan rover conducted in-situ elemental measurements of the lunar regolith at Shiv Sakti statio [3]. These measurements broadly support the lunar magma ocean (LMO) hypothesis, reveal an excess of sulphur indicating presence of primitive mantle materials, provide evidence for mixing of primordial feldspathic crust with deep (lower crustal and/or upper mantle) materials excavated from South Pole Aitken (SPA) Basin, and provide one of the firsts in-situ constraints on magnesian-anorthosite-like material in the lunar nearside highlands [3,4,5]. The geochemical resemblance of regolith of Shiv Sakti statio with the ancient lunar meteorite ALHA 81005 (Allan Hills, Antarctica) further proves its antiquity.

The Chandrayaan-3 APXS analyses provide an unparalleled opportunity for lunar research, providing the first, *in situ* view of the composition of the southern nearside FHT distant from Procellarum KREEP Terrane (PKT) and demonstrate that high-latitude feldspathic terrains can preserve geochemical signatures distinct from those represented by the Apollo, Luna and Chang'e sample collections, contributing to our advancement in understanding of key aspects of lunar science. A future comparative study of the lunar feldspathic crust between the farside and nearside is required to unravel the origin of the lunar dichotomy. Additionally, the lunar south pole and high latitude feldspathic terrain are important targets for planetary exploration because they have preserved ancient geological terrains and volatile-rich environments.

References

[1] Korotev, R.L. and Irving A.J. 2021, Meteoritics Planet Sci. [2] Gu Y. et al. 2026, NSR, [3] Vadawale S. et al. 2024, Nature, [4] Sinha, R. et al. 2025, Comm. Earth & Environment, [5] Ray, D. et al. 2026, npj Space Exploration.

HOW DID SOME BASALTS ON THE MOON BECOME SO RICH IN TITANIUM?

H. Moitra[1*], S. Ghosh[1], T. Mukherjee[1], S. Gupta[1] and K. K. Marhas[2]
[1]Department of Geology & Geophysics, Indian Institute of Technology Kharagpur, Kharagpur, West Bengal 721302, India; *himelamoitra@gmail.com
[2]Physical Research Laboratory, Navrangpura, Ahmedabad, Gujarat 380009, India

The TiO_2 content of lunar basaltic magmas may range from <1 wt. % to ~18 wt.% in some volcanic glasses. Theories about their origin have included processes such as partial melting of late stage ilmenite-bearing cumulates (IBCs), that crystallized from the primordia lunar magma ocean (LMO), direct assimilation of IBCs into ascending basaltic magmas, and physical mixing of the IBCs and the lunar mantle material at depths to produce Ti-rich magmas at the source [1], [2], [3]. However, matching the TiO_2 and MgO-contents of the melts produced by these processes with that of the lunar basalt magmas have always been a challenge [4]. This study tried to address this question by conducting high-pressure reaction experiments between a novel fayalite-included IBC composition and forsteritic olivine that represented the lunar mantle. Experiments were conducted between 1-3 GPa and at 1075–1500 °C in a piston cylinder apparatus, using a 0.5 inch talc+pyrex assembly. The resultant melts produced matched the range of TiO_2 content of the lunar basalt magmas, however were still relatively depleted in MgO (<6 wt.%) in most cases, especially for melts with TiO_2 content higher than 10 wt. %. To resolve this problem, thermodynamic modelling was pursued using the Magma Chamber Simulator programme that runs on the alphaMELTS engine. Fractionation modelling showed that high-melt fraction, moderately Ti-rich partial melts (6–8 wt.% TiO_2) of the IBC layer can directly fractionate to generate intermediate-Ti lunar basalts with appropriate MgO content (6-10 wt.%). Density calculations also showed that these melts are indeed positively buoyant enough relative to the lunar mantle for them to ascend to the lunar surface. Achieving suitable MgO contents in melts with higher-Ti contents required more steps with the initial fractionation being followed by subsequent assimilation and fractionation. Initial fractionation of low-melt fraction, high- TiO_2 partial melts of the IBC (11–19 wt.% TiO_2) may first produce more Ti-rich, Mg-poor compositions. Mixing of these fractionated melts with ascending low-Ti, picritic magmas and their subsequent fractionation during ascent may generate high-Ti basalt compositions with appropriate MgO contents. Density calculations show some of these resultant basalt compositions may also descend towards the core-mantle boundary. The mechanism proposed in this model succeeds in justifying the temporal distribution of the lunar high-Ti basalts while providing experimental support to the idea of gravitational overturn of the lunar mantle post LMO crystallization.

Acknowledgements: Financial support by Kalpana Chawla Space Technology Cell, IIT Kharagpur (Grant no. IIT/KCSTC/Chair/New/P/24-25/01), the Anusandhan National Research Foundation (ANRF), (erstwhile SERB), Department of Science and Technology (DST), India (grant number - CRG/2021/005527) and fellowship from CSIR, Government of India through the Shyama Prasad Mukherjee Fellowship scheme (Award letter no. SPM-06/081(0256)/2017-EMR-I).

References:

[1] Van Orman, J.A. and Grove, T.L. (2000). Meteoritics and Planetary Sciences 35: 783–794.
[2] Mallik, A. et al. (2019). Geochimica et Cosmochimica Acta 250:238–250
[3] Wagner, T.P. amd Grove, T.L. (1997). Geochimica et Cosmochimica Acta 61:1315–1327.
[4] Scholpp, J.L. and Dygert, N. (2024). Contributions to Mineralogy and Petrology 179(58).

IDENTIFICATION AND CHARACTERIZATION OF PREVIOUSLY UNIDENTIFIED EVENTS FROM APOLLO PASSIVE SEISMIC DATA

Omkar K. Gupta[1] and K. Durga Prasad[1]
[1]Planetary Sciences Division, Physical Research Laboratory (PRL), Ahmedabad, Gujarat 380059, India.
Emails: ogupta@prl.res.in; durgaprasad@prl.res.in

Introduction: Seismic investigations were a major component of the Apollo lunar exploration programme, providing observations that constrain lunar seismicity, interior structure, and near-surface properties. The Apollo Passive Seismic Experiment (APSE) produced the Moon's first long-duration seismic records. Although extensively studied, these archived data can be reprocessed using modern analysis methods to identify events that may not be represented in existing catalogues.

This study reanalyses Apollo 11 and Apollo 15 passive seismic data to identify and characterize previously unrecognized events, with particular emphasis on meteoroid impacts. The available Apollo 11 dataset has been systematically processed; the Apollo 15 interval examined spans 31 July to 24 October 1971. Waveforms are processed using the Python-based ObsPy framework. Candidate events are identified through manual inspection and evaluated using waveform morphology, frequency content, temporal coherence, and comparison with existing Apollo event catalogues to help distinguish seismic signals from instrumental noise and transient disturbances.

Candidate impact-generated signals are being investigated in terms of their waveform characteristics, frequency content, and arrival times. Further analysis will examine their propagation through lunar regolith and the shallow subsurface. These events may provide constraints on near-surface seismic scattering and attenuation, and thereby improve understanding of local regolith properties and shallow subsurface structure. The presentation will describe the processing workflow, candidate events, and their distribution.

Acknowledgments: We acknowledge research funding from the Physical Research Laboratory (PRL), Ahmedabad. The Apollo seismic data were obtained from the archive described by Nunn et al. (2022). We also thank the SIMPEX Laboratory, Planetary Sciences Division, PRL, for providing research facilities and support.

References:

[1] Nunn C., Nakamura Y., Kedar S. and Panning M. P. (2022) A new archive of Apollo's lunar seismic data. The Planetary Science Journal 3(9):219.

[2] Nunn C. et al. (2020) Lunar seismology: A data and instrumentation review. Space Science Reviews 216(5):89.

[3] Latham G., Ewing M., Press F. and Sutton G. (1969) The Apollo passive seismic experiment. Science 165:241–250.

[4] Duennebier F., Latham G. V., Nakamura Y. and Dorman H. J. (1975) Meteoroid flux from Apollo passive seismic data. Proceedings of the 6th Lunar Science Conference:2417–2426.

[5] Duennebier F. K., Nakamura Y. and Latham G. V. (1976) Meteoroid storms detected on the Moon. Science 192(4243):1000–1002.

[6] Oberst J. and Nakamura Y. (1991) A search for clustering among the meteoroid impacts detected by the Apollo lunar seismic network. Icarus 91(2):315–325.

LATE-STAGE SILICIC DIFFERENTIATION ON MARS: EVIDENCE FROM Si–Na–K-RICH MESOSTASIS AND INCLUSIONS IN THE SHERGOTTY SHERGOTTITE

Manoj Jat[1] and Dipak K. Panda[1]
[1]Planetary Sciences Division, Physical Research Laboratory (PRL), Ahmedabad 380009, Gujarat, India
(manojjat@prl.res.in)

Introduction: Whether Martian basaltic magmas can undergo sufficient closed-system differentiation to generate silica- and alkali-rich residual melts at the grain scale remains an open question in Martian magmatic evolution. We address this using the Shergotty shergottite, which preserves an interstitial Si–Na–K-rich mesostasis together with compositionally similar silica-rich inclusions hosted within merrillite grains. Using petrography, EPMA major-oxide analyses, wavelength-dispersive elemental mapping, k-means segmentation of elemental maps, and Raman spectroscopy, we characterise the mineralogy, composition, and origin of both features to evaluate whether they record genuine late-stage magmatic differentiation rather than shock melting.

Results: The mesostasis resolves into three compositional groups on the Total Alkali–Silica diagram — a high-alkali rhyolite–phonolite-boundary group, a transitional rhyolitic group, and an ultra-silicic, low-alkali tail — consistent with an independently derived, area-weighted bulk composition from segmented elemental maps. Merrillite-hosted inclusions show an analogous split: a normal population that overlaps the K-rich mesostasis specifically, and a compositionally distinct, ultra-silicic subset (~94–101 wt% SiO_2, <1.5 wt% total alkalis) that pairs instead with the SiO_2-rich mesostasis end-member. Exclusively interstitial, grain-conformable textures with no crosscutting features favour a late-stage residual-melt origin over shock generation, consistent with silicate liquid immiscibility driven by progressive Fe enrichment under near-anhydrous, moderately oxidising conditions. Rhyolite-MELTS modelling of candidate parental compositions is used to test whether this two-population structure is consistent with a single liquid line of descent or instead requires unmixing into immiscible conjugates.

Conclusions: Together with the granitic clasts of NWA 7533, trachytic float rocks at Gale Crater, and orbital felsic detections, the Shergotty mesostasis and its merrillite-hosted inclusions extend the evolved silicic differentiation record on Mars to the grain-interstitial scale, even in a comparatively young (~165 Ma) Amazonian basalt.

Keywords: Mars; shergottite; silicate liquid immiscibility; mesostasis; inclusions

RECONSTRUCTING THE GEOLOGICAL PAST OF MARS: INSIGHTS FROM OLIVINE ALTERATION IN THE NAKHLITE YAMATO-593

Aditya Das[1], Dwijesh Ray[1]
[1]*Physical Research Laboratory, Ahmedabad, Gujarat 380009*

Olivine alteration provides an important record of water–rock interaction and can be used to reconstruct the physicochemical conditions that prevailed during the geological evolution of Mars. The Martian nakhlite Yamato-593 (Yam-593) contains alteration features within olivine grains that provide an opportunity to investigate the nature of aqueous activity in the Martian crust. Petrographic observations show that alteration is strictly confined to fractures within olivine grains, suggesting highly localized fluid–rock interaction. Raman spectroscopic analyses confirm the presence of smectite-group clay minerals, particularly saponite, together with Fe-oxide phases. This association of clay minerals and Fe oxides represents the mineral assemblage commonly referred to as iddingsite.

The observed mineral assemblage and fracture-controlled alteration were used to reconstruct the geological conditions under which these secondary phases could have formed. Geochemical simulations were performed to examine the evolution of the reacting fluid and the conditions that favour the formation of the observed alteration products. The results indicate that limited water–rock interaction under relatively low-temperature conditions can produce alteration assemblages comparable to those observed in Yam-593. The progressive interaction between the fluid and olivine also modifies the fluid chemistry, influencing the stability and evolution of secondary minerals. The modelled alteration behaviour is consistent with the restricted nature of alteration observed petrographically and with the Fe-rich character of the Yam-593 olivine.

The combined mineralogical observations and modelling results suggest that the alteration recorded by Yam-593 developed under low-temperature, localized, and water-limited conditions, rather than through prolonged and extensive fluid circulation. The study demonstrates how alteration minerals preserved within Martian meteorites can be used to reconstruct the physicochemical environment of the Martian crust and provides further insight into the nature of aqueous activity during the geological evolution of Mars.

TEXTURAL STUDY OF THE MARTIAN METEORITE - SHERGOTTY

Mahima Sharma[1], Nachiketa Rai[1,2] and **Kuljeet Kaur Marhas[3]**, [1]Centre for Space Science and Technology, IIT Roorkee (mahima_s@sst.iitr.ac.in; n.rai@es.iitr.ac.in) , [2]Department of Earth Sciences, IIT Roorkee, [3]Physical Research Laboratory, Ahemadabad

Abstract

The only currently available samples from Mars and studied in terrestrial laboratories are Martian meteorites. These meteorites were ejected from Mars by high-energy impact events, during which fragments of Martian rocks attained sufficient velocities to escape the planet's gravitational field (escape velocity ~5 km/s [1]), potentially through near-surface spallation [2]. Traditionally, Martian meteorites have been categorized into three main groups: called the Shergottites, Nakhlites, and Chassignites (SNC) [3]. Based on their mineralogical and textural characteristics, shergottites are divided into basaltic, lherzolitic (or olivine-, pyroxene-phyric, and olivine-phyric [4]. Shergottites record complex magmatic histories involving varying degrees of partial melting, fractional crystallization, and mantle-source heterogeneity [5]. Mineralogically, shergottites exhibit similarities to terrestrial mafic igneous rocks, although they are petrologically and chemically distinct from other basaltic achondrites [6]. Shergotty is a basaltic shergottite with a reported crystallization age of approximately 165 ± 5 Ma [7]. It comprises predominantly augite and pigeonite, along with maskelynite, fayalite, titanomagnetite, ilmenite, pyrrhotite, apatite, whitlockite, baddeleyite, and silica-bearing mesostasis. The pyroxene grains in Shergotty are coarse-grained and exhibit a preferred orientation, potentially reflecting processes such as crystal accumulation or flow segregation. However, some pyroxenes exhibit continuous compositional zoning, suggesting crystallization from an evolving magma rather than a simple cumulate origin [8]. Evidence of intense shock metamorphism is also preserved in Shergotty, notably in the form of maskelynite, which is produced by shock transformation of plagioclase under high-pressure conditions, commonly associated with pressures of several tens of GPa [9].

The present study focuses on the mineralogical and petrographic characterization of the Shergotty meteorite, with particular emphasis on its textural relationships and mineral phases. Petrographic observations are used to characterize mineral zoning, alteration features, and shock-related phases such as maskelynite. The study aims to provide insights into the textural evolution and mineralogical characteristics of Shergotty, contributing to a better understanding of its magmatic crystallization and post-crystallization history.

Acknowledgement: Mahima Sharma gratefully acknowledges the receipt of DST-INSPIRE JRF.

References: [1] Fritz, J., Artemieva, N., & Greshake, A. (2005). Ejection of martian meteorites. Meteoritics & Planetary Sciences, 40(9–10), 1393–1411. https://doi.org/10.1111/j.1945-5100.2005.tb00409.x. **[2]** Head, J. N., Melosh, H. J., & Ivanov, B. A. (2002). Martian meteorite launch: High-speed ejecta from small craters. Science, 298(5599), 1752–1756. https://doi.org/10.1126/science.1077483. **[3]** Udry, A., Howarth, G. H., Herd, C. D. K., Day, J. M. D., Lapen, T. J., & Filiberto, J. (2020). What Martian meteorites reveal about the interior and surface of Mars. Journal of Geophysical Research: Planets, 125, e2020JE006523. https://doi.org/10.1029/2020JE006523. **[4]** Goodrich C. A. 2002. Olivine-phyric Martian basalts: A new type of shergottite. Meteoritics & Planetary Science 37:B31–B34. **[5]** Symes S. J. K., Borg L. E., Shearer C. K., and Irving A. J. 2008. The age of the Martian meteorite Northwest Africa 1195 and the differentiation history of the shergottites. Geochimica et Cosmochimica Acta 72:1696–1710. **[6]** Papike, J. J., Karner, J. M., Shearer, C. K., & Burger, P. V. (2009). Silicate mineralogy of martian meteorites. *Geochimica et Cosmochimica Acta*, *73*(24), 7443-7485. **[7]** Nyquist, L. E., Bogard, D. D., Shih, C. Y., Greshake, A., Stöffler, D., & Eugster, O. (2001). Ages and geologic histories of Martian meteorites. *Space Science Reviews*, *96*(1), 105-164. **[8]** Stolper, E. M., & McSween, H. Y. (1979). Petrology and origin of the Shergottite meteorites. Geochimica et Cosmochimica Acta, 43(9), 1475 1498. https://doi.org/10.1016/0016-7037(79)90142-x. **[9]** Laul, J. C. (1986). The Shergotty consortium and SNC meteorites: An overview. *Geochimica et Cosmochimica Acta*, *50*(6), 875-887.

PETROGRAPHIC AND MINERALOGICAL INSIGHTS INTO WINONA AND NWA 14344: IMPLICATIONS FOR WINONAITE PETROGENESIS

Nishant Pandey[1], Nachiketa Rai[1,2], and Kuljeet Kaur Marhas[3], [1]Centre for Space Science and Technology, IIT Roorkee (nishant_p@csst.iitr.ac.in), [2]Department of Earth Sciences, IIT Roorkee, [3]Physical Research Laboratory, Ahemdabad

Introduction: Primitive achondrites provide an important record of the earliest stages of thermal processing and differentiation of chondritic planetesimals. Unlike fully differentiated achondrites, primitive achondrites retain substantial portions of their original chondritic mineralogy and textures while recording varying degrees of metamorphism, partial melting, and melt extraction. They therefore provide an intermediate record between relatively undifferentiated chondritic materials and bodies that underwent extensive silicate and metal–silicate differentiation [1,10]. The acapulcoite–lodranite clan, winonaites, and brachinites constitute important groups within this class. Winonaites are characterized by near-chondritic bulk compositions but display textural evidence of low degrees of partial melting and heterogeneous thermal processing. Grain sizes vary widely, from fine-grained Pontlyfni to medium-grained Winona and coarse-grained varieties such as Tierra Blanca, suggesting variable thermal histories [1,2]. Mineralogically, winonaites are relatively reduced, with olivine compositions typically ranging from $Fa_{1–9}$, distinctive oxygen isotopic signatures ($\Delta^{17}O \approx -0.40$ to -0.73‰), and relatively high abundances of Fe–Ni metal and troilite compared to many chondritic groups [1,3,4]. Based on mineralogical and isotopic similarities with silicate inclusions in IAB irons, winonaites are commonly associated with the winonaite–IAB complex [5,6].

Despite extensive previous work [1,11], constraints on the evolution of the winonaite–IAB parent body remain limited by the relatively small number of well-characterized samples and the incomplete integration of petrographic, mineralogical, and geochemical datasets. This study addresses these gaps through a comparative investigation of two winonaite meteorites, Winona and NWA 14344, using detailed petrography, phase characterization, and bulk trace-element geochemistry. Winona shows heterogeneous textures, with both relatively coarse-grained and fine-grained regions. The coarse-grained areas contain interlocking grains with well-developed grain boundaries, whereas the finer regions comprise smaller grains with locally irregular or rounded morphologies. Variations in mineral distribution over short distances further suggest heterogeneous thermal processing and variable degrees of recrystallization and textural modification. In contrast, NWA 14344 exhibits relatively coarse-grained textures with metal–troilite veins, potentially indicating brecciation and localized impact-related thermal modification or partial melting. The mineral assemblages are dominated by silicates, Fe–Ni metal, and sulfides, with minor accessory phases. The observed textures are broadly comparable to those reported in other winonaites, where variations in grain size, heterogeneous mineral assemblages, and the distribution of Fe–Ni metal and Fe–S-rich phases have been associated with thermal processing, brecciation, and metamorphism [1,11]. The presence of interstitial and locally interconnected Fe-rich phases in the studied samples may indicate redistribution of Fe-rich material during thermal processing, further supporting heterogeneous thermal and petrological evolution within the winonaite–IAB parent body.

Acknowledgments: I would like to express my sincere thanks to MHRD for providing me the fellowship.

References: [1] Benedix, G. K., McCoy, T. J., Keil, K., Bogard, D. D., & Garrison, D. H. (1998) *GCA*, *62*(14), 2535-2553. [2] Benedix, G. K., McCoy, T. J., Keil, K., & Love, S. G. (2000) *Meteoritics & Planet. Sci.*, *35*(6), 1127-1141. [3] Clayton, R. N., & Mayeda, T. K. (1996) GCA, 60(11), 1999-2017. 210 [4] Greenwood, R. C., Franchi, I. A., Gibson, J. M., & Benedix, G. K. (2012) GCA, 94, 146-163. [5] Bild, R. W. (1977) *GCA*, *41*(10), 1439-1456. [6] Graham A.L. et al. (1977). Min. Mag. 41, 201 [7] Choi, B. G., Ouyang, X., & Wasson, J. T. (1995) *GCA*, *59*(3), 593-612. [8] Wasson, J. T., & Kallemeyn, G. W. (2002) GCA, 66(13), 2445-2473. [9] Kelly, W. R., Rambaldi, E. R., & Larimer, J. W. (1977) In *International Astronomical Union Colloquium* (Vol. 39, pp. 405-413). Cambridge University Press. [10] Takeda, H., Bogard, D. D., Mittlefehldt, D. W., & Garrison, D. H. (2000) *GCA*, *64*(7), 1311-1327. [11] Hunt, A. C., Benedix, G. K., Hammond, S. J., Bland, P. A., Rehkämper, M., Kreissig, K., & Strekopytov, S. (2017) GCA, 199, 13-30.

PROBING THE ORIGIN OF EARTH'S APPARENT NON-CHONDRITIC Mg ISOTOPE SIGNATURE

Soumyadip Haldar*[1], Rabindranath Mondal[1], Swastika Chatterjee[1]
[1]National Centre for High-Pressure Studies and Department of Earth Sciences,
Indian Institute of Science Education and Research-Kolkata,
Nadia, West Bengal, India.
*E-mail: sh21ip012@iiserkol.ac.in

The mantle constitutes the largest reservoir of Mg on Earth. The ability to use Mg isotopes to distinguish between undifferentiated and differentiated planetesimals is still a topic of ongoing research. There is also a continued debate regarding whether the Mg isotope composition of the Earth is chondritic or non-chondritic [1-7]. Since Earth's mantle has undergone extensive differentiation, understanding the distribution of Mg isotopes among its major mineral phases as a function of depth is essential for assessing how differentiation may have influenced the isotopic composition of different mantle layers.

In this study, we investigate equilibrium Mg isotope fractionation among the major mineral phases of Earth's mantle using quantum-chemical density functional theory (DFT) and density functional perturbation theory (DFPT). We consider the major mineralogical transitions from olivine through wadsleyite and ringwoodite to bridgmanite, as well as the transformation of bridgmanite to post-perovskite in the lowermost mantle [8,9]. Our calculations (i) predict significant Mg isotope fractionation between major mantle minerals, (ii) demonstrate the importance of crystallographically inequivalent Mg sites, and (iii) highlight the role of Fe incorporation in modifying Mg isotope fractionation.

We have also modelled the Mg isotope fractionation between the perovskite rich mantle (the first phase to have crystallized out of the magma ocean) and the residual melt (from which the upper mantle minerals crystallized) during magma ocean cooling under lower mantle conditions. If such primordial signature is not destroyed, and at least partially preserved through Earth's history, significant isotope heterogeneity could still exist between upper and lower mantle. This heterogeneity may manifest itself in the form of samples from plumes having roots within deep mantle.

Our results provide a mineral-physics basis for understanding the distribution of Mg isotopes during planetary differentiation and suggest that preferential storage of lighter Mg isotopes in the deep lower mantle could contribute to the apparent non-chondritic Mg isotopic composition of Earth.

References:

[1] B. Bourdon, E. T. Tipper, C. Fitoussi, and A. Stracke, Geochimica et Cosmochimica Acta, vol. 74, no. 17, pp. 5069–5083, Sep. 2010

[2] M. R. Handler, J. A. Baker, M. Schiller, V. C. Bennett, and G. M. Yaxley, Earth and Planetary Science Letters, vol. 282, no. 1, pp. 306–313, May 2009.

[3] F.-Z. Teng, M. Wadhwa, and R. T. Helz, Earth and Planetary Science Letters, vol. 261, no. 1, pp. 84–92, Sep. 2007.

[4] F.-Z. Teng et al., Geochimica et Cosmochimica Acta, vol. 74, no. 14, pp. 4150–4166, Jul. 2010.

[5] U. Wiechert and A. N. Halliday, Earth and Planetary Science Letters, vol. 256, no. 3, pp. 360–371, Apr. 2007.

[6] R. C. Hin et al., Nature, vol. 549, no. 7673, pp. 511–515, Sep. 2017.

[7] X.-N. Liu et al., Geochimica et Cosmochimica Acta, vol. 358, pp. 12–26, Oct. 2023.

[8] D. J. Frost, Elements, vol. 4, no. 3, pp. 171–176, Jun. 2008.

[9] M. Murakami, K. Hirose, K. Kawamura, N. Sata, and Y. Ohishi, Science, vol. 304, no. 5672, pp. 855–858, May 2004.

GEOCHEMICAL INSIGHTS INTO BASALT WEATHERING ON MARS: A CASE STUDY OF LYOT CRATER

S. Bhowmik[1], A. Mukherjee[1] and S. Gupta[1]
[1]Department of Geology and Geophysics, Indian Institute of Technology Kharagpur, Kharagpur, West Bengal 721302, India; Email: snehabhowmik.sb@gmail.com

Introduction: Understanding the geological and geochemical processes of Mars is very important to reconstruct its past environmental condition and evolution, and for assessing its potential habitability. Orbital spectroscopy observations and in-situ rover missions have revealed widespread phyllosilicates, such as smectites, on the martian surface, indicating extensive water-rock interaction and a long-term aqueous history [1,5]. So, it is therefore essential to explore basalt weathering for constraining the formation history of these minerals and the climatic evolution of Mars. As direct access to martian samples is limited, geochemical modeling has become an essential tool for reconstructing these processes. Here, we apply this particular approach to investigate the basalt weathering conditions and the formation of secondary minerals within Lyot Crater. It is an Amazonian-aged impact crater with a diameter of 215 km, located in the northern lowlands near the dichotomy boundary of Mars. Earlier studies revealed that significant amounts of Fe/Mg phyllosilicates, chlorite, illite/muscovite, prehnite, and other unidentified hydrated minerals are present in this crater and proposed that they formed through either pre-impact alteration or syn-impact basalt weathering [4]. Modeling the origin of these secondary minerals can therefore help constrain the past climate of Lyot Crater. Moreover, because the Amazonian is considered a dry period in martian history [3], this investigation can provide insights into the possibility of aqueous activity during this arid period.

Methods: Geochemical modeling was performed using the REACT module of Geochemist's Workbench (GWB) Software. The initial basaltic rock composition was based on in-situ analyses at the Zhurong rover landing site [6], and the aqueous phase was represented by a groundwater composition developed for the Gale Crater region [2]. The simulations were run under closed-system, hydrothermal basalt weathering conditions, with varying parameters.

Results and Implications: The modeling successfully reproduces the secondary mineral assemblages observed in Lyot Crater, supporting the syn-impact hydrothermal formation scenarios proposed previously for the region [4]. These results constrain Amazonian-age aqueous alteration processes and highlight Lyot Crater as an useful target for future investigations of aqueous processes and habitability.

References: [1] Ehlmann B. L. and Edwards C. S. (2014) *Annual Review of Earth and Planetary Sciences* 42:291-315. [2] Kikuchi S. and Shibuya T. (2021) *Minerals* 11:341. [3] Kolkas M. M. (2026) *The Professional Geologist* Jan-Feb-Mar:7-15. [4] Pan L. and Ehlmann B. L. (2018) *Journal of Geophysical Research: Planets* 123:1618-1648. [5] Sheppard R. Y. et al. (2021) *Minerals* 11:986. [6] Zhao Y. Y. S. et al. (2023) *National Science Review* 10:nwad056.

SPECTRAL ANOMALIES AND POSSIBLE IRON-METEORITE ORIGINS OF FE-RICH FLOAT ROCKS AT JEZERO CRATER, MARS: A MASTCAM-Z AND SUPERCAM INVESTIGATION.

S. Sarkar and R. Chakrabarti, Centre for Earth Sciences, Indian Institute of Science, Bangalore, India.
subhamrajsarkar@gmail.com.

Float rocks on Mars provide insights into impact processes, sediment transport, igneous diversity, and aqueous alteration [1]. Multispectral observations from Mars rovers have also enabled the identification of candidate meteorites based on their distinctive spectral characteristics [2]. At Jezero crater, the combined use of Mastcam-Z multispectral imaging and SuperCam visible/near-infrared (VIS/IR) spectroscopy has revealed substantial diversity in iron mineralogy, reflecting variations in lithology, oxidation, and water–rock interactions [1,3]. Here, we investigate two anomalously Fe-rich float rocks, 'Tower of Ra' and 'Phantom Creek', encountered by the Perseverance rover at Site 56 on Sols 1238 and 1241, respectively, to assess their spectral and compositional characteristics and evaluate their possible origin.

SuperCam laser-induced breakdown spectroscopy (LIBS) measurements acquired at ten observation points on 'Phantom Creek' and five on 'Tower of Ra' yield apparent FeOT abundances of approximately 82–85 wt.% and 52–78 wt.%, respectively. Mastcam-Z I/F observations of 'Phantom Creek' reveal a dark, low-albedo surface with subdued spectral characteristics and no diagnostic mafic silicate absorption features, challenging its earlier interpretation as an olivine-rich boulder. The exceptionally high apparent Fe abundances and unusual spectral characteristics of 'Tower of Ra' and 'Phantom Creek' distinguish them from typical igneous and sedimentary lithologies encountered at Jezero crater. Their characteristics raise the possibility that they represent iron meteorites or their altered remnants, consistent with the identification of other candidate Fe-rich float rocks at Mars, including 'Phippsaksla' at Jezero crater [4].

The subdued Mastcam-Z spectrum of 'Phantom Creek' does not replicate the smoothly increasing, red-sloped reflectance profile documented for candidate iron meteorites at Gale crater [2]. Furthermore, the limited representation of extremely Fe- and Ni-rich lithologies in current SuperCam LIBS training libraries introduces inherent calibration uncertainties [4,5]. Because Mastcam-Z I/F data are unavailable for 'Tower of Ra' and passive VIS/IR spectra remain broadly compatible with various Fe-oxide assemblages, alternative origins, including Fe-rich hydrothermal precipitates or secondary weathering products, cannot be definitively excluded. Discriminating between meteoritic versus secondary hydrothermal models requires targeted multi-instrument comparative analyses, improved high-Fe calibration datasets, and high-resolution textural context to constrain the complex alteration history of these unusual float rocks.

Acknowledgments: SS acknowledges the financial support provided by Anusandhan National Research Foundation (ANRF) through the National Post Doctoral Fellowship scheme (vide file no. PDF/2025/006616). All the data related to this study was acquired from https://pds-geosciences.wustl.edu/missions/mars2020/index.htm and PDS Geosciences node is duly acknowledged.

References: [1] Kathir B. S. et al. (2025) *Journal of Geophysical Research: Planets* 130, e2024JE008702. [2] Wellington D. F. et al. (2018) *LPSC XLIX,* Abstract #1832. [3] Mandon L. et al. (2024) *Journal of Geophysical Research: Planets* 129, e2023JE008254. [4] Rudin M. C. et al. (2026) *LPSC LVII,* Abstract #1180 [5] SuperCam LIBS composition documentation retrieved on 12th October 2026 from https://an.rsl.wustl.edu/help/Content/About%20the%20data/Data%20products/M20/SCLIBS%20composition.htm

THE PAH PROBLEM IN THE ISM – BOTTOM-UP OR TOP-DOWN

B Sivaraman, A Roy, W Khan, R Ramachandran, J K Meka, V Venkataraman,
B N Rajasekhar, P Janardhan, A Bhardwaj, N J Mason
Physical Research Laboratory, Ahmedabad, India.
Raman Research Institute, Bangalore, India.
Space Physics Laboratory, Thiruvananthapuram, India.
Institute of Astronomy Space and Earth Science, Kolkata, India.
University of Kent, Canterbury, UK.
Email – bhala@prl.res.in

Introduction: Polycyclic Aromatic Hydrocarbons (PAH) are at the center stage of carbon chemistry in the interstellar medium (ISM). The formation of PAH are under investigation for over many decades. To-date there are two proposed pathways in synthesizing PAH molecules: the bottom-up and the top-down formation routes. There exist experimental evidences to support both the formation pathways in explaining the PAH presence in the ISM. However, the question arises whether we know the efficient and feasible pathways owing to the reactant availability in ISM. While approaching this problem we also have to consider both the eras of astrochemistry – before and after the dust.

Experiments and results: Using the experimental systems that are capable of recreating the cold conditions and shock fronts in the ISM, we carried out experiments to understand the PAH formation from simple to complex carbon containing molecules. This ranges from single carbon containing molecule – carbon monoxide (CO) to many carbon containing molecules such as benzonitrile (C_6H_5CN) on cold ISM dust and amorphous carbon (a-C) to benzene (C_6H_6) in shock fronts.

The results obtained suggest an efficient pathway for PAH formation. In this meeting, we will present the solution [1,2] to the long standing PAH formation problem in the pre-and-post dust ISM.

References:

[1] Arijit et al., Advances in Space Research, 70:2571-2581.
[2] Wafikul et al., Life Sciences in Space Research (Astrochemistry special issue), 49: 94-100.

MID-INFRARED SPECTROSCOPIC INVESTIGATION OF A SAMPLE OF ASTEROIDS.

V. Venkataraman[1], B. Sivaraman[2], A. Roy[3] and Thirukumaran[4]
[1]Space Physics Laboratory, Vikram Sarabhai Space Center, Thiruvananthapuram
e-mail: v.venkataraman@gmail.com
[2]Physical Research Laboratory, Ahmedabad
[3]Indian Institute of Technology, Kharagpur
[4]Chikkiah Government College of Arts and Science , Erode

Introduction: Asteroids are recognized as primary tracers of the evolutionary history of the Solar System. Their surface mineralogy directly reflects the chemical reservoir and processing conditions of the early solar nebula [1]. Conventionally, these surface compositions are investigated through visible to near-infrared (0.4 - 2.5 μm) spectroscopy, which probes electronic transitions in surface minerals [2]. Current asteroid taxonomies classify these bodies using key absorption features and continuum slopes observed at these wavelengths. Alternatively, mid-infrared (MIR, 5 - 38 μm) spectroscopy directly detects fundamental molecular vibrational modes, offering detailed insight into the mineral lattice [3]. We present a mid-infrared spectral analysis of a sample of asteroids, spanning distinct dynamical populations - including Main-Belt, Jupiter Trojan, and Near-Earth asteroids - to evaluate variations across their surface regoliths. The impacts of space weathering on these mid-infrared signatures will be discussed.

References:

[1] DeMeo, F. E., Carry, B., (2014), *Nature*, 7485, 629 – 634
[2] DeMeo, F. E., et al., (2009), *Icarus*, 202(1), 160–180.
[3] Lim L. F., et al., (2005), *Icarus,* 173. 385- 408.

PULSED LASER IRRADIATION OF THREE CM CHONDRITES: MICROMETEORITE RELATED SPACE WEATHERING ON ORGANIC-RICH ASTEROIDS

S. P. Das[1*], A. Maturilli[2], K. Rammelkamp[3], A. Van den Neucker[2], S. Schroeder[3], N.Shukla[4], G.Thangjam[1] , S. S. Rout[1]

[1]School of Earth and Planetary Sciences, NISER, HBNI, Bhubaneswar,752050, India. [2]Institute for Planetary Research. [3]Institute of Optical Sensor Systems, DLR, Rutherfordstrasse 2, 12489, Berlin, Germany. [4]Applied Physics and Material Engineering, NIT Patna, 800005, India.

*Email: swarnaprava.das@niser.ac.in

Introduction: Space weathering (SW) modifies airless planetary surfaces through micrometeorite impacts and solar-wind irradiation, producing changes in their mineralogy, chemical, and optical properties [1,2]. Returned samples and spacecraft observations of the C-type asteroids Bennu and Ryugu reveal complex SW signatures, including darkening, spectral bluing, and modification/weakening of the ~2.7 μm OH absorption [3–5]. Similar effects have been observed in laboratory simulations of pulsed-laser irradiation on CM materials, including changes in spectral slope, albedo, and the ~0.7 and ~3 μm hydration bands, with the magnitude and direction of these effects depending on the material's initial composition [6–8]. Here, we investigate simulated SW effects in three CM chondrites with varying degrees of aqueous alteration to understand the effect of SW on organic-rich asteroids.

Samples and Methods: Three CM chondrites, Aguas Zarcas (AGZ; fall), Jbilet Winselwan (JBL; find), and Mukundpura (MKD; fall), were investigated. AGZ and JBL pellets were irradiated under high vacuum (~8×10^{-5} mbar) using a 1064 nm Nd:YAG laser (~6 ns, 10 mJ $pulse^{-1}$) at single laser pulse per spot (1-ps) and five consecutive pulses per spot (5-ps). Reflectance spectra of the pellets were acquired over a 0.5–18 μm spectral range using a Bruker Vertex 80V FTIR spectrometer. The infrared spectra from polished section were obtained using Bruker Hyperion 2000 Micro-FTIR in the VNIR + MIR range at an optical magnification of 15x and a resolution of 4 cm^{-1}. Raman spectra were obtained from the unirradiated and irradiated surfaces to evaluate changes in the carbonaceous material. Post-irradiation surface textures were examined using a Zeiss Gemini 450 scanning electron microscopy (SEM) and lamellas for transmission electron microscopy (TEM) study were prepared using a JIB-4700F focused ion beam scanning electron microscope (FIB-SEM).

Results and Discussions: Laser irradiation produces rapid darkening accompanied by minor bluing and flattening of the VNIR spectra in both AGZ and JBL, together with suppression of the ~0.7 μm absorption feature. The ~2.7 μm OH/H_2O band increases in depth after 1-ps irradiation but decreases at 5-ps and shifts toward longer wavelengths, indicating transient redistribution of water followed by progressive dehydration and modification of phyllosilicates. In the MIR, the Si–O stretching bands show little positional change in AGZ but shift toward longer wavelengths in JBL, demonstrating a sample-dependent response to irradiation. Raman spectral parameters show no systematic changes following irradiation, suggesting that the carbonaceous material remains comparatively insensitive to the short experimental timescales investigated. The observed VNIR darkening and bluing/flattening are likely related to the formation and redistribution of fine-grained opaque phases, including Fe-sulfides, magnetite, Fe–Ni metal, and carbonaceous material, produced through melting and alteration of Fe-sulfides, tochilinite, and Fe-rich phyllosilicates, with possible contributions from carbonization of organic matter.

Conclusion: Our results demonstrate that simulated micrometeorite impacts can induce dehydration of phyllosilicates and generate micro- to fine-grained opaque phases that substantially modify the optical properties of CM material. The contrasting responses of AGZ and JBL highlight the role of initial mineralogy and aqueous alteration in controlling SW signatures. Ongoing TEM investigations will further constrain the nanoscale mineralogical, textural, and compositional changes produced by laser irradiation, and these results will be presented to provide a more comprehensive understanding of the mechanisms responsible for the observed spectral modifications. Together, these observations provide laboratory constraints for interpreting diverse SW signatures on organic-rich carbonaceous asteroids.

References: [1] Chapman C. R. (2004), *Annu. Rev. Earth Planet. Sci.*, **32**, 539–567. [2] Clark B. E. et al. (2002), *Asteroids III*, 585–599. [3] Matsuoka M. et al. (2023), *Commun. Earth Environ.*, **4**, 335. [4] Noguchi T. et al. (2023), *Nat. Astron.*, **7**, 170–181. [5] Keller L. P. et al. (2025), *Nat. Geosci.*, **18**, 825–831. [6] Matsuoka M. et al. (2015), *Icarus*, **254**, 135–143. [7] Matsuoka M. et al. (2020), *Astrophys. J. Lett.*, **890**, L23. [8] Thompson M. S. et al. (2020), *Icarus*, **346**, 113775.

SOLAR- AND COSMIC RAY TRACKS IN REGOLITH BRECCIA METEORITES.

N. Thomas[1], S.S. Rout[2,3]
[1]Indian Institute of Science Education and Research, Berhampur (neetha21@iiserbpr.ac.in),
[2]National Institute of Science Education and Research, Bhubaneswar, Jatni, Khurdha, Odisha, India, 752050.
[3]Homi Bhabha National Institute, Training School Complex, Anushaktinagar, Mumbai, India.
*neetha21@iiserbpr.ac.in

Introduction: Gas-rich regolith breccia meteorites contain high concentrations of solar wind-implanted gases which is evidence for exposure of the surface of their parent asteroids to Solar Energetic Particles (SEPs). These SEPs can penetrate only up to a few millimetres of the regolith material [1]. Heavy ions belonging to the iron group (Z>26) produce a narrow trail of damage (<50 Å radius) in the crystal lattice of the regolith grains. This trail of damage in crystal structures is called a track and can be revealed through chemical etching methods or can be directly imaged using a transmission electron microscope (TEM) [2]. The study of these track-rich grains, which were exposed directly to the solar wind, within regolith breccia meteorites helps in understanding the exposure history and dynamics of regolith materials on their parent asteroids, possible variation in solar activity in the past and in understanding surface processes on asteroids. Here we report the study of SEP tracks in pyroxene grains from the aubrite meteorites Khor Temiki and Kapoeta.

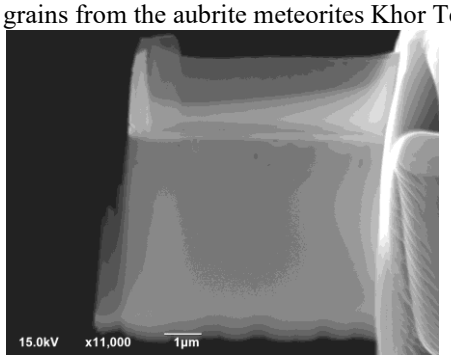


Figure 1: Secondary electron (SE) image of a focused ion beam (FIB) lamella of a pyroxene grain from Kapoeta.

Samples and Methods: Pyroxene grains of size range 80-200µm from the meteorites Khor Temiki and Kapoeta were selected since it has been shown to contain high concentrations of solar wind-implanted gases and were separated using the freeze-thaw technique followed by centrifugation [3,4]. The grains were then embedded in epoxy resin and polished using silicon carbide (SiC) foils and diamond pastes of different grit sizes. The polished epoxy mount was partially etched for 5 minutes in a boiling NaOH and water mixture in a 6:4 ratio at 120-160°C [5]. The etched grains were then examined under an optical microscope to identify those with a high track density, and a Zeiss Gemini 560 scanning electron microscope (SEM) was used to image grains with a higher track-density gradient. Two cross-sectional lamellas for TEM study were prepared using a JEOL JIB-4700F focused ion beam scanning electron microscope (FIB-SEM).

Results and Discussion: In Khor Temiki, out of 5570 grains studied, 24 grains exhibited high track densities ($6.3\pm0.5\times10^6$ tracks/cm^2), while the remaining grains showed no elevated densities. Meanwhile, out of 1300 grains studied, Kapoeta yielded 11 grains with high track densities and 2 grains with track density gradients, where the track density decreases from $(3.9\pm0.2)\times10^8$tracks/cm² at the rim to $(1.7\pm0.3)\times10^8$tracks/cm² towards the centre. Widespread darkening was also observed along rims and linear fractures of the grains after etching. The higher track densities and gradients in the pyroxene grains from Kapoeta and Khor Temiki indicate exposure to both solar cosmic rays (SCR) and galactic cosmic rays (GCR). High track density grains likely resided within the upper few centimetres of their parent asteroid regolith, while the grains exhibiting high track density gradients were located directly on the surface. Such grains can be used for estimating the surface exposure ages of grains using the known track production rates at 1 AU [1]. The grains from Kapoeta showing a gradient in track density are grains from the surface of the parent asteroid of Kapoeta, which is likely a V-type asteroid or Vestoids. These grains therefore can provide valuable information about products of interaction of solar wind with regolith on these asteroids and the rate of solar wind-induced space weathering.

Conclusion and Future Work: Various pyroxene grains showing high SEP track density gradient were found within the Kapoeta and Khor Temiki regolith breccia meteorites. These grains were directly exposed to the solar wind ions on the surface of their parent asteroids. Results from ongoing TEM studies of the etched grains will be used for estimating surface exposure ages and in understanding regolith dynamics on their parent asteroids.

Acknowledgements: We would like to extend our appreciation to the Centre for Interdisciplinary Sciences at NISER and SATHI-CISCoM at IIT, Hyderabad, for providing the necessary facilities and equipment; Prof. Maibam Baidyananda from the Department of Geological Sciences, Manipur University, and Prof. Narendra Bhandari and Nirjhari Sinha for assistance and helpful discussions regarding the sample preparation process

References: [1] Keller, L. P. et al. (2021) *Meteoritics & Planetary Science* 56.9:1685-1707. [2] Fleischer, R. L. et al. (2022). *Nuclear tracks in solids: principles and applications*. Univ of California Press. [3] Eberhardt, P. et al. (1966). *Earth and Planetary Science Letters* 1.1:7-12. [4] Eberhardt, P. et al. (1965). *Tschermaks min u petr Mitt* 10:535–551. [5] Lal, D. et al. (1968). In: *Earth and Planetary Science Letters* 5:111–119.

STONY METEORITES AT HYPERVELOCITIES IN VENUSIAN ATMOSPHERE – AN EXPERIMENTAL APPROACH

Arijit Roy[1,2,*], Jaya Krishna Meka[1], Ragav Ramachandran[3], Piyush Mishra[2], Bijesh Malla[4], T Pradeep[4], V Venkataraman[5], B N Rajasekhar[6], Anil Bhardwaj[1], Janardhan Padmanabhan[1], Nigel John Mason[7], Bhalamurugan Sivaraman[1,*]

[1] Physical Research Laboratory, Ahmedabad, 38009, India

[2] IIT-Kharagpur, Kharagpur, India.

[3] Raman Research Institute, Bengaluru, Karnataka, 560080, India

[4]Indian Institute of Technology-Madras, Chennai, 600036, India.

[5]Space Physics Laboratory, Thiruvananthapuram, 695022, India

[6] Institute of Astronomy Space and Earth Science, Kolkata, 700054, India.

[7] University of Kent, Canterbury CT2 7NH, United Kingdom

*Corresponding authors - arijit6769@gmail.com & bhala@prl.res.in

Introduction: The ultraviolet (UV) absorbers in Venusian atmosphere is an unsolved puzzled to-date although many chemical species are proposed to be the carriers. The chemical diversity in the Venusian atmosphere makes it difficult to pin-point the chemical species, or a combination of chemical species, that is responsible for such strong UV absorption. Nevertheless, the formation pathways of those proposed unknown UV absorbers are investigated and are attributed to the exogenous delivery of chemical inventories in addition those synthesized due to the photon induced reactions in the Venusian atmosphere. There may exists other formation pathways of those unknown UV absorbers.

Experiment and Result: We have recreated the ablation of stony meteorite while it enters the Venusian CO_2 atmosphere at hypervelocities using the High Intensity Shock Tube for Astrochemistry (HISTA). Silicon (Si) and Iron (Fe) nano-powder was mixed and used as an analogue representing the major composition of the grains in stony meteorites. CO_2 gas along with Ar in the driven section of HISTA is used. The shock processing of this gas-grain mixture resulted in the melting of the grains and the dissociation of CO_2 enabling reactions between the Si, Fe, C and O atoms. The result suggest the significant role of CO_2 in adding the organic inventory to the Venusian atmosphere. The impact of hypervelocity bolides can therefore synthesize new chemical species in reactive atmospheres and leave behind minor concentrations of unknown UV absorbers.

THE LARGEST PEPTIDE-LIKE MOLECULE IN THE ISM - PROPIONAMIDE IN ASTROCHEMICAL ICY CONDITIONS

Ipshita Sen[1], Bratati Bhat[2], Jaya Krishna Meka[2], Wafikul Khan[3], Ragav Ramachandran[4,5], Anil Bhardwaj[2], Janardhan Padmanabhan[2], Nigel John Mason[6], Soumabha Bag[1,*], Bhalamurugan Sivaraman[2,*]

[1]Department of Industrial Chemistry, Mizoram University, Aizawl- 796004, Mizoram India

[2]Atomic, Molecular and Optical Physics Division, Physical Research Laboratory, Ahmedabad, 38009, India

[3]Experimental Molecular Physics Laboratory, HUN-REN Institute for Nuclear Research (ATOMKI), Debrecen H-4026, Hungary

[4]Raman Research Institute, Bengaluru, Karnataka, 560080, India

[5]Institute of Astronomy Space and Earth Science, Kolkata, West Bengal, 700054, India

[6]Center for Astrophysics and Planetary Sciences, School of Physics and Astronomy, University of Kent, Canterbury CT2 7NH, United Kingdom

*Corresponding authors - soumabha@mzu.edu.in & bhala@prl.res.in

Introduction: Amide functionality is a fundamental structural motif in peptides and protein that has gained particular interest in understanding the formation of protein in cosmic environment. The simplest molecule detected is formamide in the year 1970s [1]. Our study reports the temperature dependent FT-IR study of its homologue that is propionamide ($CH_3CH_2CONH_2$)- largest peptide-like molecule in space owing its molecular complexity and tentative detection towards the Sagittarius B2(N) star forming region [2]. Its formation is driven by the presence of simple molecules such as water, methanol and ammonia yet, the finding of this molecule was challenged [3][4]. To investigate the physicochemical behaviour of this molecule in astrochemical icy condition, we used the Stimulator for Astromolecules at Low Temperature (SALT) [4] experimental facility.

Experiments and Result: High purity propionamide (97%) was deposited onto a zinc-selenide (ZnSe) substrate maintained at cryogenic temperature, with a system capable of reaching 10 K under ultra-high vacuum condition. Fourier Transform Infrared (FT-IR) spectroscopy is used to probe the astromolecule (propionamide) in the condensed phase and for providing laboratory reference spectra relevant to astronomical infrared observations. Our study investigated propionamide ices from 10 K to 200 K and revealed spectral changes which are attributed to the conformational dynamics; phase transformation, formation of dimers or higher aggregates of a molecule containing CH, CO, CC and NH_2 vibrations. The results of these experiments will be presented and discussed.

Acknowledgments: The authors acknowledge the support of the ISRO project and Physical Research Laboratory (PRL), Ahmedabad for providing access to the Stimulator for Astromolecules at Low Temperature (SALT) experimental setup and associated experimental facilities.

References:

[1] R. H. R et al. (1971) *The Astrophysical Journal* 169: L39 - L44.

[2] C. S et al. (2022) *The Astrophysical Journal* 941:102 (12 pp).

[3] J. L et al. (2021) *The Astrophysical Journal* 919:4 (18 pp).

[4] L. K et al. (2022) *Astronomy and Astrophysics* 659: A111.

[4] R. R et al. (2023) *Journal of Chemical Sciences* 135:77

ROLE OF FLUID INTO THE ORIGIN OF ANCIENT LIP RHYOLITE AND LARGE GRANITOID: IMPLICATIONS FOR MARTIAN SILICIC ROCKS.

S. Sensarma[1] and D Ray[2], [1]Department of Geology, Universityof Lucknow, Lucknow 226007(sensarma2009@gmail.com), [2]PhysicalResercah Laboratory, Ahmedabad (dwijesh@prl.res.in)

Introduction: Study of different meteorites enriches the database and our knowledge of the solar system members, including Mars. One of the major areas of resercah is to look for evidence, and deciphering the nature and extent of secondary aqueous / hydrothermal alterations that may have prevailed on these bodies due to rock-fluid interactions. There is perhaps no perfect analogue of Mars on Earth, yet the geochemical evolution of Mars, given restricted acess to meteroire samples, can be reasonably better understood through apparently similar mineralogical and geochemical condition on Earth by studying the igneous processes, including hydrothermal processes preserved in the remannts of ancient magmatic provinces, including large igneous provinces (LIPs) analogues. In addition, with the recent discoveries of silicic rocks in Mars, the study of older silicic provinces including low $\delta^{18}O$ LIP rhyolites ($\delta 18O < 5.5$ ‰) holds enormus potential. For this purpose, we utilize the mineralogical and geochmeical charcaters of two precambrain silicic to high-silicic rocks in India - the LIP rhyolites (Bijli Rhyolite in central India) and Bundelkhand graniotod, in volcanic and plutonic setting respectively.

LIP rhyolites (Bijli Rhyolite): The low-grade metamorphosed and deformed, extremely high-silica rhyolites (HSR: SiO_2 ≤81 wt. %) in the LIP (Bastar craton) comprise quartz + k-feldspar + albite ± anorthoclase + biotite + zircon + Fe-oxides; high Fe/Mg, Zr, Ga, Y, and REE (except Eu), low CaO, Ba, Sr contents and high Ga/Al; a temperature of ~900°C is estimated [1]. The REE patterns broadly similar, yet sometimes cross each other, unique to the HSR. Interaction of mantle-derived picritic/high-Mg basalts and deeper crustal melts better explains the bulk rhyolite compositions including low initial $^{87}Sr/^{86}Sr$ (0.7031 and 0.7057); upper ontinental crust input seems limited. So, high temepearture (>1200°C) basaltic magmas are involved into the origin of the HSR, both physically and chemically. The $\delta^{18}O$ rhyolites require pre-existing altered source, i.e., partial melting and assimilation of rocks that periviously experiencced hydrothermal alteration by meteoric water at high water/rock ratios in the shallow, permeable, and relatively cold upper crust (<400°C), a region nevertheless considered unfavorable for the production of large melt volumes [2]. Alternatively, aqueous fluid introduction likely occurred during brittle fracturing of the crust and/or crust-mantle interaction in a caldera setting, i.e. syn-magmatic alteration [1, 2]. Secondary silicification, on the other hand, may have led to HSR (SiO_2 77–80 wt.%) in the Amalia tuff (USA) in the Questa caldera [3].

Bundelkhand granitoid: Felsic-intermediate lower crustal litholgies, e.g., magmatic charnockites (730°C-855°C), TTG (~817°C) and felsic granulites (~616°C), and high Mg basalts/picro-basalt: 1170°C-1217°C) occur as magamtic enclaves (MEs) in the ~2.6-2.3 Ga [4] fluid-fluxed transcrustally-emplaced Bundelkhand granitoid (9-2 kbar: liquidus ~900°C); MEs represent coeval magmas that experienced variable extents of crustal-mantle melts interactions, yet coexisted in the same reservoirs that of the host granitoid and incorporated into the mush at deeper crustal levels (~5-10 kb) [5]. Low-T (≤ 800°C; mostly ≤ 750°C) hydrous silicic magmas (felsic MEs) variably crystallized before being incorporated in hotter granitoid. Hydrated OIB-like mantle caused mid- to lower crustal anataxis. Dehydration of deeply buried altered high-MgO basalt/ultramafic rocks from near surface conditions likely led to fluid-fluxed melting within the lithospheric mantle to produce hydrous basalts/picro-basalt (i.e., mafic MEs), which eventually became sources for low-T (≤800°C) TTG and felsic granulite magmas. Deep aqueous fluid sourced from altered high-MgO mantle-derived rocks thus promoted melting, mineral transformation, and element transfer.

Summary and Conclusions: Mars had an active hydrological system during ancient past, thereby leveraging the potential for a complex crust-mantle-fluid interaction history. The percolation of water and/or hydrotherammly alterated rock from shallow crustal levels to deeper parts may have potentailly caused hydrated deep crust, conducive for production of silicic to high silica melts in the form of silicic magmatism or silica enrichment in deep crust.

Acknowledgments: DST-ANRF Major project (file no. CRG/2023/006051) to SS.

References:[1] Sensarma, S. and Gaur, R. (2021) *Jour. Earth Sys. Sci. (springer)* 131 (2): 105.[2] Troch, J. et al. (2020) *Earth-Science Reviews* 208: 103299. [3] Lipman, P W. (1983) *Proceedings on the Denver Region Exploration Geologists Society Symposium*, 133-147. [4] Kaur, P. et al (2016) *Precambrian Research* 281, 384-413. [5] Sensarma, S. et al. (2026) *Geol. Mag. (in press)*.

COMBINED RADIOGENIC K–CA AND RB–SR ISOTOPIC AGE CONSTRAINTS OF THE DHALA IMPACT STRUCTURE, INDIA

Gaurav S. Papola[1*], Rahul Das Gupta[2], Ramananda Chakrabarti[1], Arindam Dutta[3], Debjani Raychaudhuri[4], Kaushlendra Kumar Sinha[5], [1]Centre for Earth Sciences, Indian Institute of Science, Bengaluru, India (*gauravpapola@iisc.ac.in), [2]Department of Earth Science, Assam University, Silchar, India, [3]Geological Survey of India, Kolkata, India, [4]Geological Survey of India, RSAS, Bengaluru, India, [5]Atomic Minerals Directorate for Exploration & Research, Jamshedpur, India

The deeply eroded, ~25-km-diameter Dhala impact structure, hosted by Archean granitoids of the Bundelkhand Craton in central India, preserves shocked basement rocks and impact-melt breccia that have undergone extensive post-impact fluid–rock interaction. Despite claims of being one of Earth's oldest preserved impact structures, its impact age remains unresolved and is currently constrained to ~2.10–1.71 Ga by shocked ~2.1 Ga giant quartz veins (GQVs) and overlying post-impact Vindhyan sediments. The Dhala impact has not been unequivocally dated, as geochronological studies have been complicated by inherited target-rock components and later hydrothermal disturbance. Additionally, younger zircon populations at ~1.83–1.77 Ga and disturbed $^{40}Ar/^{39}Ar$ systematics, including a ~0.99 Ga alteration age, demonstrate a prolonged post-impact hydrothermal history [1, 2, 3].

We utilize coupled K–Ca and Rb–Sr isotope systematics to distinguish target inheritance, impact-related resetting, and younger hydrothermal reactivation. Target granitoids (n = 4), surface breccia (n = 7), and drill-core breccia (n = 9) were analyzed for major and trace elements by quadrupole ICP-MS (Thermo XSERIES 2), while high-precision $^{40}Ca/^{44}Ca$ and $^{87}Sr/^{86}Sr$ ratios were measured by TIMS (Thermo Triton Plus) at the Centre for Earth Sciences, Indian Institute of Science, Bengaluru. Impact breccia show pronounced K enrichment (up to 14.4 wt% K_2O) accompanied by variable Na–Ca–Sr depletion, resulting in large ranges in K/Ca and Rb/Sr suitable for both chronometers. Isochrons were evaluated using IsoplotR maximum-likelihood Model 3b regression, which accommodates geological overdispersion interpreted as variable closure/resetting ages rather than analytical scatter alone [4].

Target granitoids yield discordant K–Ca and Rb–Sr ages of 2.37 ± 0.26 Ga and 2.07 ± 0.09 Ga, respectively, both younger than their ~2.58–2.49 Ga emplacement ages. The older K–Ca signature indicates greater preservation of Neoarchean target-rock memory, whereas Rb–Sr records substantially stronger Paleoproterozoic re-equilibration, broadly concurrent with regional GQV-related metasomatism [5]. Surface breccia yield 2.16 ± 0.24 Ga (K–Ca) and 1.71 ± 0.20 Ga (Rb–Sr) ages. Their discordance indicates incomplete differential resetting: the K–Ca system retains an older component overlapping the permissible impact interval, whereas Rb–Sr was more strongly modified during Paleoproterozoic fluid activity. In contrast, drill-core breccia yield mutually concordant K–Ca and Rb–Sr ages of 0.96 ± 0.24 and 0.99 ± 0.27 Ga. Their agreement with the published 994 ± 22 Ma $^{40}Ar/^{39}Ar$ alteration signal strongly identifies a distinct ca. 1 Ga post-impact hydrothermal resetting event [2]. The coupled chronometers therefore reveal progressive isotopic rejuvenation from inherited granitoid crust, through partially reset surface impactites, to strongly re-equilibrated subsurface breccia. K–Ca and Rb–Sr discordance and concordance resolve a polyphase history of target inheritance, Paleoproterozoic impact/hydrothermal modification, and ca. 1 Ga tectono-hydrothermal reactivation at Dhala.

References: [1] Pati, J. K. et al. (2008) *Meteoritics & Planetary Science*, *43*(8), 1383-1398. [2] Pati, J. K. et al. (2010) *GSA,* Large Meteorite Impacts and Planetary Evolution IV. [3] Dwivedi, S. et al. (2026) *Meteoritics & Planetary Science*, *61*(7), 1494-1527. [4] Vermeesch, P. (2018) *Geoscience Frontiers*, *9*(5), 1479-1493. [5] Deb, T., & Bhattacharyya, T. (2022) *Earth-Science Reviews*, *235*, 104238.

SIGNIFICANCE OF TERRESTRIAL ANALOGUES FOR LUNAR EXPLORATION: INSIGHTS FROM THE SITTAMPUNDI ANORTHOSITE COMPLEX, INDIA

V.J. Rajesh
Department of Earth and Space Sciences, Indian Institute of Space and Science Technology, Valiamala P.O., Thiruvananthapuram, 695547, INDIA

Terrestrial analogues play a crucial role in planetary exploration by providing accessible natural environments and geological materials on Earth that help investigate the composition, evolution, and surface processes of extraterrestrial bodies. They also facilitate the development and validation of analytical techniques, remote-sensing approaches, and technologies required for future space missions. With the growing advancement in space exploration and the increasing emphasis on lunar missions by the Indian Space Research Organisation (ISRO) and other space agencies, terrestrial analogues of lunar materials have become increasingly important for understanding the Moon's primordial crust, mineralogical diversity, impact history, and regolith characteristics, while supporting the development of in situ resource utilization (ISRU) technologies. The Sittampundi Anorthosite Complex in Tamil Nadu, southern India, represents a promising terrestrial analogue for lunar highland materials owing to its anorthositic composition, plagioclase-rich lithology, and complex geological evolution. An integrated investigation of this complex provides valuable insights into its petrographic characteristics, mineralogical assemblages, and major- and trace-element geochemistry, enabling comparisons with lunar anorthosites and assessment of their compositional similarities and differences. Spectroscopic characterization across the visible, near-infrared, and shortwave-infrared regions helps establish diagnostic spectral signatures for mineral identification, supporting the interpretation of lunar orbital remote-sensing data and rover-based observations. Furthermore, geotechnical and geomechanical assessments of representative lithologies and derived regolith simulants help evaluate their physical and mechanical properties for applications such as rover mobility, excavation, surface infrastructure development, and habitat construction. The complex also offers a potential setting for microbial investigations to examine interactions between microorganisms and anorthositic substrates, including mineral alteration, nutrient availability, and the feasibility of biologically assisted resource utilization under controlled simulated planetary conditions. Additionally, anorthosite-derived materials can be evaluated for space-brick fabrication and other construction applications using locally available lunar resources, while experimental shock-related studies can investigate impact-induced deformation, microstructural modifications, and mineral transformations relevant to lunar impact processes. Collectively, these multidisciplinary investigations establish the Sittampundi Anorthosite Complex as a valuable natural laboratory that bridges fundamental geological research with the development of exploration technologies, resource-utilization strategies, and construction materials for future lunar missions and sustained human presence on the Moon.

EVAPORATIVE POLYGONS – AN INDICATION OF TRANSIENT BRINE ACTIVITY ON MARS

A. Samanta[1], A. Mukherjee[2], P. B. Hiral[3], T. Nimura[3], J. Kameda[3] and T. Ruj[3], [1]Indian Institute of Technology Bombay, Powai, Mumbai 400076, India (25n0209@iitb.ac.in), [2]Indian Institute of Technology Kharagpur, Kharagpur 721302, West Bengal, India (adritajam25@kgpian.iitkgp.ac.in), [3]Institute for Planetary Materials, Okayama University, 827 Yamada, Misasa, Tottori 682-0193, Japan (trishitruj@okayama-u.ac.jp)

Polygonal landforms are widespread in the mid to high latitudes of Mars. Many have been attributed to thermal contraction and desiccation-related processes. Our study extends to the peripheral North polar region, where some polygonal morphologies may require additional processes involving evaporation and sublimation. If evaporation contributed to their formation, their evolution must have involved a liquid phase, implying transient liquid activity in this region. Obliquity induced pressure and temperature variations, together with abundant polygonal terrains further make this region a plausible setting for transient brine activity.

However, morphology observed from orbit alone cannot establish whether these Martian polygons formed through brine-related processes. Terrestrial saline playas are therefore used as process analogues to examine how brine evaporation and salt redistribution are expressed in polygon morphology under natural conditions. Previous field studies at Winnemucca Lake, a desiccated lake in Nevada revealed characteristic polygon morphologies -- raised rim in the central part of the lake and low rim towards the peripheral part. Although these terrestrial polygons form under very different pressure, temperature, and hydrological conditions from those on Mars, they provide a useful morphological and process reference for evaluating how evaporation and salt concentration could influence polygon development.

The next question is whether brines exposed to Martian atmospheric conditions can develop comparable polygonal surface organization. To test this directly, we conducted a series of experiments in the MISASA (Mars Innovative Simulator for Assessing Surface Aqua-environment) chamber at pressure of 4-6 hPa, in CO_2 or N_2 atmospheres, using 1-4 wt.% $CaCl_2$, $MgCl_2$, NaCl and mixed brines. Evaporative cooling under reduced pressure initiated ice formation, as the system approached the triple-point of water. Although the effect of specific brine composition remains unresolved, pressure and salinity clearly influenced the freezing behavior and hence polygon formation in the brine. Raised-rim polygons, morphologically similar to those observed in the central part of Winnemucca Lake, with sizes of 0.100-0.600 cm were observed.

The experiments revealed a six-stage evolutionary sequence for raised-rim morphology- **(1) Ice nucleation** and subsequent crystal growth in a thin surface layer, followed by **(2) a compositional and mechanical heterogeneity** due to salt-rejection during freezing. **(3) Linear ridge and trough development** occurs as spatial differences in salinity and water activity produce differential sublimation, progressively amplifying small surface irregularities. As sublimation continues, **(4) ridge linkage** occurs as these linear heterogeneities propagate and connect, **initiating the first closed polygonal cells.** Boundary relief increases, producing more organized polygonal network with well-defined junctions and rounded cells indicating **(5) polygon maturation.** With prolonged sublimation, polygon boundaries lose definition, resulting in **(6) degradation of the polygonal pattern.**

This experimental sequence provides a basis for interpreting the Martian polar polygons that motivated this study, linking ice surface morphology to the progressive modification of transient liquid brine under Martian conditions. If similar stages occur on Mars, the relative maturity of polygonal forms may help identify regions where brine activity occurred most recently, with less mature morphologies potentially marking younger episodes of near-surface liquid-water activity whereas more evolved forms record longer exposure to sublimation. In this framework, terrestrial playa polygons provide morphological context, while the MISASA experiments test whether comparable surface evolution can occur under Martian atmospheric conditions. Such morphological indicators could help constrain the recent hydrological evolution of the Martian polar environment and identify regions of particular interest for investigating transient liquid water and potential habitability.

Acknowledgments: We sincerely acknowledge the MISIP Internship Program and Okayama University for providing us with the opportunity, facilities, and support to undertake this project.

3D PRINTING OF SPACE BRICKS AND RADIATION SHIELD USING PLANETARY ANALOGUES

Thirukumaran Venugopal [1&2] Hariharan P.K.[1], Aastha Jhala[3], Bhalamurugan Sivaraman[4], Vijayan Sivaprahasam[4], Vinoth Srinivasan[5] , Sanil R[6]., Nigel John Mason[7]

[1]Government Arts College (Autonomous), Salem - 636007, Tamil Nadu

[2]Chikkaiah Government Arts and Science College, Erode- 638004, Tamil Nadu

[3]Aaka Space Studio, Ahmedabad, 380059, India.

[4]Physical Research Laboratory, Ahmedabad, 380009, India.

[5]NIT, Surathkal, Karnataka

[6]Government Arts and Science College, Coonoor, Ooty - 643101, Tamil Nadu

[7]University of Kent, Canterbury, United Kingdom.

E-mail : mailkumaran75@gmail.com

Introduction: The near-future colonisation of Mars and the Moon warrants suitable construction materials to be prearranged. Selecting appropriate and readily available rocks, as well as obtaining a cementing medium to make the rocks feasible for 3D printing, provide obstacles that must be overcome before preparing for Martian and Lunar settlement. Olivine, a mineral of significant presence, is widely distributed across the planetary surface of Mars, it is noteworthy to mention that Nili Fossae region and is observed in Ganges Chasma, which is situated on the eastern side of Valles Marineris. The presence of Calcium or iron carbonates along the Huygens Crater, which is situated in the Iapygia quadrangle, so, the calcium carbonate may be used as cementing media.

Analogue site and sample: The terrestrial analogue of the olivine mineral is collected from the ultramafic complex of Chalk Hills, Salem, Tamil Nadu. The monomineralic rock Dunite is pulverised in a jaw crusher and sieved using a mechanical sieve shaker. Two different types of cement are intended for making cubical blocks of 7.5 cm^3. Pulverised sedimentary Marly lime stones were collected from sedimentary deposits in Ariyalur district, Tamil Nadu, which may be an analogue of the sedimentary sequence reported from Gale crater.

The spacebricks made from the lunar and Martian simulant with natural binders with different proportions were set to cure for 7 days under natural drying atmospheric conditions, and the blocks were tested for engineering properties. The second set of samples is left to cure for 30 days of natural drying under nominal atmospheric conditions. The third set of samples was heated up to 105 degrees centigrade before testing for geomechanical properties.

The bricks were tested for geomechanical properties, including compressive strength, density, porosity and durability. "compressive strength of 3 MPa for lunar bricks versus 1 MPa for Martian bricks." The findings suggest that locally available regolith-like material could be used to build shelters and structures on the Moon and Mars, reducing the need to ferry materials from Earth. With this achieved strength, many alternative ideas can float to build structures.

Based on the idea pitched at Vikram Discussions-2 (at PRL) by the authors, followed by discussions, a completed 3D-printed radiation structure using a simulant from Martian analogue rocks was planned. With support from AAKA Space studio, a 3D-printed structure was attempted in the month of October 2025 in Ahmedabad, and a structure was successfully built. Because the atmosphere of Mars is thin, radiation and temperature swings are severe, so thick shielding structures are needed. For the first time in Asia, a radiation-shielding structure was created.

Acknowledgement: The authors acknowledge MicoB, Ahmedabad, for providing the facilities for 3D printing.

References [1]Anbazhagan, S., & Arivazhagan, S., (2010) *58*(5), 752–760. [2] Anbazhagan et al., (2021) *Icarus, 366*, 114511. [3]Dikshit, et al., (2021) Ceramics International 47(11), 16047–16053. [4] Dikshit et al.,(2022) PLOS ONE 17(4), e0266415. [5] Kakkassery et al., (2022), *Planetary and Space Science*, *221*, 105528.

LABORATORY STUDIES FOR PLANETARY SCIENCE: DEVELOPING A NEW EXPERIMENTAL FACILITY AT SINP, KOLKATA, INDIA

Dr. Sankhabrata Chandra
Associate Professor-E, Nuclear Atomic and Particle Physics Division (NAPPD)
Saha Institute of Nuclear Physics (SINP)
1/AF, Bidhan Nagar, Kolkata 700064, India
sankhabrata.chandra@saha.ac.in

Understanding planetary processes driven by electron and ion radiation is a key area of research in planetary science. Airless planetary bodies are immersed in high-energy electron and ion radiation. For example, the solar wind, low-energy (keV) electrons, and protons bombard Solar System bodies; Jupiter's and Saturn's local magnetospheric trapped energetic particles, such as H^+, O^+, S^+, and He^+ with keV to MeV energies, constantly bombard Jupiter's and Saturn's moons. Therefore, understanding radiation processes on planetary surfaces under extreme conditions is necessary. However, studying ion- and electron-induced processes under extreme conditions presents unique experimental challenges, such as maintaining a planetary environment in a laboratory. The primary objective of this laboratory is to explore electron- and ion-induced processes on planetary analog surfaces to understand physical processes such as sputtering of surface species and modifications of surface species during radiation processes in the context of planetary science. These studies also aim to understand the origin of prebiotic species and their evolution from dense molecular clouds to planetary systems via protoplanetary disks. This will be studied using mass spectrometry and near- to mid-infrared spectroscopy during electron and ion irradiation, as well as during the warming up the sample using temperature-programmed desorption following electron and ion bombardment.

Currently, at SINP, I am establishing the **APRIS** Laboratory — **A**strophysical and **P**lanetary **R**adiation-**I**ce **S**urface Laboratory. This will be a state-of-the-art laboratory dedicated to investigating electron- and ion-induced processes on astrophysical and planetary dust surfaces. The laboratory will provide a platform for studying fundamental physical processes under space-relevant conditions and will contribute to different areas of space science, including astrophysics and planetary science. In this presentation, I will discuss the current development of the APRIS Laboratory and its potential contributions to India's space missions, particularly ISRO missions, as well as to international space missions, including missions led by NASA and ESA.

EXTREMOPHILE MICROBIOMES HOSTED IN PLANETARY ANALOGUE SITES ACROSS THE INDIAN SUBCONTINENT

Y. Jangir* and D.Dey
(jangir@iitk.ac.in)
Department of Space, Planetary and Astronomical Sciences and Engineering, IIT Kanpur

Extreme environments provide natural laboratories for understanding the ecological limits, evolutionary trajectories and biological patterns of microbial life. Many such extreme environments can be found across the Indian subcontinent [1], and numerous studies have explored microbial biodiversity in these extreme habitats. However, due to differences in sequencing platforms, analytical workflows and sampling strategies, cross-ecosystem comparisons have been limited. In this study, we performed a standardised meta-analysis of publicly available 16S rRNA gene amplicon sequence datasets to generate a unified view of microbial diversity across extreme environments in the Indian Subcontinent. A total of 2127 sequenced runs were downloaded from public repositories and processed through a harmonised bioinformatic workflow. Sequence denoising and Amplicon Sequence Variant (ASV) inference were performed using the DADA2 [2] workflow. Out of the downloaded datasets, 1423 runs passed quality filtering and 1137 datasets were retained following sequence merging, chimera removal and contaminant filtering for downstream analyses. The final dataset represented a broad environmental gradient encompassing marine and terrestrial ecosystems, including forests, mines, basaltic rocks and alpine regions. Downstream comparative analyses revealed pronounced differences in microbial community composition across habitats, indicating strong environmental filtering across physicochemical extremes. However, we also found a lot of common microbes across vastly different environments. We observed that high-pressure environments like the seabed, hydrothermal vents and coastal basins are dominated by *Bacillota*, while cold environments like permafrost and alpine areas were populated by *Actinomycetota* and *Acidobacteriota*. Saline environments are dominated by *Verrucomicrobiota*. Thus, we can observe that marine and terrestrial environments formed distinct ecological groupings. Individual ecosystem categories displayed unique microbial assemblages, highlighting the influence of habitat-specific selective pressures over geographic proximity. Through this study, several environments emerged as underexplored reservoirs of microbial diversity, especially the subsurface. Our work provides a harmonised framework for assessing microbial diversity across extreme environments hosted in the Indian subcontinent. It lays a foundational groundwork for future planetary research by studying extremophiles across underexplored planetary analogues.

Acknowledgments

We are grateful to Prof. Kunal Mooley, Department of Space, Planetary and Astronomical Sciences and Engineering, IIT Kanpur, for providing us access to HPC hosted in his lab.

References

[1] Jangir Y and Dutta S (2026) Planetary analogue sites in the Indian subcontinent and the Indian Ocean: underexplored environments suited for astrobiological and space research. Front. Astron. Space Sci. 12:1712191. doi: 10.3389/fspas.2025.1712191

[2] Callahan BJ, McMurdie PJ, Rosen MJ, Han AW, Johnson AJ, Holmes SP (2016) DADA2: High-resolution sample inference from Illumina amplicon data. *Nat. Methods.* 13:581–583. doi: 10.1038/nmeth.3869.

BIOSIGNATURE PRESERVATION IN TRAVERTINE DEPOSITS FROM TAPOVAN HOTSPRING, UTTARAKHAND: IMPLICATIONS FOR MARS

Pallabi Das[1,2*], Dwijesh Ray[1], Anil D. Shukla[3], Uttam K. Bhui[4], Subham Sarkar[5], Satadru Bhattacharya[6] and Himangshu Deka[1,2]

[1]Physical Research Laboratory, Ahmedabad, Gujarat, India

[2]Amity Centre of Excellence in Astrobiology, Amity University Maharashtra, Mumbai, India

[3]Dept. of Geology, School of Earth Science, Hemwati Nandan Bahuguna University (HNBGU), Srinagar Garhwal-246174,
Uttarakhand, India

[4]School of Petroleum Technology, Pandit Deendayal Energy University, Raisan, Gandhinagar, Gujarat 382007, India

[5]Center for Earth Science, Indian Institute of Science, Bangalore, India

[6]Space Applications Centre, Ahmedabad 380017, India

*daspallavi95@gmail.com

Abstract: Hot springs serve as exceptional analogue sites for studying hydrothermal systems on Earth and identifying traces of past water on Mars [1]. Carbonate travertines are particularly valuable because rapid precipitation of calcite and aragonite can preserve organic molecules within a durable mineral matrix. We examined travertine deposits from the Tapovan hot spring in the Garhwal Himalaya, Uttarakhand, India, using X-ray diffraction, micro-Raman, scanning electron microscopy, isotope analyses, and optical spectroscopic characterization of solvent-extracted organic matter. The Tapovan hot spring discharges near-boiling waters (86–94 °C) with near-neutral pH, enriched in silica, sulfur, sodium, chloride, and bicarbonate from fractured crystalline rocks along the Main Central Thrust. The deposits consist mainly of calcite and aragonite. This mineral distribution mirrors settings detected in Jezero, Gusev, and Gale Craters, where carbonates and hydrated silicates indicate past aqueous habitability [2]. Isotopic analyses indicate that meteoric water circulated through fractured crystalline basement along the Main Central Thrust and dissolved inorganic carbon was derived from thermal dissolution of existing marine carbonates or organic-bearing rocks rather than from magmatic or mantle sources. Solvent extracts contain relatively immature organic compounds, including lipids, aromatic hydrocarbons, esters, carboxylic acids, and functional groups linked to proteins, polysaccharides, and humic substances, indicating rapid entrapment during carbonate precipitation. These results provide a well-characterized example of mineralogical, isotopic, and organic preservation in a high-altitude travertine system, offering a valuable reference dataset for interpreting carbonate deposits and assessing potential biosignatures in ancient Martian hydrothermal environments.

Acknowledgments: We acknowledge Department of Space (Govt. of India) for financial help.

References: [1] Boulesteix, D., Buch, A., Masson, G., Kivrak, L.L., Havig, J.R., Hamilton, T.L., Teece, B.L., He, Y., Freissinet, C., Huang, Y. and Santos, E., 2024. Environmental analogs from Yellowstone hot springs on geochemical and microbial diversity with implications for the search for life on Mars. *Planetary and Space Science*, *250*, p.105953.

[2] Zastrow, A.M. and Glotch, T.D., 2021. Distinct carbonate lithologies in Jezero crater, Mars. *Geophysical Research Letters*, *48*(9), p.e2020GL092365.

GEOCHEMICAL STUDIES OF IMPACT-MELT ROCKS FROM THE LONAR CRATER.

S M Anagha[1,2*], Yogita Kadlag[1], Hridya T V[1, 3], Anil Chavan [4], and Hadi Muhammed Rahil K. K.[1,2]
[1]*Geosciences Division, PRL Ahmedabad-380009* anaghasm@prl.res.in
[2]*Department of Earth Sciences, IIT Gandhinagar- 382355*
[3]*Department of Geology, Central University of Karnataka, Gulbarga, Karnataka- 585367*
[4]*Earth and Planetary Exploration Group, BSIP, Lucknow, Uttar Pradesh- 226007*

Impact craters are geological structures formed on the surface of planetary objects as a result of collisions with asteroids, meteorites and comets. The Lonar crater in Maharashtra, India, is one of the rare simple craters formed in basaltic terrain and is situated within the Poladpur Formation of the Deccan Traps[1]. Although the impact origin of the Lonar crater has long been established, the nature of the impactor remains a matter of debate. To investigate the type and contribution of the impactor, textural and compositional analyses of impact-melt rocks from the Lonar crater have been carried out in this study. The abundances of rare earth elements (REEs) and other trace elements (e.g., Cr, Co, Ni, Sr, Ce, Th, U, Yb, Hf, Pb, Sc, Y) were determined to assess the contribution of the impactor.

The presence of melt schilerien in the impactites suggests incomplete mixing of compositionally distinct melts. Textural observations, together with the observed compositional heterogeneity suggest that impactites record selective melting, incomplete mixing and rapid cooling. Abundance patterns of REEs and concentrations of siderophile elements (eg., Ni (~76.6 µg/g) and Cr (~59.2 µg/g) are similar to that of the target basalt with slight enrichment in REEs, which suggests the dominant target contribution in the studied impactites. Previous studies of impact spherules from the Lonar crater, based on the abundances and ratios of siderophile elements, particularly Ir, Cr, Co, and Ni suggested an enstatite-chondrite-type impactor[2-4]. The impactites investigated in this study indicate chondrite impactor contribution ranging from 0 to 1.6 wt.%, consistent with previously reported impactite data[5]. This further suggests that the chondritic contribution to the impact-melt rocks is lower than that estimated for impact-derived spherules[5]. Further isotopic studies will be carried out to trace the nature of the impactor and impactor and processes associated with the impact.

Acknowledgement: We thank Mr. Shivansh Verma for maintaining SEM facility at PRL which was used for the textural analysis.

References: [1] Nayak, V. K. (1972) *Earth and Planetary Science Letters* 14. [2] Misra, S. et al. (2009) *Meteoritics & Planetary Science* 44(7):1001–1018. [3] Gupta, R. D. et al. (2017) *Geochimica et Cosmochimica Acta* 215:51–75. [4] Ray, D. et al. (2017) *Meteoritics & Planetary Science* 52:1577–1599. [5] Schulz, T. et al. (2016) *Meteoritics & Planetary Science* 51:1323–1339.

IMPACT-MELT SPHERULES AT LONAR CRATER, INDIA, AND JEZERO CRATER, MARS: A TERRESTRIAL ANALOGUE PERSPECTIVE

Himangshu Deka[1,2] and Dwijesh Ray[1],
[1]Physical Research Laboratory, Ahmedabad, Gujarat, India
[2]Amity Centre of Excellence in Astrobiology, Amity University Maharashtra, Mumbai, India
himangshudeka1210@gmail.com

Abstract: Hypervelocity impacts on basaltic targets produce melt-derived spherules whose morphology, texture, and chemical composition preserve signatures of the impact-melting and quenching processes. On sol 1442, NASA's Perseverance rover imaged a float rock named "St. Pauls Bay" within the Witch Hazel Hill outcrop on the rim of Jezero crater, which is coated by millimeter-sized glassy, vesicular, and locally agglutinated spherules. These spherules are texturally distinct from earlier discovered hematite spherules (aka *Martian Blueberries*) in Meridiani Planum. Recent investigations of the various impact products at Witch Hazel Hill region interpret the spherules as more consistent with an impact-ejecta origin than with a volcanic one [1]. Therefore, the St. Pauls Bay spherules provide a rare, preserved record of impact-melt products on the Martian crust.

Lonar crater (1.8 km diameter; ~150 m depth), excavated into the Deccan Continental Flood Basalt, India, is an important terrestrial analogue for investigating impact processes and products [2]. Lonar impact spherules formed by rapid quenching of shock-induced melt, provide an opportunity for detailed petrographic, and geochemical analyses at spatial resolutions that are currently not possible for the Mars impact spherules.

Both Lonar and Jezero impact spherules show a relatively homogeneous, high luster texture with vesicles. Spherules from both localities occupy the basaltic field on a total alkali-silica (TAS) diagram. Furthermore, the impact origin of St. Pauls Bay spherules was supported using a CaO/Al2O3 vs. MgO/Al2O3 plot where Lonar and Martian spherules cluster at CaO/Al2O3 ratios of ~0.6-0.8, and~0.4-0.8, respectively, and both spherules fall below MgO/Al2O3 ratio of 1.25 indicating a non-volcanic basaltic glass composition [3]. On the CaO-MgO-(FeOt+TiO2) ternary diagram, Lonar target basalt and Lonar melt spherules plot as a tightly overlapping cluster, an expected result due to geochemical homogenization by impact. But St. Pauls Bay spherules plot as a distinct, comparatively CaO-enriched cluster offset from the bulk of the Jezero basalt field, overlapping only marginally with its most CaO-rich, MgO-poor members. This mismatch seems to be more consistent with the spherules representing an allochthonous component: an impact spherule-bed perhaps from a different target lithology elsewhere on the Martian crust, subsequently transported to and deposited at Witch Hazel Hill rather than formed by the Jezero impact itself. We suggest this as a working interpretation rather than a settled conclusion as the Jezero target basalt field is broad and a larger LIBS dataset will be needed to test whether any subpopulation of the basalt more closely matches the spherule composition.

Acknowledgments: We acknowledge Department of Space for financial help. All mission data are available at the NASA Planetary Data System (PDS) Geoscience Node at https://pds-geosciences.wustl.edu/missions/mars2020/supercam.htm

References: [1] Jones, A.J. et al. (2026) "Stratigraphy Preserved on the Jezero Crater Rim Reveals Repeated Impacts on Early Mars," *Journal of Geophysical Research: Planets*, 131(7), p. e2026JE009779. [2] Ray, D. et al. (2017) "New insights on petrography and geochemistry of impactites from the Lonar crater, India," *Meteoritics & Planetary Science*, 52(8), pp. 1577–1599. [3] Delano, J.W. (1986) "Pristine lunar glasses: Criteria, data, and implications," *Journal of Geophysical Research: Solid Earth*, 91(B4), pp. 201–213.

MINERALOGICAL SIGNATURES OF BASALTIC LATERITES FROM INDIA: IMPLICATIONS FOR Fe-RICH ALTERATION HISTORY ON MARS

Aindrila Mukherjee[1] and Dwijesh Ray[1]
[1]Physical Research Laboratory, Ahmedabad, India (Email: aindrila36@gmail.com)

Laterites, products of prolonged, intense chemical weathering, serve as important archives of paleoclimate, hydrological conditions, and parent-rock interactions. Laterites developed on basaltic terrains preserve mineralogical evidence of chemical weathering, oxidation, and aqueous alteration, providing valuable terrestrial analogues for investigating alteration processes on Mars. This study compares the X-ray diffraction (XRD) characteristics of weathering materials from the Deccan and Rajmahal volcanic provinces of India, representing distinct geological and palaeogeographical settings associated with the Late Cretaceous–early Paleogene and Early Cretaceous volcanism, respectively, to evaluate contrasting mineralogical pathways and their implications for Martian Fe-rich alteration.

The Deccan laterites exhibit characteristic XRD reflections consistent with hematite ($d \approx 2.70$ and 2.51 Å) and gibbsite ($d \approx 4.85$ Å), accompanied by quartz and a probable kaolin-group mineral. This assemblage indicates the occurrence of Fe- and Al- bearing secondary phases and is consistent with chemical weathering involving ferric iron formation and aluminium enrichment. In contrast, the Rajmahal samples are characterized by prominent quartz reflections ($d \approx 3.35$ Å), together with additional reflections potentially attributable to feldspar- and mica-bearing phases. These patterns indicate substantial preservation of silicate components relative to the secondary mineral assemblage identified in the Deccan sample. However, preliminary Rietveld refinement of Deccan and Rajmahal laterites highlights discrepancies between observed and calculated diffraction profiles, providing initial insights towards the possible present phases, where further refinement could help to improve prominent phase identification and quantify mineral abundances. These contrasting mineralogical frameworks suggest that the Deccan laterites underwent more intense weathering during their formation, potentially reflecting differences in paleoclimate and geographic position, and exhibit pronounced desilication and residual Fe–Al enrichment.

In addition to their terrestrial significance, basalt-derived laterites provide useful process-based analogues for interpreting the alteration of basaltic crust on Mars, where Fe-oxide-bearing assemblages have been linked to aqueous alteration. Earlier studies of Deccan weathering profiles have also highlighted their relevance to understanding the Martian regolith. Diverse Fe-bearing alteration assemblages are also evident in Jezero Crater, Mars, where Fe^{3+}-bearing oxides may indicate intense water–rock interaction and/or a higher degree of diagenesis under oxidizing conditions, whereas Fe^{2+}-bearing phases may reflect reducing environments or short-lived aqueous activity within an otherwise oxidizing regime. The contrasting mineralogical pathways identified in these basaltic provinces therefore provide a terrestrial framework for evaluating basalt alteration, Fe-oxide formation, oxidation states, and mineral crystallinity, including their potential relevance to assessing biogenicity in Martian surface environments.

SHOCK DRIVEN CHEMICAL PROCESSING OF LUNAR ANALOGUES

R. Nath[1], S. Chakraborty[1]*, M. Bhatt[2],N. Srivastava[2], V. J. Rajesh[3] and S. Narendranath[4]
[1]Department of Chemistry, GITAM University, Bengaluru, India
[2] Planetary Science Division, Physical Research Laboratory, Ahmedabad, India
[3] Department of Earth and Space Sciences, IIST, Thiruvananthapuram, India
[4] U. Rao Satellite Centre, Indian Space Research Organization, India
*E-Mail: schakrab4@gitam.edu

Detailed characterisation of returned lunar samples suggests a significant effect of shock metamorphism [1]. The continuous churning due to impacts driven shock waves influences the chemical composition and volatiles on the topmost layer of the regolith. More specifically, volatile elements such as Na and H_2O may vary due to impact induced processes [2]. The goal of this work is to investigate the influence of shock induced modification to lunar analogues and understand the formation of volatiles in airless planetary bodies like Moon and Mercury.

We will present results of shock induced modification of Sittampundi anorthosite (SA) lunar analogues [3]. The results are derived using newly established hypersonic shock wave facility at the GITAM Bengaluru under an ongoing ISRO-RESPOND project. The analogue materials were sieved to different grain sizes, and powder XRD (p-XRD), VNIR reflectance measurements, SEM, TEM and Raman microscopy was performed to determine their structural and optical properties. Following, the SA samples were subjected to controlled shock exposure of a Mach number varying from 2.5 to 7 with a calculated reflected shock temperature varying from approximately 2400K to 7000K. p-XRD showed shifts towards high 2θ after subjecting it to multiple shocks. Scanning electron microscopy (SEM) study revealed irregular morphology and formation of spherules. Band Area Ratio of shocked samples have decreased. These shock induced results will be compared with the pre-shock characteristics of samples and the outcomes will be discussed and put in the context of impact processing in planetary surfaces.

Acknowledgement

The research leading to this work is funded by the Indian Space Research Organization (ISRO) Respond basket (RES-PRL-2023-009). We thank the central instrumental facility GITAM Bengaluru, FESEM TESCAN MIRA S6123, MURTI-SAIF, GITAM University for the SEM analysis We thank Dr. S. Anbazhagan from Periyar University for their insights on SA.

References

[1] Lucey et al. 2006 Rev. Mineral. Geochem, 60, 83-219, [2] Pieters et al. 2003, Geophys. Res. Lett., 30, 2048, [3] Anbazhagan et al. 2010, Plan. Space. Sci. 58, 752

MRO-HIRISE OBSERVATIONS OF AEOLIAN CHARACTERISTICS AT THE ARKHANGELSKY CRATER ON MARS

Anirban Mandal[1], Deb Deep Mandal[2], Satyaki Banerjee[3], and Jagabandhu Panda[1]
[1]Department of Earth and Atmospheric Sciences, National Institute of Technology Rourkela, Odisha, India, e-mail: anirbanm0101@gmail.com
[2]Department of Petroleum Engineering, Indian Institute of Technology (Indian School of Mines) Dhanbad, Jharkhand, India
[3]Department of Earth Sciences, Indian Institute of Technology Kanpur, Uttar Pradesh, India

Abstract: The aeolian environment provides valuable information about the planetary surface and current climatic conditions. This study examines the aeolian characteristics in the Arkhangelsky crater on Mars using observations from the High-Resolution Imaging Science Experiment (HiRISE) onboard the Mars Reconnaissance Orbiter (MRO). Specific emphasis is given on their morphometry and migration pattern to gain an understanding of the Martian land-atmosphere interaction. Aeolian features like barchan and barchanoid dunes, ripples, and megaripples are observed in the crater. The total dune length varies between 341–1219 m, the body width ranges from 266–633 m, and the height varies between 21–62 m. The right horn is typically bigger than the left one, owing to the sand supply and wind dynamics. The sand supply towards the right horn is further confirmed by moderate correlations between its length and body width and body length. While asymmetric horns indicate different wind directions, a high correlation between dune length and width indicates sand transport patterns. A strong negative correlation between ASI (asymmetry index) and slipface angle points to the asymmetry between the orientation of the stoss and lee side. The wavelength of ripples is in the range of 2–3 m, while the megaripple wavelength varies between 5–17 m. Dune migrates primarily in the NNE–NE direction at a rate of 0.25–0.61 m/Earth year, while the ripple migration is observed between 0.26–0.97 m/Earth year, also in the NNE–NE direction. The development and removal of new slip face scars suggest the ongoing mass wasting processes. The observation of dust devil tracks over the years offers insight into the robust wind dynamics inside the crater. The current analysis on the aeolian characteristics at the Arkhangelsky crater advances our understanding of Mars' present surface dynamics and helps plan for future missions.

Acknowledgments: The authors acknowledge the technical help provided by Mr. Animesh Choudhury, a PhD scholar at the Modeling and Simulation Lab, Department of Earth and Atmospheric Sciences, National Institute of Technology Rourkela, Odisha, India. The HiRISE images used in this study are publicly available (https://www.uahirise.org/), provided by NASA and the University of Arizona. The CTX images are obtained from the image explorer of the Arizona State University (https://viewer.mars.asu.edu/viewer/ctx/#T=0).

SIMULATION OF NEUTRON AND GAMMA SPECTRA OF MARS: CONSTRAINTS ON THICKNESS OF CO_2 FROST LAYER

Debabrata Banerjee[1] and Shipra[2], [1]Planetary Sciences Division, Physical Research Laboratory (deba@prl.res.in), [2]Planetary Sciences Division, Physical Research Laboratory.

Introduction: Neutron and gamma-ray spectroscopy are important remote-sensing techniques for investigating the composition and volatile distribution of the Martian surface and shallow subsurface. These techniques are particularly useful for studying seasonal carbon dioxide (CO_2) frost, estimating water abundance, and understanding the interaction between the Martian atmosphere, surface, and subsurface materials. Neutron spectroscopy measures neutrons produced when high-energy cosmic rays interact with the Martian soil. The energy distribution of these neutrons is strongly affected by the presence of hydrogen. Areas containing water ice (> 0.1 wt.%) show characteristic changes in neutron flux compared with dry soil. Measurements of epithermal and thermal neutrons can therefore be used to estimate the hydrogen concentration and, with suitable assumptions about soil composition, convert it into an estimate of water-equivalent hydrogen or water abundance. By comparing neutron observations during different seasons, the contribution from seasonal CO_2 deposition and utilizing forward models and Monte Carlo neutron-transport simulations, the CO_2 frost thickness that best reproduces the measured neutron spectra can be estimated. Repeated observations during accumulation and sublimation phases can provide information about both the spatial distribution and seasonal evolution of the frost. Measurements acquired before frost formation, during maximum seasonal deposition, and after sublimation provide useful constraints.

.

Results and Discussion: We have built a Geant4 based code which builds a Mars environment in the simulation. The geometry consists of a large vacuum world, regolith layers, an optional solid CO_2 layer, and a 100 km atmosphere. The bottom regolith is 20 m thick with a hydrogen concentration of 5.6 wt.% (50% water equivalent hydrogen), while the middle regolith is 0.10 m thick with 0.34 wt.% hydrogen. Both use a density of 1.7 g/cm³ and a specified elemental composition. The solid CO_2 layer thickness is varied from zero to 1 m. The atmosphere is divided into ten 10-km layers, extending from 0 to 100 km. Density, temperature, and pressure are calculated using linear interpolation between the supplied reference points and evaluated at the midpoint of each layer. The thickness of seasonal CO_2 frost can be estimated by modeling how different layer thicknesses modify neutron and gamma-ray transport. Epithermal Neutron fluxes measured in northern hemisphere high latitudes (> 65°N) by Mars Odyssey HEND show a decrease with increasing L_s (solar longitude) from 0-100 degrees and is explained by sublimation of CO_2, after winter ends in the northern hemisphere. Our results simulate this effect, and we infer that the reduction in epithermal neutron fluxes near polar regions are consistent with an 80 cm thick CO_2 layer above a 10 cm dry layer and a thick underlying water-ice rich layer of ~50 wt.% (WEH). Integrating these observations with atmospheric temperature, surface pressure, and thermal-infrared measurements can further improve estimates of frost thickness.

References:

[1] Shipra, D. Banerjee and S. K. Goyal, 2026, Advances in Space Research, https://doi.org/10.1016/j.asr.2026.02.085

CHANDRAYAAN-3 PROVIDES INTRIGUING INSIGHTS INTO THERMOPHYSICS AND GEO-TECHNICAL ENVIRONMENT AT LUNAR HIGH-LATITUDES

K. Durga Prasad
[Email: durgaprasad@prl.res.in]
Physical Research Laboratory (PRL), Ahmedabad, India,

The successful soft landing of the ISRO Chandrayaan-3 mission in the lunar southern polar region has provided unprecedented ground-truth observations regarding surface composition, regolith properties, and the potential for water-ice. Although situated in a sunlit area, the Chandra's Surface Thermophysical Experiment (ChaSTE) payload on the Vikram lander delivered critical constraints on volatile stability and high-latitude thermophysics. ChaSTE instrument successfully measured the temperature profile and thermal conductivity within the uppermost 10 cm of the lunar regolith, revealing a pronounced thermal gradient and significant vertical heterogeneity. Crucially, the ChaSTE data suggests that lunar water-ice could be more prevalent than previously assumed, potentially extending beyond deep polar craters into broader high-latitude zones. Analyses of the surface temperature distribution also indicate that poleward-facing slopes in these regions may offer favorable conditions for preserving volatiles, including water-ice. Furthermore, subsequent measurements taken after the lander's hop experiment identified distinct local stratigraphy, evidence of surface modification, and notable variations in geotechnical and thermophysical properties at the secondary location. ChaSTE data along with other observations revealed a complex layering within top 10 cm and surface erosion due to Vikram’s landing at Shiv Shakti point on the Moon. These scientific outputs and operational insights provide essential constraints on the near-surface lunar environment, carrying significant implications for future exploration strategies and in-situ resource utilization.

3D THERMOPHYSICAL MODELLING OF MARTIAN SURFACE AND SUBSURFACE TEMPERATURES: VALIDATION AGAINST IN-SITU OBSERVATIONS

K. Samadhanam Raju, K. Durga Prasad*, Omkar Kumar Gupta
Physical Research Laboratory, Ahmedabad-380009, India.
*Corresponding author: durgaprasad@prl.res.in

Introduction: The thermal behaviour of Mars is influenced by surface topography, regolith properties, atmospheric dust, and seasonal variations in solar heating. Understanding these effects is essential for interpreting regolith thermophysical properties, investigating surface–atmosphere interactions, and supporting planetary mission operations. This study applies a three-dimensional (3D) thermophysical model to investigate surface and subsurface temperature variations across diverse Martian terrains. The model incorporates high-resolution topography, surface thermophysical properties, and atmospheric radiative effects to simulate diurnal temperature variations. Simulated surface temperatures are compared with observations from the Rover Environmental Monitoring Station (REMS) aboard NASA's Curiosity rover at Gale Crater, while subsurface temperature predictions are evaluated against measurements from NASA's InSight mission. The model is further applied to examine the influence of terrain morphology, thermal inertia, atmospheric dust opacity, and seasonal solar forcing on surface and subsurface thermal behaviour. The simulations characterize spatial variations in surface temperature and the attenuation and phase delay of the diurnal thermal wave with increasing depth. This study demonstrates the applicability of 3D thermophysical modeling to Martian thermal characterization, interpretation of planetary observations, exploration-site assessment, and thermal management for future robotic and human missions.

References:

[1] Appelbaum, J. and Flood, D. J. (1990) *Solar Energy* 45:353–363. [2] Kieffer, H. H. (2013) *Journal of Geophysical Research: Planets* 118:451–470. [3] Atri, D. et al. (2023) *Monthly Notices of the Royal Astronomical Society: Letters* 518:L1–L6. [4] Raju, K. S. et al. (2026) *Monthly Notices of the Royal Astronomical Society* 549:stag932. [5] Spohn, T. et al. (2024) *Geophysical Research Letters* 51(18):e2024GL108600.

DESIGN AND DEVELOPMENT OF A MINIATURIZED NEUTRAL AND ION MASS SPECTROMETER (NIMS) FOR FUTURE PLANETARY MISSIONS

S. K. Mishra*, S. K. Goyal, P. K. Kushwaha, A. J. Verma , D.K. Painkara, M. K. Soni, C. Raghavan, Alka, J. Sebastian, P. Kumar, N. Upadhyay, Sanjay K. Mishra, K. Acharyya, R.R. Mahajan, M. Shanmuagm, V. Sheel, D. Chakrabarty, and A. Bhardwaj
*Corresponding Author Email: sanjeevm@prl.res.in
Physical Research Laboratory, Ahmedabad

Introduction: We are developing a compact and versatile mass spectrometer for future planetary missions such as the upcoming lunar landing missions and future missions to Mars and other planetary bodies. The current Neutral & Ion Mass Spectrometer (NIMS) being developed covers a mass range of 2 - 150 amu and the design can very well be scaled to study species of higher masses. The objective of the instrument is to determine the composition and abundances of neutral and ion species present in the atmosphere. Additionally, the instrument can give key insights to characterize the local plasma environment using in-situ ion measurements. The instrument consists of three main subsystems- the ionizer, the quadrupolar mass filter, and the detector. Each of these sub-systems have their own mechanical and associated electronics counterparts. The ionizer control electronics, RF control electronics, and the Current readout electronics, all have been tested and demonstrated. The detector head assembly has also been completed and the total integrated NIMS testing is underway with comprehensive testing covering different aspects of ionization, mass discrimination, and signal readout strategies. The development is being undertaken in-house at PRL and the performance of different sub-systems of the mass spectrometer have already been tested and demonstrated successfully. At present, the integrated testing has shown a mass range capability of up to 100 amu with mass resolution better than 0.5 amu. Further design updates, configuration optimization and comprehensive test, calibration and characterization activities are being carried out. Additional operational flexibilities are being designed and tested to make NIMS highly flexible and adaptable to a wide range of environmental conditions. In this paper, we will present the design, development and some of the interesting testing results of the NIMS.

References: Internal Technical Reports and Documents

CHEMICAL FINGERPRINTS OF PLANETARY EVOLUTION

Liton Majumdar
National Institute of Science Education and Research, Jatni 752050, Odisha, India

How do the chemical and isotopic signatures established during planet formation survive and evolve into the diverse compositions of planetary bodies and their atmospheres? In this talk, I will present our group's efforts to connect the chemistry of molecular clouds and protoplanetary disks with early Solar System processes, meteoritic records, rocky planetary interiors, and atmospheric evolution. Combining remote sensing observations with astrochemical, geochemical, and atmospheric modelling, I will discuss how molecular inheritance, isotopic fractionation, condensation, volatile depletion, and planetary differentiation shape the composition of planetary building blocks. I will further explore how photochemistry, atmospheric escape, and surface–atmosphere interactions modify these inherited chemical signatures, drawing connections between Earth, Mars, Venus, and their exoplanetary analogues. Together, these studies aim to establish a unified framework for tracing planetary chemical evolution, from its interstellar origins to the diversity, atmospheric evolution, and potential habitability of planetary systems.

STUDIES ON INTERANNUAL VARIABILITY OF ARGON IN THE MARTIAN ATMOSPHERE

Shipra[1] and Debabrata Banerjee[2]
[1]Planetary Sciences Division, Physical Research Laboratory, Ahmedabad (shipra@prl.res.in),
[2]Planetary Sciences Division, Physical Research Laboratory, Ahmedabad (deba@prl.res.in).

Introduction: Argon is an important minor constituent of the Martian atmosphere, comprising approximately 1.9% of its composition. Because argon is chemically inert, its spatial and temporal variability provides a useful tracer of atmospheric circulation, seasonal mass exchange, and the redistribution of atmospheric constituents. Gamma-ray spectroscopy, together with complementary spacecraft observations, provides an additional means of investigating the spatial and temporal behaviour of argon and the radiation-induced processes associated with the Martian surface–atmosphere system. Gamma-ray spectroscopy detects characteristic gamma-ray emissions generated by interactions between cosmic rays and the Martian surface and atmosphere. Although atmospheric argon is more commonly investigated using mass spectrometry and direct atmospheric measurements, gamma-ray observations provide a complementary perspective on the spatial environment and seasonal processes associated with argon redistribution. The seasonal behaviour of Martian argon is closely linked to the planet's CO_2 cycle. During polar winter, atmospheric CO_2 condenses onto the polar caps, producing substantial changes in atmospheric pressure and total atmospheric mass. Because argon remains gaseous under Martian surface conditions while CO_2 undergoes seasonal condensation and sublimation, its relative atmospheric abundance can vary significantly throughout the seasonal cycle. Atmospheric circulation can subsequently redistribute argon from the polar regions toward lower latitudes and between the two hemispheres, producing measurable seasonal and potentially interannual variations.

Results and Discussion: Our analysis of Mars Odyssey Gamma Ray Spectrometer (GRS) observations reveals a pronounced seasonal variation in the continuum-corrected 1294 keV Argon (Ar) gamma-ray signal within the 75–90°S latitude band. The production of thermal neutrons at Mars varies with season and location; hence by taking a ratio of the 1294 keV gamma ray line of atmospheric Ar to the Titanium (Ti) based 1382 keV gamma ray line, we remove possible systematic variations caused by the changing thermal neutron population as a function of season and location. The variation of Argon peak area with Martian solar longitude (L_s) for MY 26 reveals a clear seasonal dependence in its spatial distribution. The Ar area remains essentially negligible from $L_s \approx 22.5°$ to 67.5°, followed by a pronounced increase beginning near $L_s \approx 75°$. It reaches a maximum at $L_s = 142.5°$, after which it generally decreases, with a smaller secondary enhancement around $L_s = 217.5°$. The Ar area becomes negligible again beyond $L_s \approx 247.5°$. In contrast, the Ti peak area is consistently much larger than the Ar area throughout the Martian year. It increases from approximately $L_s = 22.5°$ to a maximum at $L_s = 172.5°$, before gradually declining toward the end of the solar-longitude cycle. The Ar/Ti ratio remains below 0.08 for most observations, and its peak is observed near $L_s = 97.5°$ reaching approximately 0.075. Taken together, these observations imply that the observed temporal evolution is consistent with seasonal modulation of the Martian atmosphere and polar mass exchange associated with the CO_2 cycle. The results demonstrate the potential of Mars Odyssey GRS observations as a complementary tool for investigating the seasonal redistribution of atmospheric argon, while further comparison with atmospheric measurements and independent neutron-monitoring proxies is required to separate genuine atmospheric variability from changes in cosmic-ray-induced excitation and instrumental/background effects.

Acknowledgments: 23 PDS data products from the Mars Odyssey SGS Data Set were used for the analysis contained within this paper (https://pds-geosciences.wustl.edu/missions/odyssey/grs_sgs.html).

DEEP LEARNING CLASSIFICATION OF MARTIAN IMPACT CRATER DEGRADATION FROM CTX IMAGERY.

Saksham, Department of Applied Geophysics, IIT (ISM) Dhanbad, Dhanbad, Jharkhand, India.

Introduction: Impact craters record the geologic history of Mars. Crater counts date Martian surfaces [1], and a crater's preservation state shows how strongly erosion, infilling and burial have modified it. Deep learning is widely used to detect craters and other landforms in orbital images [2,3], and recent global catalogs also carry degradation states [4,5], but grading degradation by eye is slow and subjective. We test whether a compact convolutional neural network (CNN) can classify crater degradation state directly from Context Camera (CTX) image patches, giving a reproducible way to map crater preservation across the planet.

Methodology: We used the Mars Crater CTX Images with Dual Degradation Labels dataset [6]: 33,901 grayscale 1024×1024 patches from the Global CTX Mosaic of Mars [7], labelled with the four ordered Robbins & Hynek preservation states [4], from pristine to highly degraded. Patches were downsampled to a small fixed size and split into training and held-out validation sets. The model is a compact CNN (about 0.42 million parameters) with four convolutional layers (32–256 filters) with batch normalization and ReLU, three max-pooling stages, global average pooling and a two-layer classifier, trained in PyTorch for 10 epochs; the checkpoint with the best validation accuracy was retained. We report overall accuracy, per-class precision, recall and F1, and a confusion matrix, and use Grad-CAM [8] to inspect which image regions drive each prediction. The model is deployed as an interactive web application (single-image, batch, evaluation and map modes).

Results: On the 5,086-patch held-out validation set the model reached 61% overall accuracy (macro-F1 0.58), well above the 39% obtained by always predicting the most frequent class (state 3); validation accuracy peaked at 0.613 at epoch 8 (Fig. 1). Per-class F1 was highest for state 1, the most degraded class (0.74; precision 0.87, recall 0.65), and lowest for state 2 (0.41), with states 3 and 4 at 0.66 and 0.52 (Fig. 2). Errors concentrate between neighbouring states: 96% of misclassifications (1,882 of 1,970) fell between adjacent classes, so 98% of predictions were within one state of the catalog label. This is consistent with degradation being a continuum graded into discrete states, with ambiguity between intermediate states, state 2 in particular, a main source of error. Fig. 3 shows a Grad-CAM overlay for an example CTX image.

```
Epoch 01/10 | train_loss=1.0449 train_acc=0.4962 | val_loss=0.8984 val_acc=0.5495
  -> saved new best checkpoint (val_acc=0.5495)
Epoch 02/10 | train_loss=0.9315 train_acc=0.5500 | val_loss=0.8819 val_acc=0.5952
  -> saved new best checkpoint (val_acc=0.5952)
Epoch 03/10 | train_loss=0.8918 train_acc=0.5779 | val_loss=0.9237 val_acc=0.5230
Epoch 04/10 | train_loss=0.8766 train_acc=0.5842 | val_loss=0.8604 val_acc=0.5942
Epoch 05/10 | train_loss=0.8637 train_acc=0.5936 | val_loss=0.8417 val_acc=0.6048
  -> saved new best checkpoint (val_acc=0.6048)
Epoch 06/10 | train_loss=0.8556 train_acc=0.5966 | val_loss=0.8301 val_acc=0.5586
Epoch 07/10 | train_loss=0.8467 train_acc=0.6088 | val_loss=0.8854 val_acc=0.5665
Epoch 08/10 | train_loss=0.8351 train_acc=0.6094 | val_loss=0.8605 val_acc=0.6127
  -> saved new best checkpoint (val_acc=0.6127)
Epoch 09/10 | train_loss=0.8301 train_acc=0.6155 | val_loss=0.9804 val_acc=0.4978
Epoch 10/10 | train_loss=0.8311 train_acc=0.6152 | val_loss=0.8131 val_acc=0.6030
```

Figure 1. Training log over 10 epochs (loss and accuracy); the epoch-8 checkpoint (best validation accuracy) was retained.

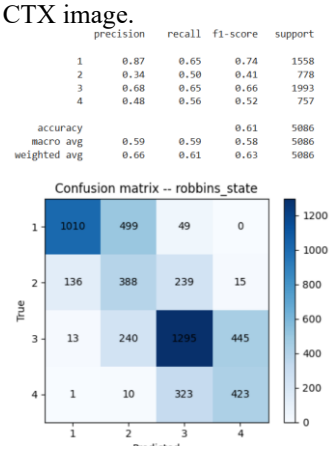


Figure 2. Per-class precision, recall, F1 and confusion matrix on the validation set (states 1–4: most degraded to pristine).

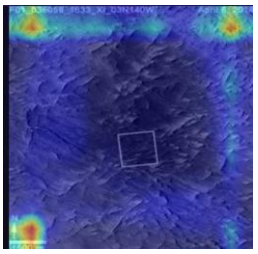


Figure 3. Grad-CAM overlay for an example CTX image; warmer colours contribute more to the predicted class.

Conclusion and Future Prospects: A compact CNN can grade Martian crater degradation from CTX imagery well above chance (61% four-class accuracy, macro-F1 0.58), with nearly all errors falling on a neighbouring state, but accuracy remains modest and intermediate states are hard to separate. Training accuracy plateaued near 0.62, pointing to room for higher-capacity models and longer training. Next steps are ordinal-aware losses, class weighting, transfer learning from pretrained networks, evaluation on a spatially separated test set, and comparison with the Liu et al. labels [5]. Predicted degradation could later be combined with crater size-frequency analysis to estimate relative ages, and the method extended to the Moon and other bodies.

References: [1] Hartmann W. K. and Neukum G. (2001) Space Science Reviews 96:165–194. [2] Palafox L. F. et al. (2017) Computers & Geosciences 101:48–56. [3] Lee C. (2019) Planetary and Space Science 170:16–28. [4] Robbins S. J. and Hynek B. M. (2012) Journal of Geophysical Research: Planets 117. [5] Liu D. et al. (2024) International Journal of Applied Earth Observation and Geoinformation, doi:10.1016/j.jag.2024.103952. [6] Hammer A. (2026) Mars Crater CTX Images with Dual Degradation Labels (v1.0.0), Zenodo, doi:10.5281/zenodo.20801959. [7] Dickson J. L. et al. (2024) Earth and Space Science 11(7). [8] Selvaraju R. R. et al. (2017) Proceedings of the IEEE International Conference on Computer Vision 618–626.

CAN THE EXPERIMENTAL MATURITY SEQUENCE HELP TO LOCATE RELATIVELY RECENT BRINE ACTIVITY ON MARS?

Mukherjee Adrita [1*], Samanta Angana [2], P.B. Hiral [3], Nimura Tokuhiro [3], Kameda Jun [3] and Ruj Trishit [3]
1 Indian Institute of Technology Kharagpur (adritajam25@kgpian.iitkgp.ac.in)
2 Indian Institute of Technology Bombay (25n0209@iitb.ac.in)
3 Institute for Planetary Materials, Okayama University, Misasa, Japan (trishitruj@okayama-u.ac.jp)

The Martian polar cap is not simply a frozen ice cap but a patterned ground of ice mixed with sediments. This typically consists of polygons occurring from mid to high latitudes. At lower latitudes, the cause of formation is thermal cracking, while at higher latitudes it is desiccation. Our study focuses on the periphery of the north polar ice cap, where we find various morphologies within similar polygonal type. A specific type of raised rim/low-centered polygon has been observed in the polar and circumpolar regions of Mars. Moving towards the pole, these polygons generally become larger and their rims more pronounced. We investigate whether this morphological variation represents different stages of polygon evolution associated with evaporation-driven freezing and subsequent sublimation. If such a mechanism operated on Mars, transient liquid brine must have been present during at least part of the evolution of these surfaces. We therefore ask whether polygon maturity can be used as a relative indicator of comparatively recent brine activity.

To test whether comparable polygonal surface organization can develop from brines under Martian atmospheric conditions, we conducted experiments in the MISASA chamber under simulated Martian boundary conditions of 4–6 hPa in N_2 and CO_2 environments, using brines (NaCl, $MgCl_2$, $CaCl_2$, and mixed brine) of varying concentrations (1–4 wt%). Pressure reduction produced evaporative cooling and initiated freezing of a thin surface ice layer. Continued sublimation subsequently modified this layer and generated raised-rim polygonal structures. We did not observe any distinctive variation in morphology based on composition, but brine concentration and pressure produced a clear difference, with observable polygon sizes of 0.100–0.600 cm. The experiments revealed six stages of polygon formation, progressing from ice nucleation and development of surface heterogeneity, through linear ridge formation and ridge linkage, to closed polygon formation, maturation, and eventual degradation. This sequence provides a relative maturity framework for comparison with Martian polygons.

Using the six-stage formation model and HiRISE images of raised-rim polygons across the polar and circumpolar latitudes of the north polar ice cap, we examined variations in polygon maturity and morphology with latitude. Mature polygons are found near the pole (84°N) and less developed ones in the circumpolar region (73°–74°N). Moving away from the pole, polygon size decreases and the rims become less pronounced. Near 73°N, the onset of ridge formation is observed.

If the experimentally derived sequence is applicable to Mars, these latitudinal differences may represent different stages of surface evolution rather than entirely different formation mechanisms. The relative maturity of raised-rim polygons may therefore provide a morphological indicator of where brine-related activity occurred comparatively recently, with less mature forms potentially preserving younger episodes of near-surface liquid-water activity

Acknowledgments: MISIP Student internship program and Okayama university

DEEP-LEARNING-BASED SEMANTIC SEGMENTATION OF LUNAR SWIRLS

Subhangini Soni[*1,2] and Megha Bhatt[1], [1]Physical Research Laboratory, Ahmedabad-380009, India, [*]subhangini@prl.res.in, [2]Indian Institute of Technology Gandhinagar, Gandhinagar-382055, India

Lunar swirls are enigmatic, sinuous, high-albedo surface features associated with localized crustal magnetic anomalies, although not every anomaly region hosts swirls [1,2]. Their formation mechanism has been debated since the Apollo era [1–7] and is attributed either to magnetic shielding of the surface from solar-wind-driven space weathering [1,6] or to cometary impacts that expose optically immature material, which is then preserved by magnetic shielding [3–5]. To understand the origin of swirls, this study investigates their shape, presence, and extent across the equatorial and mid-latitude regions (±60° latitude). The existing global swirl map was derived by visually interpreting a false-color composite of optical and UV spectral ratios [2], in which swirls were identified manually, primarily based on their albedo contrast with the surroundings. Because swirls occupy less than 1% of the lunar surface and often have diffuse margins, this map likely favors prominent, well-preserved swirls. It therefore remains unclear whether anomalies without mapped swirls truly lack swirls or instead host swirls too faint to detect.

In this work, we use deep-learning-based semantic segmentation to identify, map, and categorize swirls. Chuang et al. [8] applied K-means clustering and Maximum Likelihood Classification regionally over portions of Reiner Gamma and Mare Ingenii. However, this approach cannot be extended globally because it requires multiple co-registered meter-scale NAC observations per site and does not account for swirl morphology.

We therefore developed, for the first time, a deep-learning-based framework for the semantic segmentation of swirls at the global scale, which incorporates multiple remote sensing datasets to identify plausible swirls across ±60° latitude. We used LRO WAC 643-nm data [9,10], a multispectral RGB composite (R: 415 nm, G: 321/415 nm, B: 321/360 nm) [2], and a LOLA digital elevation model [11] to train an Attention U-Net architecture [12] for swirl detection. After multiple iterations, our preliminary results indicate that high-resolution skip connections [13] preserve thin, curvilinear swirl structures, while attention gates [12] suppress irrelevant background features. The model was trained on known swirls in mare, mare–highland boundary, and highland regions to capture the variability associated with different terrain types. To account for the large imbalance between the positive (swirl) and negative (background) classes, we combined focal [14] and focal Tversky [15,16] losses. We will discuss our preliminary low- to mid-latitude results and ongoing work to fine-tune the model to improve its generalization. The validated model will also be extended to the lunar polar regions to identify and map swirls and their associated parameters (such as magnetic field strength), to better constrain how swirls form and are preserved

References: [1] Blewett et al. (2011) JGR, 116, E02002. [2] Denevi et al. (2016) Icarus, 273, 53. [3] Hess et al. (2020) A&A, 639, A12. [4] Schultz & Srnka (1980) Nature, 284, 22. [5] Syal & Schultz (2015) Icarus, 257, 194. [6] Kramer et al. (2011) JGR, 116, E04008. [7] Garrick-Bethell et al. (2011) Icarus, 212, 480. [8] Chuang et al. (2022) PSJ, 3, 231. [9] Robinson et al. (2010) Space Sci. Rev., 150, 81. [10] Boyd et al. (2012) LPSC XLIII, Abstract 2795. [11] Smith et al. (2010) Space Sci. Rev., 150, 209. [12] Oktay et al. (2018) arXiv:1804.03999. [13] Ronneberger et al. (2015) MICCAI, LNCS 9351, 234. [14] Lin et al. (2017) IEEE ICCV, 2980. [15] Salehi et al. (2017) MLMI, LNCS 10541, 379. [16] Abraham & Khan (2019) IEEE ISBI, 683.

INTEGRATED ASSESSMENT OF SAFE LANDING ZONES AND TRAVERSE PLANNING AT THE LUNAR SOUTH POLE

Suyash Sharma[1] (ssharmaco07@gmail.com), Rajesh V J[1] (rajeshvj@iist.ac.in), Shyama Narendranath[2] (shyama.kc@gmail.com), 1. Indian Institute of Space Science and Technology, Thiruvananthapuram, India 2. U R
Rao Satellite Centre, ISRO, Bengaluru, India

The coming decade of lunar exploration will focus on the south polar region, which holds strategic and scientific significance, mainly because of the presence of permanently shadowed regions (PSRs). The lunar axial tilt creates extreme angles of sunlight and low temperatures (< 110 K), making it ideal for volatile sequestration [1,2]. The South Pole-Aitken (SPA) basin significantly shapes the region; it spans approximately 2,500 kilometres in diameter, making it the Moon's largest and oldest impact structure [3]. Very few in-situ measurements have been conducted at higher latitudes. This study develops an integrated framework by identifying safe landing zones and evaluating their scientific potential, enabling in-situ measurements at two candidate regions, **Nobile Rim 1 (NR1; 85.4°S, 35.3°E)** and **Nobile Rim 2 (NR2; 84.2°S, 60.7°E)**. We developed a multi-parameter geospatial workflow using 5 m/pixel LOLA and Shape-from-Shading DEMs [5,6], LOLA-derived illumination products [7], Diviner temperature [8,9] and ice-stability products [10], and NAC images. We evaluated four geomorphological hazards: topographic slope using [11], sub-pixel surface roughness, crater/degraded-rim boundaries, and solar illumination. Slope with >10° was treated as a hazardous tipping limit for landers. Roughness was estimated from DEM [12], with >0.48 m considered hazardous, while profile curvature was used to identify concave crater-related terrain using a threshold of $<-0.005\ m^{-1}$ for rover trafficability. Solar illumination regions receiving <11 continuous days of sunlight were classified as unsuitable for solar-powered assets. PSRs and thermally stable cold traps were independently evaluated using illumination and Diviner temperature data. Geometric PSRs were defined by <2% illumination, while thermally stable regions were identified using average summer temperatures <100 K.

The candidate region Nobile Rim 1 (NR1) is situated on the SPA massif at an elevation of around 4500m, characterized by ancient, degraded crust and pre-Nectarian ejecta [4], producing hummocky and structurally complex terrain associated with the early lunar bombardment history. Elevation provides higher Solar illumination and Earth visibility for longer operation; NR1 has 79.2% of its area above the 10° slope threshold. In contrast, Nobile Rim 2 (NR2) is surrounded by relatively fresh Lower Imbrian craters [4], with well-preserved crater walls providing exposures of subsurface material. NR2 has 56.7% of its area above the 10° slope threshold and higher roughness due to ejecta, but it is in proximity to large PSRs. After combining all four hazard layers, NR1 contains a narrow safe corridor along the northern ridge crest, whereas NR2 contains a thin, illuminated ridge zone strongly constrained by crater density. NR1 offers a larger, safer landing area and better-illuminated terrain optimal for long-term mission sustainability but has less cold-trap coverage (2.5% of the area) and only a few micro PSRs. NR2 provides substantially greater cold-traps (13% of the area) and volatile potential with fresh crater exposures but has a smaller safe landing zone and greater terrain constraints.

Acknowledgements: The authors thank NASA Planetary Data System (PDS) for providing data used in this study.

References: [1] Shearer C. K. et al. (2024) *Proceedings of the National Academy of Sciences* 121: e2321071121. [2] Zhang J. A. and Paige D. A. (2009) *Geophysical Research Letters* 36: L16203. [3] Spudis P. D. et al. (1994) *Science* 266:1848-1851. [4] Krasilnikov S. S. et al. (2023) *Icarus* 394:115422. [5] Barker M. K. et al. (2021) *Planetary and Space Science* 203:105119. [6] Bertone S. et al. (2026) *The Planetary Science Journal* 7:118. [7] Mazarico E. et al. (2011) *Icarus* 211:1066-1081. [8] Paige D. A. et al. (2010) *Science* 330:479-482. [9] Williams J.-P. et al. (2019) *Journal of Geophysical Research: Planets* 124:2505-2521. [10] Schorghofer N. and Williams J.-P. (2020) *The Planetary Science Journal* 1:54. [11] Horn B. K. P. (1981) *Proceedings of the IEEE* 69:14-47. [12] Florinsky I. V. (2017) *Progress in Physical Geography: Earth and Environment* 41:723-752.